30th YEAR ANNIVERSARY SUPPLEMENT

THREE-DIMENSIONAL MICROSURGICAL AND TRACTOGRAPHIC ANATOMY OF THE WHITE MATTER OF THE HUMAN BRAIN

Juan C. Fernández-Miranda, M.D.
Department of Neurosurgery,
University of Florida,
Gainesville, Florida

Albert L. Rhoton, Jr., M.D.
Department of Neurosurgery,
University of Florida,
Gainesville, Florida

Juan Álvarez-Linera, M.D.
Department of Radiology,
Hospital Ruber Internacional,
Madrid, Spain

Yukinari Kakizawa, M.D., Ph.D.
Department of Neurosurgery,
Shinshu University School of Medicine,
Matsumoto, Japan

Chanyoung Choi, M.D.
Department of Neurosurgery,
Ilsan Baek Hospital,
Inje University,
Goyang, Korea

Evandro P. de Oliveira, M.D.
Department of Neurosurgery,
State University of Campinas,
São Paulo, Brazil

Received, May 31, 2007.
Accepted, September 12, 2007.

OBJECTIVE: We sought to investigate the three-dimensional structure of the white matter of the brain by means of the fiber-dissection technique and diffusion-tensor magnetic resonance imaging to assess the usefulness of the combination of both techniques, compare their results, and review the potential functional role of fiber tracts.

METHODS: Fifteen formalin-fixed human hemispheres were dissected according to Klingler's fiber-dissection technique with the aid of ×6 to ×40 magnification. Three-dimensional anatomic images were created with the use of specific software. Two hundred patients with neurological symptoms and five healthy volunteers were studied with diffusion-tensor magnetic resonance imaging (3 T) and tractographic reconstruction.

RESULTS: The most important association, projection, and commissural fasciculi were identified anatomically and radiologically. Analysis of their localization, configuration, and trajectory was enhanced by the combination of both techniques. Three-dimensional anatomic reconstructions provided a better perception of the spatial relationships among the white matter tracts. Tractographic reconstructions allowed for inspection of the relationships between the tracts as well as between the tracts and the intracerebral lesions. The combination of topographical anatomic studies of human fiber tracts and neuroanatomic research in experimental animals, with data from the clinicoradiological analysis of human white matter lesions and intraoperative subcortical stimulation, aided in establishing the potential functional role of the tracts.

CONCLUSION: The fiber-dissection and diffusion-tensor magnetic resonance imaging techniques are reciprocally enriched not only in their application to the study of the complex intrinsic architecture of the brain, but also in their practical use for diagnosis and surgical planning.

KEY WORDS: Cerebrum, Diffusion-tensor magnetic resonance imaging-based tractography, Disconnection syndromes, Fiber dissection, Three-dimensional anatomy, White matter tracts

Neurosurgery 62[SHC Suppl 3]:SHC-989–SHC-1027, 2008 DOI: 10.1227/01.NEU.0000297076.98175.67

The neurosurgeon must advance into the unshaped magma that characterizes the white matter of the brain in dealing with many lesions, including primary or secondary brain tumors, intraventricular lesions, intracerebral hematomas, cavernomas, arteriovenous malformations, hippocampal sclerosis, and others. For this reason, knowledge of the organization that underlies white matter, although complex and not completely elucidated, is of significant neurosurgical importance.

In basic structure, white matter is composed of myelinated fibers grouped into three types of tracts or fasciculi: association fibers interconnecting different cortical regions of the same hemisphere, commissural fibers interconnecting the two hemispheres across the median plane, and projection fibers passing up and down the neuraxis and connecting the cortex with caudal parts of the brain and spinal cord (113). Although current neuroanatomic texts and atlases describe the fiber bundles, there is a lack of anatomic explanations and illustrations suitable to acquire an appropriate three-dimensional knowledge for surgical practice (17, 95, 127). Several recent publications have demonstrated the usefulness of the white fiber-

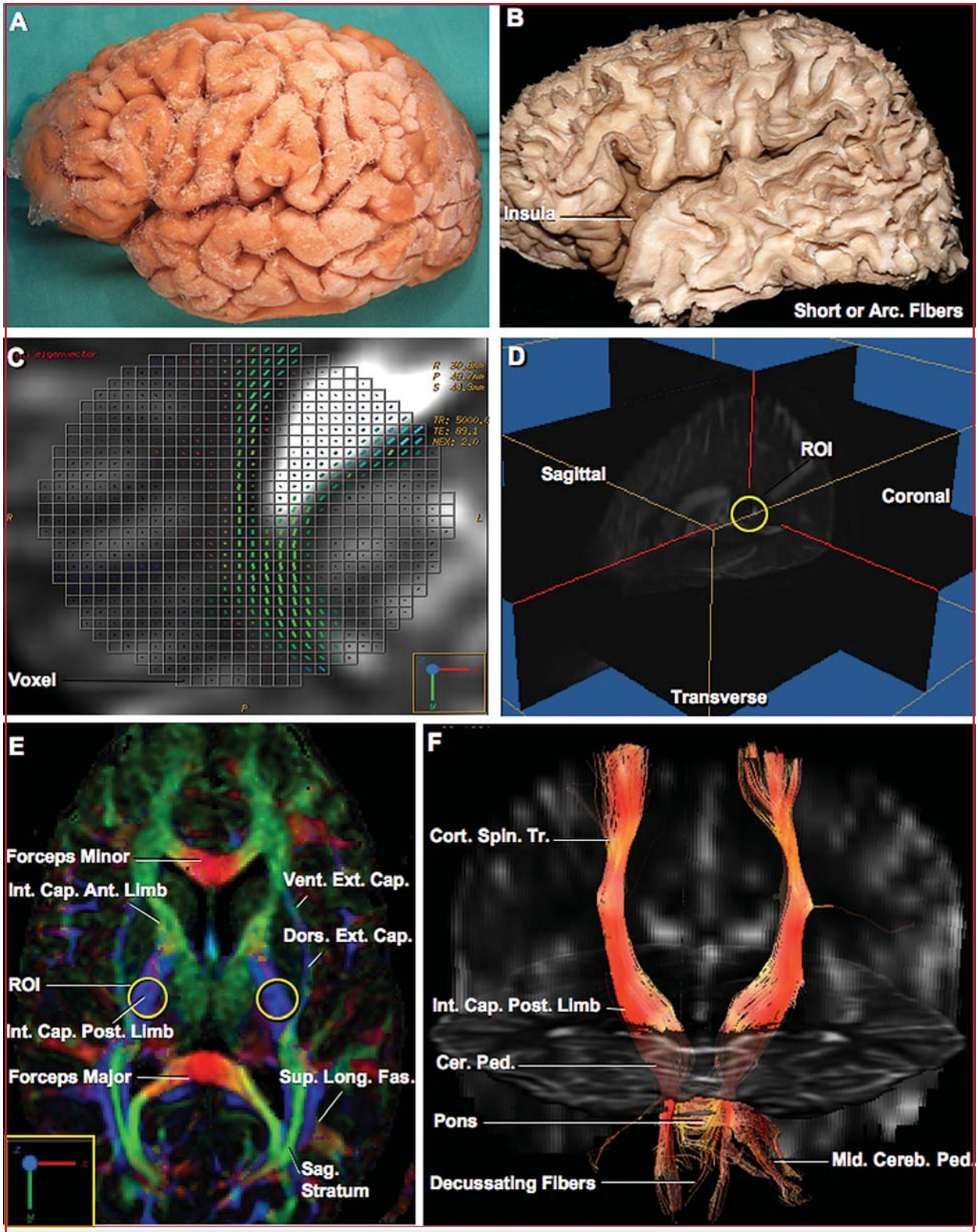

FIGURE 1. **A**, *left hemisphere fixed in 10% formalin solution. After removal of the arachnoidal and vascular structures, the anatomic specimens were frozen at −16°C for 2 to 4 weeks. The freezing process promotes the formation of formalin ice crystals between the nerve fibers, expanding and separating them and, thus, facilitates the dissection of fine fiber bundles in particular.* **B**, *the cortical gray matter of the lateral surface of the hemisphere has been removed, exposing the short associational or intergyral or arcuate or U fibers, which interconnect neighboring gyri at the subgyral sector. Peeling away the white matter fibers and following their direction is the basis of the fiber dissection technique.* **C**, *the diffusion tensor imaging (DTI)-based tractography is based on the fact that the magnetic resonance (Continues)*

FIGURE 1. *(Continued) imaging (MRI)-detectable diffusivity of water molecules depends on the principal orientation of the fiber tracts within white matter. The orientation dependence of the diffusion signal enables the DTI to measure the fiber orientation within each voxel of the image, showing the voxel-averaged estimate of orientation, which is codified as follows:* green, *anteroposterior;* blue, *craniocaudal; and* red, *lateromedial (see* inset *in* right bottom corner*).* **D**, *region of interest (ROI)* (yellow circle*) is the selected subset of samples for tractographic reconstruction. Volume-One and dTV software for diffusion-tensor analysis and fiber tracking (available free at http://volume-one.org) permits the selection of ROIs using the three spatial T2-weighted MRI planes. In this example, the ROI is located at the isthmus of the cingulate gyrus.* **E**, *color-coded DTI map of an axial plane at the level of the frontal horn. Several white matter tracts are identified by virtue of their anatomic location and color-coded orientation* (inset*). The forceps minor and major of the corpus callosum are formed by lateromedial commissural fibers* (red*), which turn forward and backward respectively, acquiring an anteroposterior orientation* (green*); the anterior limb of the internal capsule, the ventral part of the external capsule, and the sagittal stratum have a partially oblique but predominantly antero-posterior orientation* (green*). The posterior limb of the internal capsule, the dorsal part of the external capsule, and the vertical segment of the superior longitudinal fasciculus, have a predominant vertical orientation* (blue*). An ROI* (yellow circle*) has been selected at the level of each posterior limb of internal capsule.* **F**, *example of a tractographic reconstruction of the corticospinal tract using the ROIs shown in* **E**. *The middle cerebellar peduncle and some decussating fibers are identified.* Ant., *anterior;* Arc, *arcuate;* Cap, *capsule;* Cer, *cerebral;* Cereb, *cerebellar;* Cort, *cortical;* Dors, *dorsal;* Ext, *external;* Int, *internal;* Long, *longitudinal;* Mid, *middle;* Ped, *peduncle;* Post, *posterior;* Sag, *sagittal;* Spin, *spinal;* Sup, *superior;* Tr, *tract;* Vent, *ventral.*

dissection technique for the neurosurgeon (21, 36, 38, 40, 43, 44, 107, 113, 117, 120). However, only one of these articles, a study of the anterior optic radiations, used three-dimensional reconstruction to aid the reader in understanding the spatial relationships (117). The primary objective of this study is to create a collection of three-dimensional images that are useful in assimilating the topography and intricate relationships of the most important white fiber tracts.

The importance and necessity of a precise understanding of the white fiber anatomy for the neurosurgeon are greater than ever because of the recent introduction of diffusion-tensor imaging (DTI)-based tractography, a rapid and noninvasive magnetic resonance imaging (MRI) study that is capable of tracing white matter tracts in vivo (18, 81). The method is based on the fact that the MRI-detectable diffusivity of water molecules depends on the principal orientation of the fiber tracts within white matter. Diffusion-weighted MRI sequences probe such mobility along multiple directions to fully characterize its orientational distribution within an image voxel (*Fig. 1C*). Under the assumption that this distribution may be mathematically represented by a tensor, the principle axis of the corresponding diffusion ellipsoid coincides with the direction of the greatest diffusion coefficient, which can then be identified with the orientation of the underlying fiber bundle. Anisotropy measurements reflect the degree to which diffusion is preferred along this direction relative to other directions (5, 57). The incorporation of DTI-based tractography to the diagnostic neurosurgical armamentarium is already a reality. Its importance and usefulness for preoperative and even intraoperative planning have been demonstrated by Berman et al. (8), Nimsky et al. (96–98), and Kamada et al. (62, 64, 65). For this reason, we also conducted a study of the intrinsic anatomy of the brain using DTI-based tractography.

The findings obtained by both techniques, anatomic and radiological, were then compared and their relationship delineated. Selected clinical cases were used to illustrate the relevance of DTI-based tractography. Finally, with the goal of investigating the function of the fiber tracts, we correlated our anatomic and radiological results with published data from experimental animal research, clinicoradiological diagnosis of human white matter lesions, and intraoperative human brain electric stimulation.

MATERIALS AND METHODS

Anatomic Study

Fifteen human cerebral hemispheres were fixed in a 10% formalin solution for at least 3 weeks. The first step in the preparation of the specimens was the removal of the arachnoidal and vascular structures by use of surgical magnification (×6–×40). The hemispheres were frozen at −16°C for 2 to 4 weeks (*Fig. 1*). Twenty-four hours after completion of the freezing process, the white fiber dissection was started with fine and self-shaped wooden spatulas. We took numerous digital photographs while we performed the technique as described in the literature (114, 119) and, with the use of specific software (Anamaker 3D; available free from www.stereoeye.com), we fused the images to obtain an anaglyphic image.

Radiological Study

Two hundred patients with a neurological abnormality and five healthy volunteers were studied with brain MRI performed on a whole-body 3.0-T scanner (Signa Infinity 3T; General Electric Medical Systems, Milwaukee, WI) with an eight-channel head coil. DTI was performed using a single-shot multislice spin echo-echo planar sequence with the following attributes: diffusion sensitization, 1000 s/mm^2; repetition time, 7000 ms; echo time, 74 ms; slice thickness, 3 to 5 mm; no gap between slices; matrix, 128 × 128; field of view, 24 cm. Fifteen diffusion-gradient directions were obtained. The DTI data sets and anatomic MRI scans were analyzed with Functool software (General Electric Medical Systems) for diffusion-tensor analysis and fiber tracking. The DTI data sets of the healthy volunteers were also analyzed using Volume-One and dTV software (available free from http://volume-one.org) for diffusion-tensor analysis and fiber tracking (*Fig. 1*). We applied a knowledge-based multiple region-of-interest approach (ROI) in which the tracking algorithm was initiated from user-defined seed regions. Axonal projections were traced in both antero- and retrograde directions according to the direction of the principal eigenvector in each voxel of the region of interest. Tracking terminated when the fractional anisotropy value was lower than 0.18.

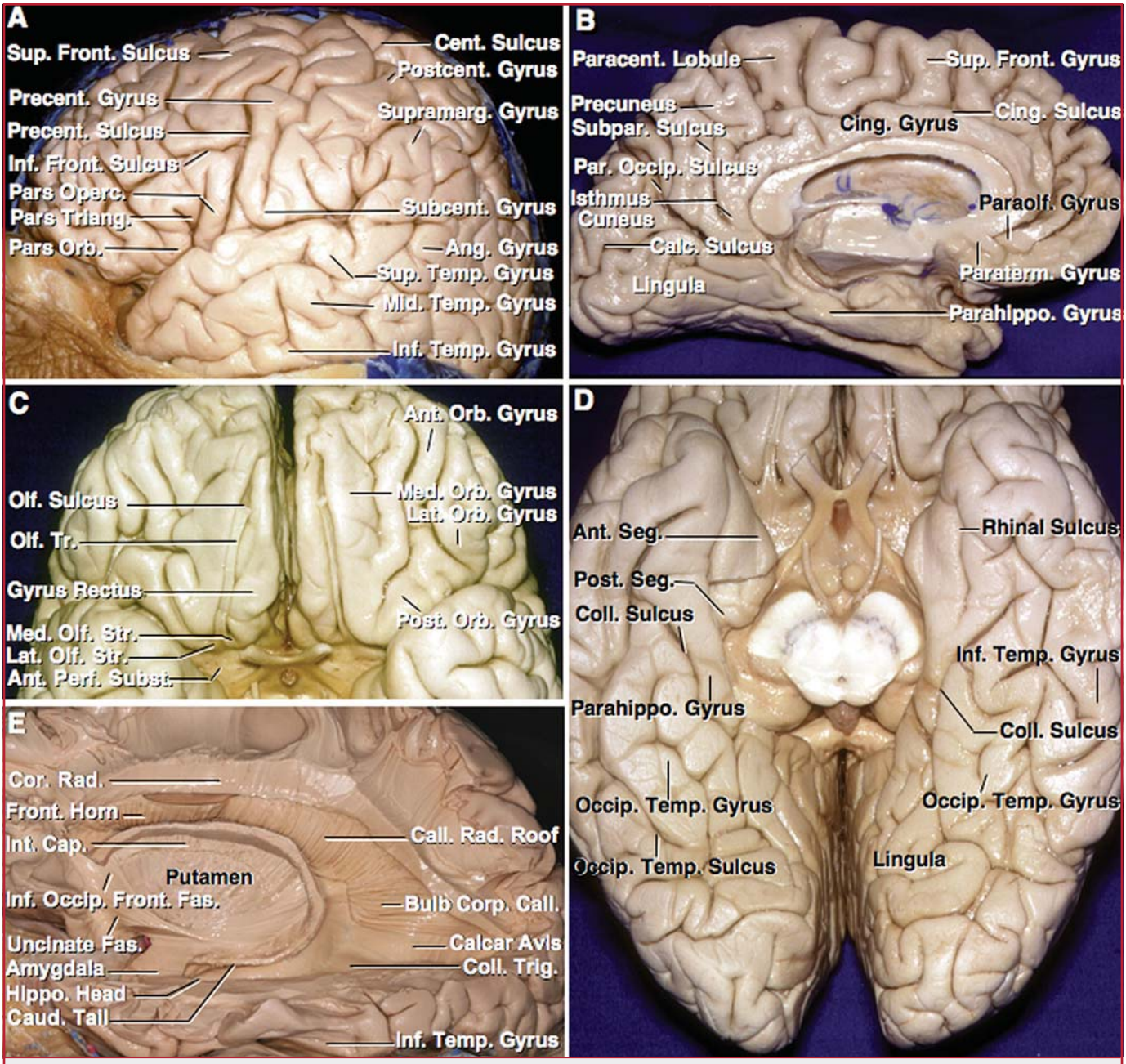

FIGURE 2. *Identification of sulci and gyri.* **A**, *lateral view, left cerebrum. The inferior frontal gyrus is formed by the pars orbitalis, triangularis, and opercularis and is limited superiorly by the inferior frontal sulcus. In this specimen, the inferior frontal sulcus is continuous and intersects with the precentral sulcus, and the superior frontal sulcus, which separates the middle frontal gyrus from the superior frontal gyrus, is an interrupted sulcus that does not intersect the precentral sulcus. The anterior limit of the precentral gyrus is formed by the precentral sulcus, which is frequently an interrupted sulcus, as seen in this specimen. The central sulcus lies between the pre- and postcentral gyri and is always continuous. The subcentral gyrus, which surrounds the lower end of the central sulcus, is visible on the lateral hemispheric surface and separates the central sulcus from the sylvian fissure. The postcentral sulcus, a commonly continuous sulcus, separates the postcentral gyrus from the superior and inferior parietal lobules. The intraparietal sulcus is also a commonly continuous sulcus, which frequently intersects the postcentral sulcus and separates the inferior from the superior parietal lobule. The inferior parietal lobule is divided into an anterosuperior part formed by the supramarginal, which arches over the upturned end of the posterior ramus of the sylvian fissure, and a posteroinferior part formed by the angular gyrus, which arches over the upturned end of the superior temporal sulcus. The lateral temporal surface is divided into three parallel gyri: the superior, middle, and inferior temporal gyri, by the superior and inferior temporal sulci. Although the superior temporal sulcus is largely continuous, the inferior temporal sulcus is commonly discontinuous, thus the middle and inferior temporal gyri are frequently formed by two or three gyral segments separated by sulcal bridges, giving the gyri an irregular discontinuous appearance.* **B**, *medial surface of the left medial hemisphere. The majority of the medial surface of the frontal lobe is formed by the superior frontal gyrus and the cingulate gyri, which are separated by the cingulate sulcus. The paraterminal and paraolfactory gyri are located below the rostrum of the corpus callosum. The ascending ramus of the cingulate sulcus passes behind the paracentral lobule, the site of extension of the pre- and postcentral gyri onto the medial surface of the hemisphere.* (Continues)

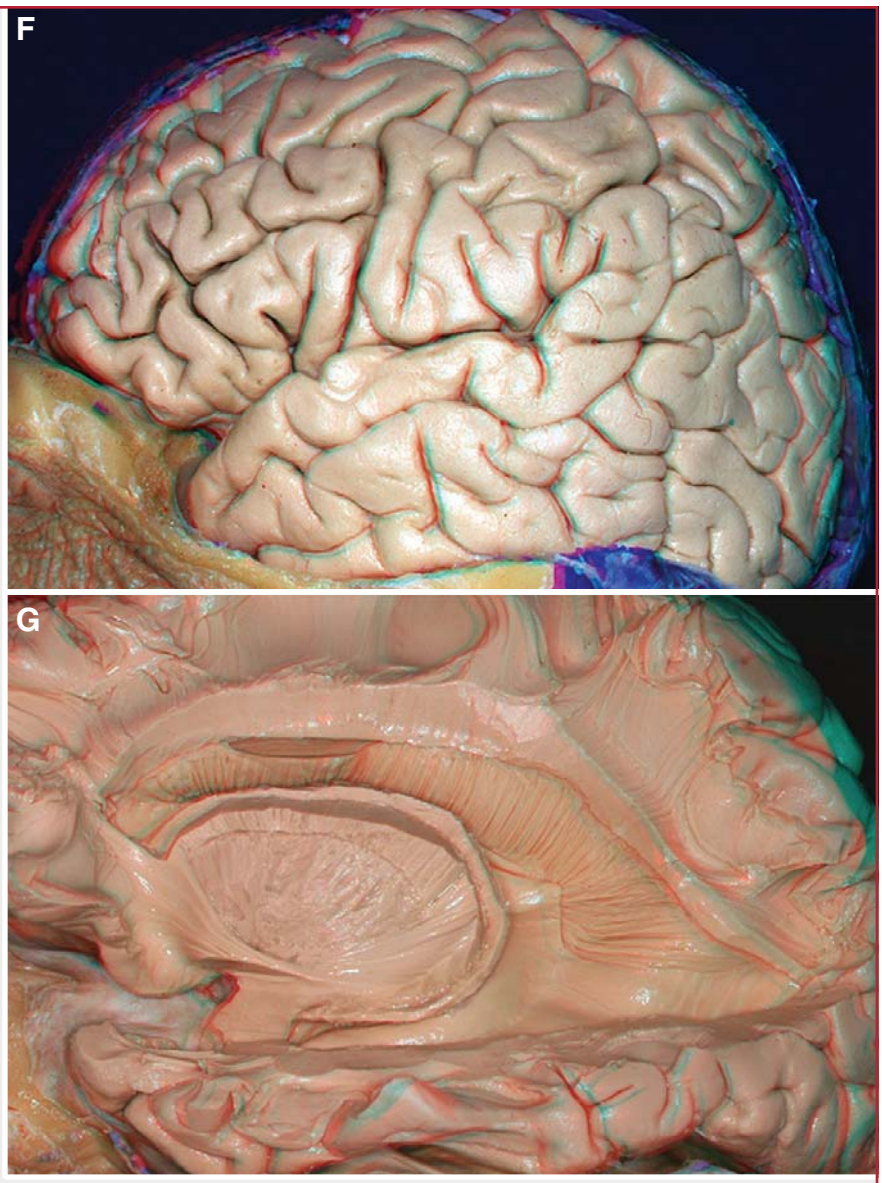

FIGURE 2. (*Continued*) *The medial surface behind the paracentral lobule is formed by the precuneus, cuneus, lingula, and posterior part of the cingulate gyrus. The precuneus is located between the ascending ramus of the cingulate sulcus, the parieto-occipital sulcus, and the subparietal sulcus, a posterior extension of the cingulate sulcus, which separates the precuneus from the isthmus of the cingulate gyrus. The cuneus is located between the parieto-occipital and the calcarine sulci, and the lingula is located below the calcarine sulcus. The parieto-occipital and calcarine sulci, always continuous sulci, join to create a Y-shaped configuration. The parahippocampal gyrus forms the majority of the medial surface of the temporal lobe, and is separated from the occipitotemporal or fusiform gyrus by the commonly continuous collateral sulci. The anterior part of the calcarine sulcus divides the parahippocampal gyrus posteriorly in a superior branch, which joins the isthmus of the cingulate gyrus, and an inferior branch, which blends into the lingula.* **C**, *orbital surface of the frontal lobe. The olfactory tract extends along the olfactory sulcus on the lateral side of the gyrus rectus and divides at the edge of the anterior perforated substance into the medial and lateral olfactory striae. The orbital surface lateral to the gyrus rectus is divided by an H-shaped sulcus into anterior, posterior, medial, and lateral orbital gyri. The posterior orbital gyrus is continuous with the transverse insular gyrus, and the lateral orbital gyrus is continuous with the pars orbitalis of the inferior frontal gyrus.* **D**, *basal surface of the temporal and occipital lobes. The collateral sulcus separates the parahippocampal gyrus from the occipitotemporal gyrus, which forms the middle strip along the long axis of the basal surface. The occipitotemporal sulcus, which separates the occipitotemporal gyrus from the inferior temporal gyrus, is continuous on the right side and discontinuous on the left side. The rhinal sulcus forms the anterior and lateral margins of the uncus, and, in most cases, is not continuous with the collateral sulcus. The uncus is divided in an anterior segment, which contains the amygdala, and a posterior segment, which contains the hippocampal head.* **E**, *fiber dissection of the left lateral cerebral hemisphere. The frontal horn, body, atrium, and temporal horn of the lateral ventricle have been exposed. The inferior frontal sulcus is located on the convexity at the deep level of the roof of the body of the lateral ventricle, which is formed by the callosal radiations. The supramarginal gyrus is located superficial to the atrium, and the middle temporal gyrus is located superficial to the temporal horn. The insular cortex, extreme and external capsules, and claustrum have been removed to expose the putamen. The internal capsule courses medial to the lentiform nucleus, the outer segment of which is formed by the putamen. The lower part of the uncinate and inferior occipitofrontal fasciculi, and the anterior part of the optic radiations have been removed to expose amygdala and head of hippocampus. The amygdala forms the anterior wall of the temporal horn. The caudate tail courses in the roof of the temporal horn. The collateral trigone bulges upward over the posterior end of the collateral sulcus and forms the floor of the atrium. The calcar avis, overlying the deep end of the calcarine sulcus, and the bulb of the corpus callosum, overlying the fibers of the forceps major, are exposed in the medial wall of the atrium.* **F**, *three-dimensional (3-D) illustration. The two dimensional (2-D) illustration is labeled in* **A** *to facilitate understanding the same illustration in three dimensions. The 3-D photograph should be viewed with red and blue anaglyph glasses.* **G**, *3-D illustration. The 2-D illustration is labeled in* **E** *to facilitate understanding the same illustration in three dimensions. The 3-D photograph should be viewed with red and blue anaglyph glasses.* Ang, *angular;* Ant, *anterior;* Calc, *calcarine;* Call, *callosal, callosum;* Cap, *capsule;* Caud, *caudate;* Cent, *central;* Cing, *cingulate;* Coll, *collateral;* Cor, *corona;* Corp, *corpus;* Front, *frontal;* Hippo, *hippocampal;* Inf, *inferior;* Int, *internal;* Lat, *lateral;* Med, *medial;* Mid, *middle;* Occip, *occipital;* Olf, *olfactory;* Operc, *opercularis;* Orb, *orbital, orbitalis;* Parahippo, *parahippocampal;* Paraolf, *paraolfactory;* Par, *parieto;* Paracent, *paracentral;* Paraterm, *paraterminalis;* Perf, *perforated;* Post, *posterior;* Postcent, *postcentral;* Precent, *precentral;* Rad, *radiata, radiations;* Seg, *segment;* Str, *striae;* Subcent, *subcentral;* Subpar, *subparietal;* Subst, *substance;* Sup, *superior;* Supramarg, *supramarginal;* Temp, *temporal;* Tr, *tract;* Triang, *triangularis;* Trig, *trigone.*

RESULTS

Identification of Sulci and Gyri

The anatomic dissection started with a detailed study of the most important sulci and gyri of each hemispheric surface. Their identification is important to define the trajectory and cortical relationships of the fasciculi that are identified later in the dissection (*Fig. 2*). Although the variability of the sulcal and gyral pattern is significant, detailed inspection reveals a relatively constant basic organization. Ono et al. (100) classified the cerebral sulci into three groups depending on their degree of continuity. In accordance with their criterion, in this study the uniformly continuous sulci (100%) were the sylvian fissure and the callosal, parieto-occipital, calcarine, and central sulci; those with a high index of continuity (60–87%) were the postcentral, cingulate, intraparietal, superior temporal, and collateral sulci; and the commonly interrupted sulci (7–33%) were the superior and inferior frontal, precentral, inferior temporal, and occipitotemporal sulci (*Table 1*). The relationship between the intersections of sulci of surgical interest was also analyzed (115). In two-thirds of the hemispheres, the superior and inferior frontal sulci were continuous with the precentral sulcus, and the intraparietal sulcus was continuous with the postcentral sulcus. In one-third of the hemispheres, the collateral sulcus was continuous with the rhinal sulcus, and the subcentral gyrus, which surrounds the lower end of the central sulcus, was located inside the sylvian fissure without being visible on the lateral hemispheric surface. Only two of 15 cingulate sulci were continuous with the subparietal sulcus (*Table 1*).

Gyral Dissection

The removal of cortical gray matter began in the depth of the sulcus and advanced progressively toward each gyral surface. Removing the outer layer of gray matter exposes the subcortex, a thin, gray layer on the outer surface of the white matter. After removal of the gray matter, the dissection progressed to the subgyral sector (148), beginning on the gyral surface and extending to the depth of the sulcus. At this level, two types of white fibers are identified: the so-called short associational fibers (also known as intergyral, arcuate, or U fibers), which interconnect neighboring gyri, and the vertical (or incorporation) fibers that are directed toward the long association, projection, or commissural fasciculi. The short fibers are located on the surface of the gyral white matter, whereas the long fibers are situated in the deep part of the gyral white matter (*Fig. 1*).

Superior and Inferior Longitudinal Fasciculi

Anatomic Study

The first of the fasciculi, identified in dissections beginning on the lateral hemispheric surface, is the superior longitudinal fasciculus or arcuate fasciculus. Traditionally, this fasciculus is described as a reversed C-shaped structure that surrounds the insula and interconnects the frontal and temporal lobes (95, 127, 138). To expose the superior longitudinal fasciculus, we removed the cortical gray matter and adjacent superficial short fibers of the frontal, temporal, and parietal opercula; the middle frontal, superior, and middle temporal gyri; and the inferior parietal lobule. Removal of the short fibers exposed the deeper long-association fibers that descend from the gyri and travel a variable distance toward distant gyri. The horizontal orientation of the long fibers in the depth of the inferior and middle frontal gyri, where they form a compact fasciculus of approximately 20 mm of lateromedial diameter, situated 22 to 25 mm from the cortical surface, is evident (*Fig. 3*). Interestingly, we observed that many of the frontal fibers of the superior longitudinal fasciculus ended at the region of the inferior parietal lobule to form what we call the frontoparietal or horizontal segment of the superior longitudinal fasciculus.

At the level of the temporoparietal junction area and at approximately 20 to 25 mm from the cortical surface, we noted a well-defined group of vertically oriented fibers that travel between the posterior part of the middle and superior temporal gyri and the inferior parietal lobule region. They form the temporoparietal or vertical segment of the superior longitudinal fasciculus. At a deeper level in the temporoparietal area, a group of fibers that arch around the posterosuperior insular border is seen traveling between the posterior temporal region and the prefrontal area. They form the frontotemporal or arcuate segment of the superior longitudinal fasciculus (*Fig. 3, C* and *I*).

Dissecting at the inferolateral hemispheric surface exposes a group of fibers deep to the temporoparietal segment of the superior longitudinal fasciculus, which runs from the anterior temporal lobe in a posterior direction. This group of fibers forms the inferior longitudinal fasciculus or temporo-occipital fasciculus (*Figs. 3, G* and *J*, and *4G*). As we will show later, this fasciculus is located lateral to the optic radiations.

Tractographic Study

The superior longitudinal fasciculus is identified in the color-coded DTI maps as the most lateral fasciculus with an anteroposterior orientation (green). In the T2-weighted sagittal images, the superior longitudinal fasciculus is identifiable as the white substance surrounding the posterior margin of the insula. The critical point is to properly select the ROIs for the tracking process. First, an ROI at the deep level of the inferior parietal lobule was selected to obtain a representation of the superior longitudinal fasciculus that is faithful to its traditional anatomic description (*Fig. 3B*). Then, three different ROIs were selected at the deep level of the middle frontal, inferior parietal, and posterior temporal regions to obtain a representation of the frontoparietal, temporoparietal, and frontotemporal segments of the superior longitudinal fasciculus, previously described by the fiber-dissection technique (*Fig. 3D*). Selecting an ROI slightly lateral to the inferolateral wall of the temporal horn displayed the fibers of the inferior longitudinal fasciculus without revealing the optic radiations, which run medially. The simultaneous exposure of the inferior and superior longitu-

TABLE 1. Sulci variability identified in 15 cadaveric hemispheres

Sulci	Continuity, no (%)	Discontinuity, no (%)	Relationship, no (%)
Sylvian fissure	15 (100)		
Callosal	15 (100)		
Parieto-occipital	15 (100)		
Calcarine	15 (100)		
Central	15 (100)		5 (33), subcentral
Postcentral	13 (87)	2 (13), 1 bridge	
Collateral	13 (87)	2 (13), 1 bridge	4 (27), continuous with rhinal sulcus
Supratemporal	12 (80)	3 (20), 1 bridge	
Cingulate	11 (73)	4 (27), 1 bridge	2 (13), continuous with subparietal sulcus
Intraparietal	9 (60)	5 (33), 1 bridge	10 (67), continuous with postcentral sulcus
		1 (7), 2 bridges	
Inferotemporal	5 (33)	4 (27), 1 bridge	
		4 (27), 2 bridges	
		2 (13), 3 bridges	
Superofrontal	3 (20)	8 (53), 1 bridge	10 (67), continuous with precentral sulcus
		4 (27), 2 bridges	
Occipitotemporal	3 (20)	7 (47), 1 bridge	
		4 (27), 2 bridges	
		1 (7), 3 bridges	
Precentral	2 (13)	10 (67), 1 bridge	
		3 (20), 2 bridges	
Inferofrontal	1 (7)	12 (80), 1 bridge	9 (60), continuous with precentral sulcus
		2 (13), 2 bridges	

dinal fasciculus revealed the spatial relationship between them (*Fig. 3H*).

Insular Region

Anatomic Study

Progressive dissection of the fibers of the superior longitudinal fasciculus exposes the insular cortex. The insula has an irregular, triangular shape, and its lateral surface is divided by the central sulcus of the insula in an anterior part formed by the short gyri and a posterior part formed by the long gyri. The short gyri converge into the insular pole, whereas the long gyri merge with the limen insulae. The insular pole is located at the anteroinferior edge of the insula, and the insular apex is the highest and most prominent laterally projecting area on the insular convexity. The insular apex is located above and behind the pole on the short gyri deep to the lower edge of the pars triangularis of the inferior frontal gyrus. The limen insulae is a slightly raised, arched ridge located at the junction of the sphenoidal and operculoinsular compartments of the sylvian fissure, and it extends from the temporal pole to the orbital surface of the frontal lobe (133). It is composed of olfactory cortex in continuity with lateral olfactory striae, and is considered a transition zone between the allocortex ("old" cortex) of the anterior perforated substance and the insular mesocortex ("transition" cortex) (137). The anterior surface of the insula is formed by the transverse and the inconstant accessory gyri of the insula, which converge into the insular pole inferiorly and are continuous with the posterior orbital gyri (*Fig. 4*) (133).

After we studied the topography of the insula, we proceeded with the decortication of the insular surface. Removal of the insular subcortex exposed the white fibers of the extreme capsule and, at the level of the limen insula, the fibers of the uncinate and inferior occipitofrontal fasciculi.

The extreme capsule is defined in the classic description as the group of fibers situated between the insular cortex and the claustrum (17, 95, 127). At the dorsal (or posterosuperior) part of the insular region and underlying the insular subcortex, we observed a thin layer of short fibers traveling between the insular gyri and the frontal, parietal, and temporal opercula. They form the dorsal part of the extreme capsule. The resection of these fibers reveals the characteristic ovoid lateral surface of the insular, dorsal, or compact claustrum (11, 48, 49, 90, 109, 110, 127), which is located dorsal and superior to the uncinate and inferior occipitofrontal fasciculi (*Fig. 4, C, E, G,* and *H*). The ventral (or anteroinferior) part of the extreme capsule is thicker

than the dorsal part and is composed of a superficial layer of short fibers traveling between the insular gyri and between these and the frontal and temporal opercula, and a deeper layer formed by fibers of the uncinate and inferior occipitofrontal fasciculi, which traverse the amygdalar, ventral, or fragmented claustrum (11, 48, 49, 90, 109, 110, 127).

The external capsule is classically described as a layer of fibers situated between the claustrum and the putamen. Removal of the fibers of the dorsal extreme capsule exposes the fibers of the dorsal (or posterosuperior) external capsule at the periphery of the dorsal claustrum, forming a characteristic spoke-and-wheel pattern with its center at the dorsal claustrum. As dissection of the external capsule progresses, the radiation pattern of the fibers between the claustrum (and/or toward it) and the corona radiata (and/or from it) becomes more evident (*Fig. 4, C*, *E*, *G*, and *H*). A detailed and delicate dissection of these fibers, starting at the periphery of the external capsule, where they join or become a part of the corona radiata, and proceeding centripetally toward the claustrum, reveals that most fibers converge and merge with the gray matter of the dorsal claustrum; thus, we can affirm that their origin (and/or termination) is in the dorsal claustrum. Removal of the white fibers is associated with removal of the gray mater of the dorsal claustrum, so that as the dorsal external capsule is being removed, the dorsal claustrum is also being removed. Only in the deepest layer do the dorsal external capsule fibers present a clear attachment to the external surface of the putamen, which is almost totally exposed at this point (*Fig. 5*).

The uncinate fasciculus is exposed under the cortical surface of the limen insulae. This thick, hook-shaped fasciculus forms the anterior part of the frontotemporal transition (also known as the temporal stem) and interconnects, in its most lateral portion, the fronto-orbital region with the temporal pole to form part of the ventral portion of the extreme and external capsule (*Figs. 4, C* and *E*, and *5*). As the uncinate fasciculus fibers are removed, several island-like gray-matter masses intermingled with the fibers are exposed. These gray-matter islands form the ventral claustrum, which is related in the superficial plane with the dorsal claustrum located superior and posterior to the uncinate fasciculus (*Figs. 4* and *5*). Extending the dissection of the uncinate fasciculus medially exposes the white fibers of the ventral portion of the external capsule that connect the frontomesial (gyrus rectus, subcallosal area) and the temporomesial regions, and the gray matter of the ventral claustrum blending into the amygdaloid nucleus, which is situated inferomedial to the uncinate fasciculus (*Fig. 6*).

Removing the white matter underlying the limen insulae also exposes the inferior occipitofrontal fasciculus, which is formed by a group of fibers traversing from the prefrontal region dorsal to the frontal fibers of the uncinate fasciculus. At the frontotemporal transition zone, the fasciculus narrows as it swings around the lower external side of the putamen and continues posteriorly toward the middle and posterior temporal region. Its fibers are so closely related to the fibers of the dorsal external capsule and the temporo-occipital fibers of the inferior longitudinal fasciculus that it was impossible to separate them. The inferior occipitofrontal fasciculus forms the main part of the ventral portion of the extreme and external capsule (*Fig. 4*).

Tractographic Study

Three ROIs (anterior, middle, and posterior) were selected in the region of the insula between the insular cortex and the putamen. The anterior ROI revealed the fibers of the uncinate fasciculus traveling between the fronto-orbital and temporopolar regions and the fibers of the inferior occipitofrontal fasciculus running between the precentral and temporo-occipital regions (*Fig. 4D*). Individual reconstructions of both fasciculi were also performed (*Figs. 4F* and *5B*). They course through the ventral claustrum and form the ventral portion of the extreme and external capsule. The middle ROI showed a group of fibers from the precentral and postcentral gyrus converging on an area situated just superior and dorsal to the uncinate fasciculus and inferior occipitofrontal fasciculus fibers. This area, as we have described previously, corresponds to the anatomic location of the dorsal claustrum. These fibers radiating from the dorsal claustrum form the anterior part of the dorsal external capsule (*Fig. 4D*). The posterior ROI showed a group of fibers coursing between the superior parietal lobule and the area of the dorsal claustrum, where they converge more posteriorly than the precentral and postcentral fibers displayed by the middle ROI. This group of fibers forms the posterior part of the dorsal external capsule (*Fig. 4D*). Some fibers appear to continue toward the prefrontal and orbitofrontal regions. On the basis of the fiber-dissection findings, these fibers are thought to be an artifact of tractography.

Basal Ganglia Region

Anatomic Study

The putamen, an ovoid, well-defined, gray-matter mass that appears after dissection of the external capsule and claustrum, is removed by use of an aspiration system (138) or fine spatulas. The identification of the external medullary lamina that separates the putamen from the globus pallidus is difficult, but both nuclei are differentiated by the higher density and pale coloration of the globus pallidus.

The anterior commissure is identified at the anterior and basal pole of the globus pallidus; it has a mediolateral and slightly anteroposterior trajectory (*Figs. 5, C*, *E*, and *H*, and *6*). The substantia innominata (or basal forebrain), located in front and beneath the anterior commissure and above the anterior perforated substance, is the site of the nucleus basalis of Meynert, the main cholinergic input of the cortex (*Fig. 5, E* and *H*) (17, 87). Medially, the substantia innominata is continuous with the base of the septal region, which contains the accumbens nucleus, an intermediate nucleus between the extrapyramidal and limbic system, which is anatomically and functionally related to the head of the caudate nucleus and the septal nuclei (17, 95).

After resection of the medial globus pallidus is complete, the internal capsule is totally exposed in continuity with the corona radiata. The internal capsule has an anterior limb situated between the lenticular nucleus and the head of the caudate nucleus, a posterior limb between the lenticular nucleus and the thalamus, a genu between the two limbs, a retrolenticular portion posterior to the lenticular nucleus, and a sublenticular portion below the lenticular nucleus.

The anterior limb of the internal capsule is composed of frontopontine and thalamofrontal (anterior thalamic peduncle) fibers (113, 127, 151). During dissection, the fibers of the anterior limb were observed as a large group of fibers emerging from the anterior frontal (orbitofrontal, prefrontal) region with an oblique orientation and an anteroposterior direction. Transcapsular bridges of gray matter between the lenticular and caudate nucleus intermingle with the fibers of the anterior limb. These fibers of the anterior limb are positioned medially in relation to the fibers of the posterior limb at the lower level of the internal capsule (*Fig. 5, C*, *E*, and *H*).

The genu of the internal capsule contains fibers that connect the precentral cortex with the motor nuclei of the cranial nerves and the most anterior fibers of the superior thalamic peduncle (thalamoprecentral fibers) (113, 127, 151). These fibers were exposed in the dissections to emerge from the prefrontal and precentral regions with a craniocaudal orientation and to be positioned lateral to the lower part of the anterior limb of the internal capsule (*Fig. 5, C*, *E*, and *H*).

The posterior limb is formed by corticospinal, thalamopostcentral (superior thalamic peduncle), corticopontine, and corticotegmental fibers (113, 127, 151). In the dissection, the fibers of the posterior limb were exposed as a large group of fibers appearing from the precentral and postcentral regions in a slightly oblique posteroanterior direction.

The retrolenticular portion of the internal capsule is composed of parietopontine fibers, occipitopontine fibers, and the posterior thalamic peduncle, which includes not only the geniculocalcarine fibers or optic radiations, but also the fibers extending between the pulvinar of the thalamus and the parieto-occipital cortex (113, 127, 151). During the dissections, the fibers of the retrolenticular portion were identified as coursing from the posterior parietal (precuneus) and occipital (cuneus) cortices and oriented in a sagittal plane in passage toward the internal capsule (*Fig. 6, B*, *E*, and *G*). Such an orientation justifies their inclusion as a component of the sagittal stratum, which is the equivalent of the internal capsule at the posterior part of the hemispheres (118). The sagittal stratum is formed by two fiber layers: the external layer, which is formed by the optic radiations, and the internal layer, which is composed of the parietopontine and occipitopontine fibers (118). The fibers of the inferior longitudinal fasciculus, inferior occipitofrontal fasciculus, and posterior limb of the anterior commissure are located lateral to the sagittal stratum. Differentiation among all of these layers of fibers via the dissection technique is impossible, and only the most anterior portion of the inferior longitudinal fasciculus, the frontal extension of the inferior occipitofrontal fasciculus, and the main stem of the anterior commissure can be differentiated. This explains the inclusion of all of these fasciculi in a single layer, identified as the sagittal stratum, in several anatomic works in which the fiber-dissection technique was used (79, 107, 120, 138).

The sublenticular portion of the internal capsule contains temporopontine fibers, the anterior component of the optic radiations (Meyer's loop), and the auditory radiations. Removal of the inferior occipitofrontal fasciculus and inferior longitudinal fasciculus fibers exposes Meyer's loop. This group of fibers departs from the lateral geniculate nucleus, travels in an anterior direction for 8 to 16 mm, and curves posteriorly to join the middle and posterior parts of the optic radiations passing toward the calcarine cortex (*Fig. 6, B*, *C*, *E*, *I*, and *J*). The anterior limit of Meyer's loop was located between 28 and 34 mm (average, 31 mm) posterior to the temporal pole, reaching (in all cases) the anterior limit of the temporal horn.

Removal of the fibers of the internal capsule, sagittal stratum, and corona radiata exposes the caudate nucleus, thalamus, and the fibers of the tapetum (callosal radiations) covering the lateral wall of the lateral ventricle (*Fig. 6C*). Removal of the tapetum fibers and the underlying ependymal layer exposes the lateral ventricle. The caudate nucleus has a characteristic C shape. The head of the caudate is positioned in the lateral wall of the frontal horn, the body in the lateral wall of the body of the lateral ventricle and atrium, and the tail of the caudate in the roof of the temporal horn. The thalamus is located within the C-shaped internal edge of the caudate nucleus. The anterior half of the thalamus is positioned in the floor of the body of the lateral ventricle, the posterior pole (pulvinar) of the thalamus is in the anterior wall of the atrium, and the lateral geniculate nucleus is positioned medial to the roof of the temporal horn (*Fig. 6, D* and *H*).

Finally, the complete removal of the fibers of the uncinate fasciculus exposes the amygdala, which has a close relationship with the ventral claustrum and substantia innominata. The amygdala forms the anterior wall and anterosuperior part of the roof of the temporal horn; the stria terminalis, which is the main amygdalar efferent pathway, runs in the roof of the temporal horn medial to the tail of the caudate nucleus and toward the septal region (*Fig. 6, C* and *H*). Resection of the lateral extension of the anterior commissure exposes the ansa peduncularis (ventral amygdalofugal fibers) that courses from the amygdala and through the anterior perforated substance to the septal region, lateral hypothalamic area, and medial thalamic nucleus (70, 95, 138).

Tractographic Study

Several ROIs were selected at different portions of the internal capsule, including the anterior limb, genu, posterior limb, and retrolenticular portion. The results were similar to those displayed with the anatomic dissections. However, tractographic studies allowed observation of not only the fibers of the corona radiata, internal capsule, and cerebral peduncle, but also the corticopontocerebellar fibers of the middle cerebellar peduncle and the contralateral fibers of the pyramidal tract at the same time

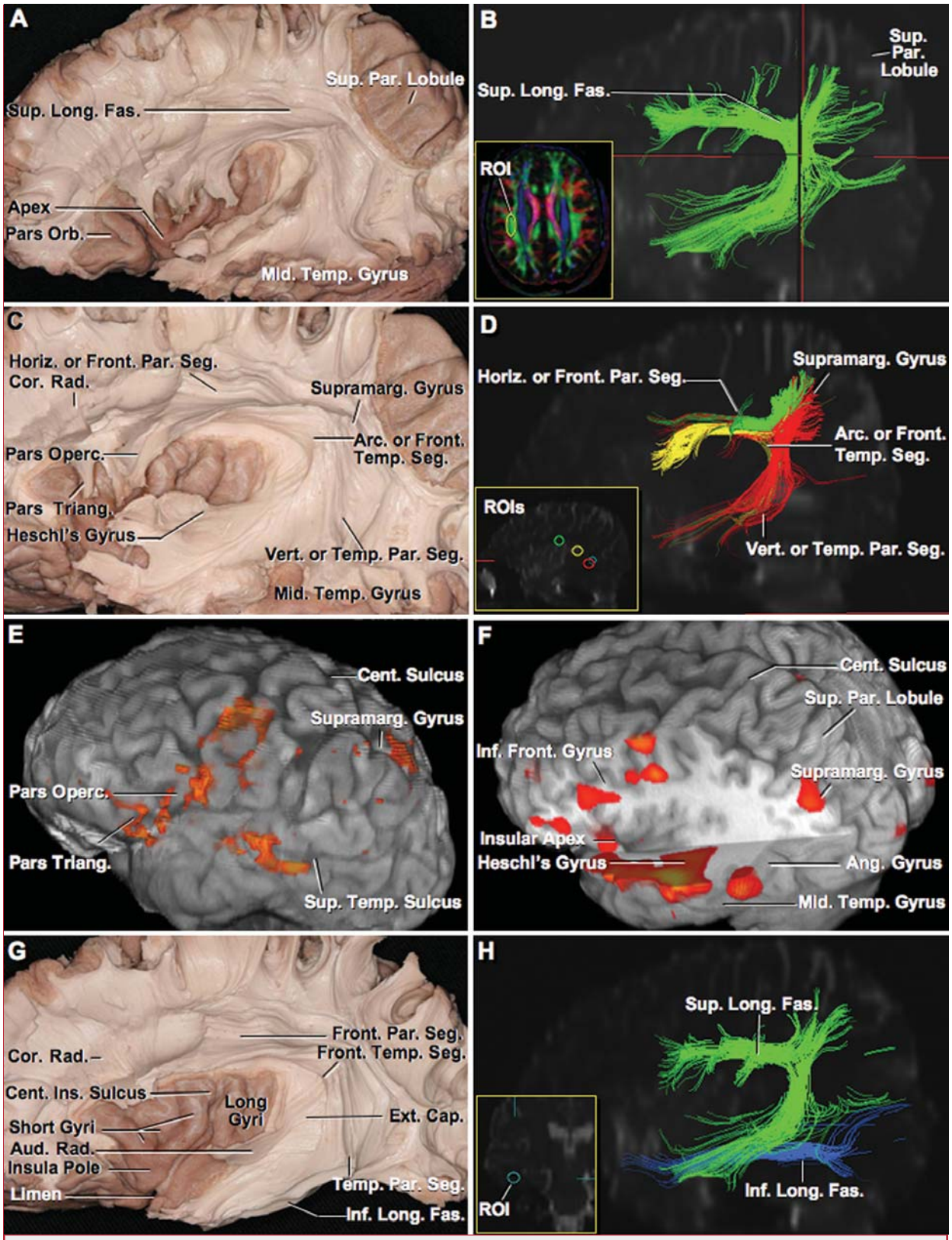

FIGURE 3. *Superior and inferior longitudinal fasciculi.* **A**, *removal of the cortical gray matter and adjacent superficial short fibers of the frontal, temporal, and parietal opercula, the middle frontal, superior temporal, and middle temporal gyri, and the inferior parietal lobule exposes the superior longitudinal fasciculus arching around the outer edges of the insula. The superior parietal lobule and the pars orbicularis of the inferior frontal gyrus are intact. Long fibers are observed descending from the frontal opercula, precentral and postcentral gyri, inferior parietal lobule, and transverse superior and middle temporal gyri.* **B**, *tractographic reconstruction of the superior (Continues)*

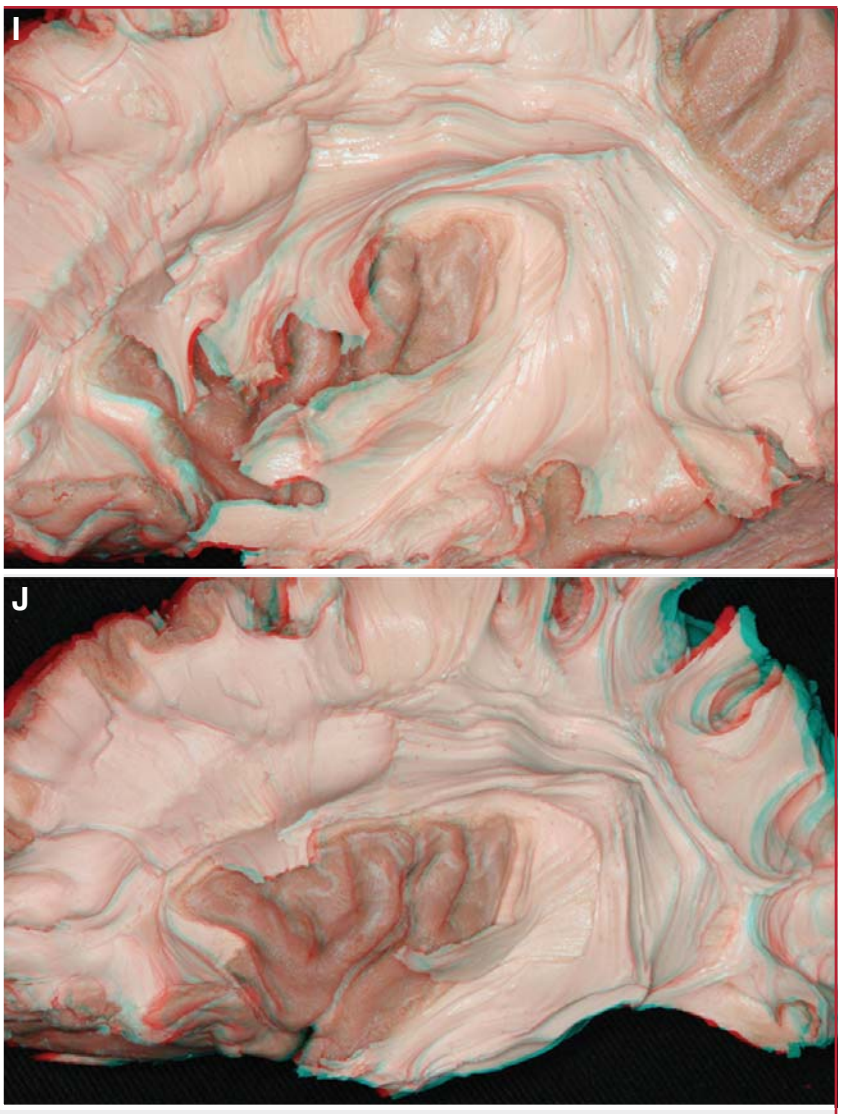

FIGURE 3. *(Continued) longitudinal fasciculus. The location of the superior parietal lobule is displayed to facilitate the comparison with* Figure 3A. *The ROI is selected in the color-coded DTI axial map at the most lateral fasciculus with an anteroposterior orientation* (green) *and at the deep level of the inferior parietal lobule* (inset). **C**, *further step in the dissection of the superior longitudinal fasciculus. Many of the frontal fibers of the superior longitudinal fasciculus end at the region of the inferior parietal lobule, forming the frontoparietal or horizontal segment of the superior longitudinal fasciculus. At the level of the temporoparietal junction area, and at approximately 20 to 25 mm from the cortical surface, a group of vertically oriented fibers travels between the posterior part of the middle and superior temporal gyri and the inferior parietal lobule region to form the temporoparietal or vertical segment of the superior longitudinal fasciculus. At a deeper level in the temporoparietal area, a group of fibers arches around the posterosuperior insular border connecting the posterior temporal region and the prefrontal area to form the frontotemporal or arcuate segment of the superior longitudinal fasciculus.* **D**, *tractographic reconstruction of the superior longitudinal fasciculus after selection of different ROIs* (inset) *at the deep level of the middle frontal* (green), *inferior parietal* (yellow), *and posterior temporal regions* (red). *A segmentation pattern in frontoparietal* (green), *frontotemporal* (yellow), *and temporoparietal* (red) *parts, as described in* **C**, *is observed. The supramarginal gyrus, a high order association cortical area, is the intermediate station between the frontal and temporal cortices connected by the superior longitudinal fasciculus.* **E**, *left hemisphere. Activation map of functional MRI during verb generation in a healthy volunteer. The task involves different aspects of language: audition, comprehension, selection of an appropriate response, and motor speech response. Cortical activations are observed in the inferior frontal gyrus (pars triangularis and opercularis), pre- and postcentral gyrus, supramarginal gyrus, and posterior superior temporal gyrus and sulcus. The superior longitudinal fasciculus provides anatomic interconnection between these cortical areas, as shown in* **A**–**D**. **F**, *left hemisphere. Activation map of functional MRI during verb generation in a different healthy volunteer. The anatomic image shows the white matter deep to the inferior frontal gyrus, inferior parietal lobule, and superior temporal gyrus. This white matter arches around the outer edges of the insula and corresponds to the superior longitudinal fasciculus. Cortical activations are observed in the inferior frontal gyrus (pars orbicularis, triangularis, and opercularis); precentral, supramarginal, and angular gyrus; anterior and posterior superior temporal gyrus and sulcus; and insular apex. The superior longitudinal fasciculus is the anatomic substrate of a high-order multisensory associative system that coordinates various inputs as required in higher human brain functions such as language in the dominant hemisphere.* **G**, *the superior longitudinal fasciculus courses superficial to the corona radiata and external capsule. The central insular sulcus separates the insula into larger anterior and smaller posterior portions. The anterior portion consists of three short gyri (anterior, middle, and posterior) arranged in a radiating pattern that converges at the insular pole located at the anteroinferior edge of the short insular gyri. The anterior and posterior long gyri extend backward and upward from the limen insulae. The distal portion of the auditory radiation courses inside Heschl's gyrus. The gray matter and superficial short fibers of the inferotemporal and temporo-occipital gyrus have been removed to expose the inferior longitudinal fasciculus, which runs from the anterobasal temporal region to the occipital lobe.* **H**, *tractographic reconstruction of the inferior and superior longitudinal fasciculi. For the reconstruction of the inferior longitudinal fasciculus, an ROI* (blue) *slightly lateral to the inferolateral wall of the temporal horn and in the deep white matter of the inferior temporal and fusiform gyri, is selected* (inset). *The inferior longitudinal fasciculus* (blue) *courses deep to the superior longitudinal fasciculus* (green), *and runs from the anterobasal temporal region to the occipital lobe.* **I**, *3-D illustration. The 2-D illustration is labeled in* **C** *to facilitate understanding the same illustration in three dimensions. The 3-D photograph should be viewed with red and blue anaglyph glasses.* **J**, *3-D illustration. The 2-D illustration is labeled in* **G** *to facilitate understanding the same illustration in three dimensions.* Ang, *angular;* Arc, *arcuate;* Aud, *auditory;* Cap, *capsule;* Cent, *central;* Cor, *corona;* Ext, *external;* Fas, *fasciculus;* Front, *frontal, fronto;* Horiz, *horizontal;* Inf, *inferior;* Ins, *insular;* Long, *longitudinal;* Mid, *middle;* Operc, *opercularis;* Orb, *orbitalis;* Par, *parietal;* Rad, *radiata, radiations;* ROI, *region of interest;* Seg, *segment;* Sup, *superior;* Supramarg, *supramarginal;* Temp, *temporal, temporo;* Triang, *triangularis;* Vert, *vertical.*

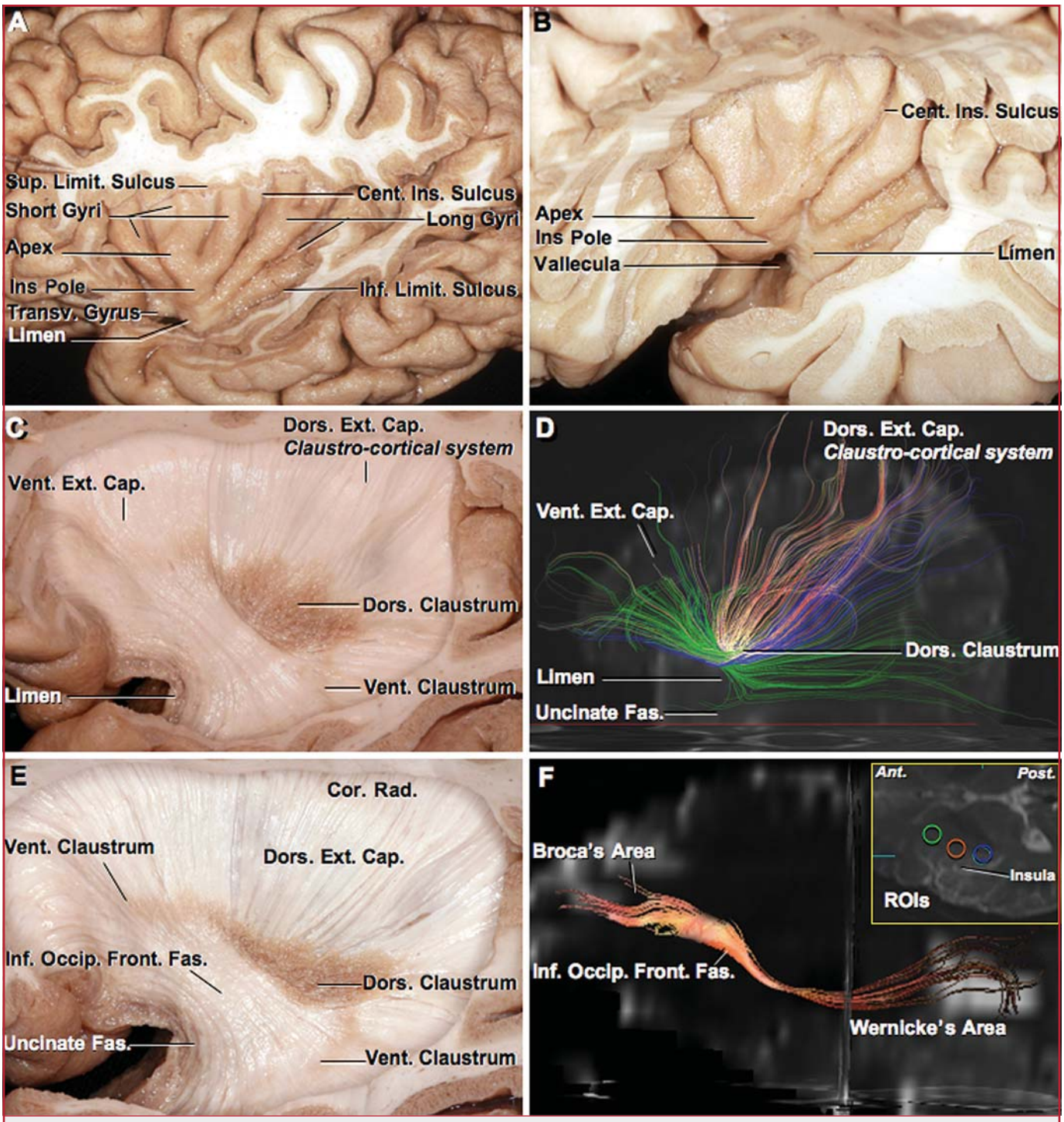

FIGURE 4. *Insular region.* **A**, *the opercular lips of the sylvian fissure have been removed to expose the insula. The central sulcus, the deepest insular sulcus, separates the insula into larger anterior and smaller posterior portions. The anterior portion consists of three short gyri (anterior, middle, and posterior) arranged in a radiating pattern that converges at the insular pole located at the anteroinferior edge of the short insular gyri. The anterior and posterior long gyri extend backward and upward from the limen insulae. The transverse insular gyrus is directed medially from the insular pole and is continuous with the posterior orbital gyri anteriorly. The inferior limiting sulcus is positioned below the long gyri of the insula and separates the insula from the sylvian surface of the temporal lobe. The superior limiting sulcus separates the insula from the sylvian surface of the frontal and parietal (Continues)*

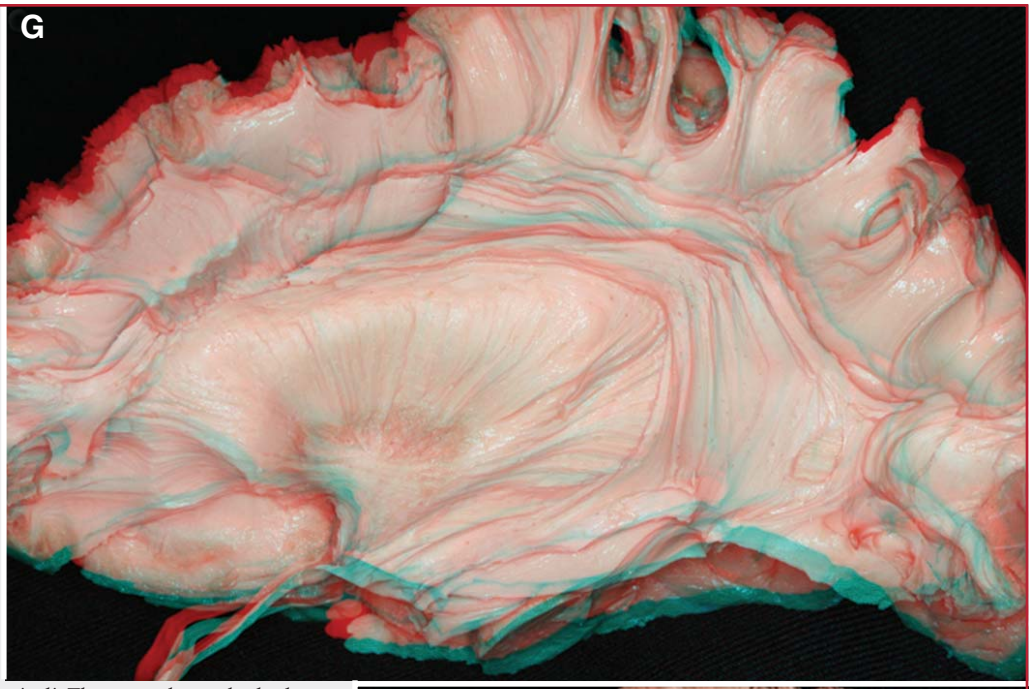

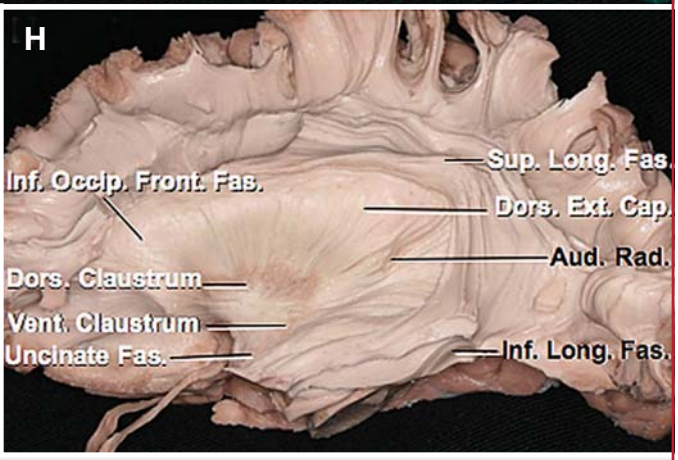

FIGURE 4. *(Continued) lobes.* **B**, *lateral view of the insula in another specimen. The opercular lips of the sylvian fissure have been removed. The limen insulae is a slightly raised, arched ridge located at the junction of the sphenoidal and operculoinsular compartments of the sylvian fissure and extends from the temporal pole to the orbital surface of the frontal lobe. The insular pole is located at the anteroinferior edge of the insula, and the insular apex is the highest and most prominent laterally projecting area on the insular convexity.* **C**, *removal of the cortical gray matter of the long and short insular gyri and extreme capsule, exposing the claustrum and external capsule. The claustrum has a dorsal (posterosuperior) part, composed of compact gray matter, and a ventral (anteroinferior)part, formed by islands of gray matter intermixed with and fragmented by fibers of the uncinate and inferior occipitofrontal fasciculi. The external capsule also has a ventral (anteroinferior) part composed of the fibers of the uncinate and inferior occipitofrontal fasciculi exposed under the cortex of the limen insulae, and a dorsal (posterosuperior) part formed by a group of radiating fibers, the claustrocortical fibers, which converge in and merge with the gray matter of the dorsal claustrum, forming a characteristic spoke-and-wheel pattern with its center at the dorsal claustrum.* **D**, *DTI-based tractogram showing the ventral and dorsal portions of the external capsule after selecting three ROIs, anterior* (green)*, middle* (orange)*, and posterior* (blue)*, in the region of the insula between the insular cortex and putamen* (inset in **F**)*. The ventral portion* (green) *is formed by the uncinate and inferior occipitofrontal fasciculi, and the dorsal portion has been divided in anterior and posterior parts. The anterior part of the dorsal portion* (orange) *is formed by multiple fibers coursing between the superior frontal, precentral, and postcentral gyri and the dorsal claustrum area just above the uncinate and occipitofrontal fasciculi. The posterior part of the dorsal portion* (blue) *is formed by several loops connecting the superior parietal lobule and parieto-occipital region to the dorsal claustrum. The dorsal external capsule contains the claustrocortical system, which has a topographical organization.* **E**, *further step in the dissection of the claustrocortical fibers. Removal of the claustrocortical fibers of the dorsal external capsule peels away the gray matter of the dorsal claustrum. The fibers from the posterior part of the dorsal external capsule enter the posterior part of the dorsal claustrum, and the fibers coming from the anterior part enter the anterior part of the dorsal claustrum. The fibers of the ventral portion of the external capsule belong to the uncinate and inferior occipitofrontal fasciculi, which traverse the most anterior and inferior parts of the claustrum to create the gray matter islands forming the ventral claustrum.* **F**, *tractographic reconstruction of the inferior occipitofrontal fasciculus, which is formed by a group of fibers coming from the prefrontal region and situated dorsal to the frontal fibers of the uncinate fasciculus. At the frontotemporal transition zone, the fasciculus narrows in section as it swings around the lower external side of the putamen and continues posteriorly toward the middle and posterior temporal region. It forms part of the ventral portion of the extreme and external capsule. Inset shows orientation* **G** *and* **H**, *3-D (***G***) and 2-D (***H***) illustrations. The 2-D illustration (***H***) is labeled to facilitate understanding the same illustration in three dimensions. The 3-D photograph should be viewed with red and blue anaglyph glasses. Fiber dissection of the left cerebral hemisphere is shown. The long and short insular gyri, and the extreme capsule have been removed to expose the claustrum and external capsule. The claustrum has a dorsal part, composed of compact gray matter, and a ventral part, formed by islands of gray matter fragmented by fibers of the uncinate and inferior occipitofrontal fasciculi. The external capsule has a ventral part composed of the fibers of the uncinate and inferior occipitofrontal fasciculi exposed under the cortex of the limen insulae, and a dorsal part formed by claustrocortical fibers, which join the corona radiata. The superior longitudinal fasciculus courses above the external capsule and lateral to the corona radiata. The inferior longitudinal fasciculus is located medial to the temporal fibers of the superior longitudinal fasciculus.* Ant, *anterior;* Aud, *auditory;* Cap, *capsule;* Cent, *central;* Cor, *corona;* Dors, *dorsal;* Ext, *external;* Fas, *fasciculus;* Front, *Frontal;* Inf, *inferior;* Ins, *insular;* Limit, *limiting;* Long, *longitudinal;* Occip, *occipito;* Post, *posterior;* Rad, *radiata, radiations;* ROIs, *regions of interest;* Sup, *superior;* Transv, *transverse;* Vent, *ventral.*

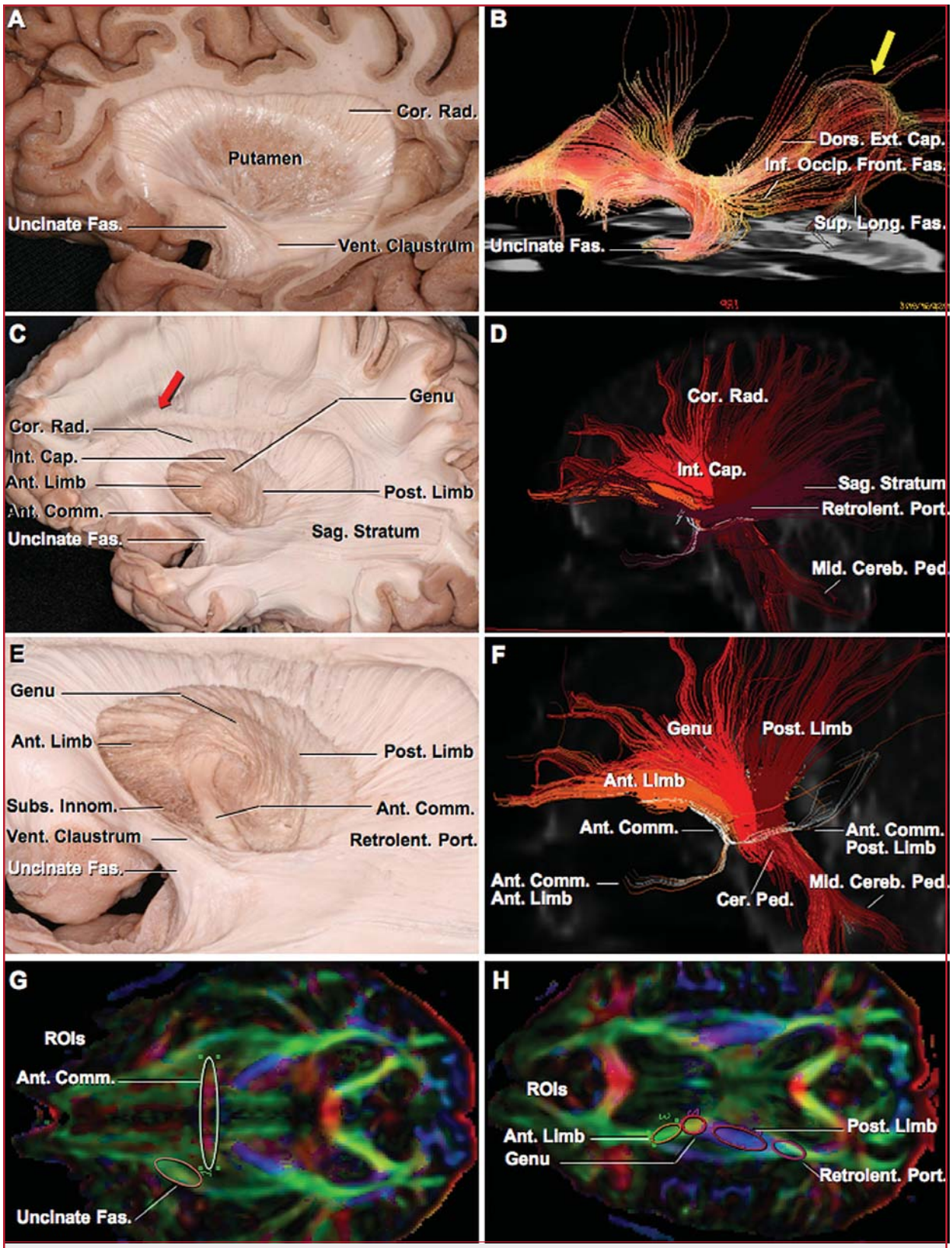

FIGURE 5. *Basal ganglia region.* **A**, *the dorsal external capsule and claustrum have been removed to expose the lateral surface of the putamen. The uncinate fasciculus, exposed by removing the cortical gray matter of the limen insulae, interconnects, in its most lateral portion, the orbitofrontal region with the temporal pole. Several island-like gray matter masses of the ventral claustrum are intermingled with the fibers of the uncinate fasciculus. The corona radiata spreads out around the putamen.* **B**, *tractographic reconstruction of the uncinate fasciculus, analogous to the fiber dissection shown in* **A**. *Some radiating fibers of the dorsal external capsule are also displayed in continuity (Continues)*

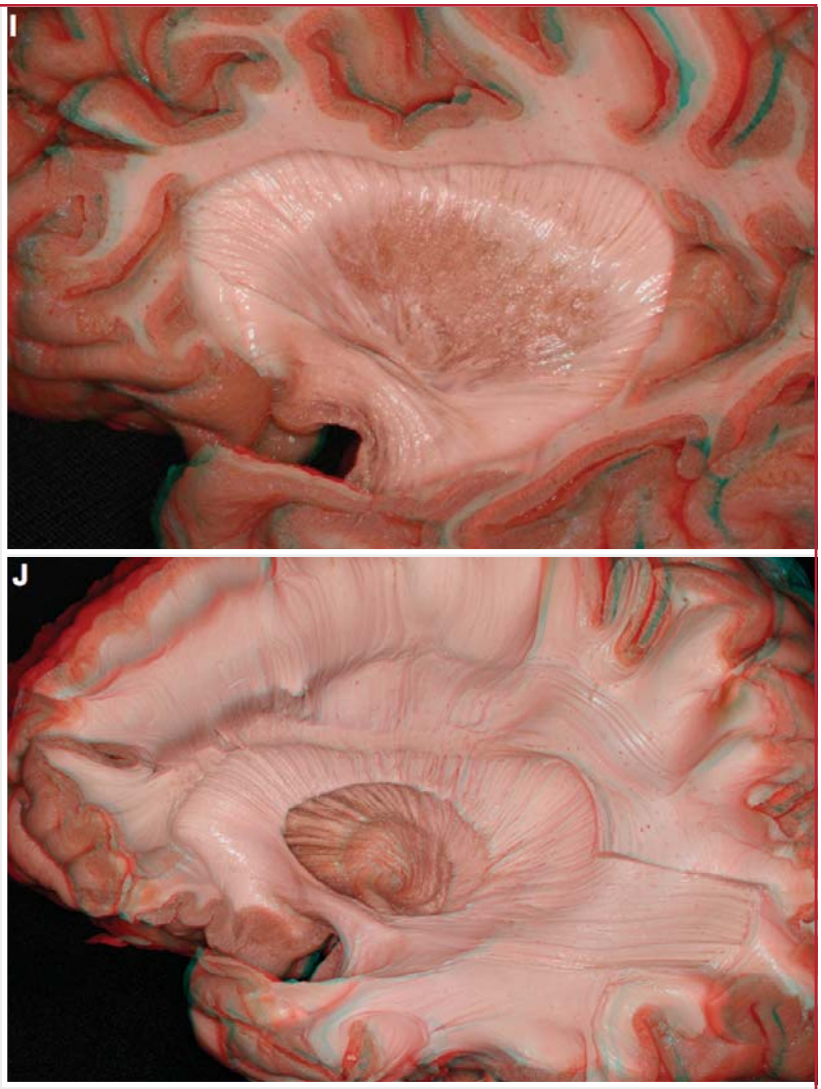

FIGURE 5. *(Continued) with vertical fibers of the superior longitudinal fasciculus* (yellow arrow). *This represents an artifact of the tractographic technique. When the voxel-averaged estimate of orientation cannot summarize the orientation of the underlying fibers, the tractography introduces continuity between the fibers where there is none. An accurate knowledge of the anatomy of the fiber systems acquired by means of the fiber-dissection technique aids in the interpretation of the tractographic results.* **C**, *the putamen and globus pallidus have been removed to expose the internal capsule and anterior commissure. The internal capsule is continuous with the corona radiata, located deep to the superior longitudinal fasciculus. A characteristic white matter prominence is created by the intersection of the fibers of the corpus callosum and the corona radiata* (red arrow). *The lower part of the vertical and arcuate segments of the superior longitudinal fasciculus have been removed to expose the sagittal stratum, which contains the optic radiations and is the equivalent of the internal capsule at the posterior part of the hemispheres. The medial fibers of the uncinate fasciculus interconnect the frontomesial (gyrus rectus, subcallosal area) and the temporomesial (amygdala, anterior parahippocampal gyrus) regions.* **D**, *tractographic reconstruction of the internal capsule and sagittal stratum. The internal capsule* (orange *and* light *and* dark red) *is in continuity with the corona radiata, which radiates toward the cortical hemispheric surface. The sagittal stratum* (purple) *is formed by the optic radiations and the parietopontine and occipitopontine fibers.* **E**, *enlarged view of the internal capsule. The anterior limb of the internal capsule has an oblique anteroposterior orientation, and is composed of a group of fibers exiting and entering the anterior frontal region (orbitofrontal, prefrontal area). The intercapsular gray matter between the lenticular and caudate nucleus is intermingled with the fibers of the anterior limb to give it a dark appearance. The fibers of the anterior limb are positioned medially to the fibers of the posterior limb at the lower level of the internal capsule. The genu of the internal capsule has a craniocaudal orientation, is positioned lateral to the lower part of the anterior limb, and is formed by fibers from the prefrontal and precentral region. The posterior limb of the internal capsule is formed by fibers from the precentral and postcentral region, and has a slightly oblique posteroanterior direction. The retrolenticular portion of the internal capsule is composed of fibers coming from the posterior parietal (precuneus) and occipital (cuneus) cortex, and is oriented in a sagittal plane in their passage toward the internal capsule. The anterior commissure, which follows a mediolateral and slightly anteroposterior trajectory, is exposed at the anterior and basal pole of the globus pallidus. The substantia innominata (or basal forebrain) is a mass of gray matter located in front and beneath the anterior commissure, and above the anterior perforated substance. The medial fibers of the uncinate fasciculus are intermingled with islands of gray matter belonging to the ventral claustrum.* **F**, *tractographic reconstruction of the internal capsule and anterior commissure. The anterior limb of the internal capsule* (orange) *is composed of frontopontine and thalamofrontal (anterior thalamic peduncle) fibers. The genu of the internal capsule* (light red) *contains fibers connecting the precentral cortex with the motor nuclei of the cranial nerves and the most anterior fibers of the superior thalamic peduncle (thalamoprecentral fibers). The posterior limb of the internal capsule* (dark red) *is formed by corticospinal, thalamopostcentral (superior thalamic peduncle), cortico-pontine, and cortico-tegmental fibers. As in the fiber dissections, the anterior limb is situated medial to the genu, and the posterior limb lateral to the genu. Tractography allows observation of the fibers of the corona radiata, internal capsule, cerebral peduncle, and middle cerebellar peduncle at the same time. The anterior commissure* (white) *bifurcates in an anterior limb directed toward the temporal pole and a posterior limb that enters the sagittal stratum, and is directed toward the posterior temporal and occipital regions.* **G**, *color-coded DTI map showing the ROIs selected for the reconstruction of the anterior commissure* (white) *in* **D** *and* **F** *and the uncinate fasciculus* (orange) *in* **B**. **H**, *color-coded DTI map showing the ROIs selected for the reconstruction of the anterior limb* (orange), *genu* (light red), *posterior limb* (dark red), *and retrolenticular portion* (purple) *of the internal capsule displayed in* **D** *and* **F**. **I**, *3-D illustration. The 2-D illustration is labeled in* **A** *to facilitate understanding the same illustration in three dimensions. The 3-D photograph should be viewed with red and blue anaglyph glasses.* **J**, *3-D illustration. The 2-D illustration is labeled in* **C** *to facilitate understanding the same illustration in three dimensions.* Ant, *anterior;* Cap, *capsule;* Cer, *cerebral;* Cereb, *cerebellar;* Comm, *commissure;* Cor, *corona;* Dors, *dorsal;* Ext, *external;* Fas, *fasciculus;* Front, *frontal;* Inf, *inferior;* Innom, *innominate;* Int, *internal;* Long, *longitudinal;* Mid, *middle;* Occip, *occipito;* Ped, *peduncle;* Port, *portion;* Post, *posterior;* Rad, *radiata;* Retrolent, *retrolenticular;* ROIs, *regions of interest;* Sag, *sagittal;* Seg, *segment;* Subs, *substantia;* Sup, *superior;* Vent, *ventral.*

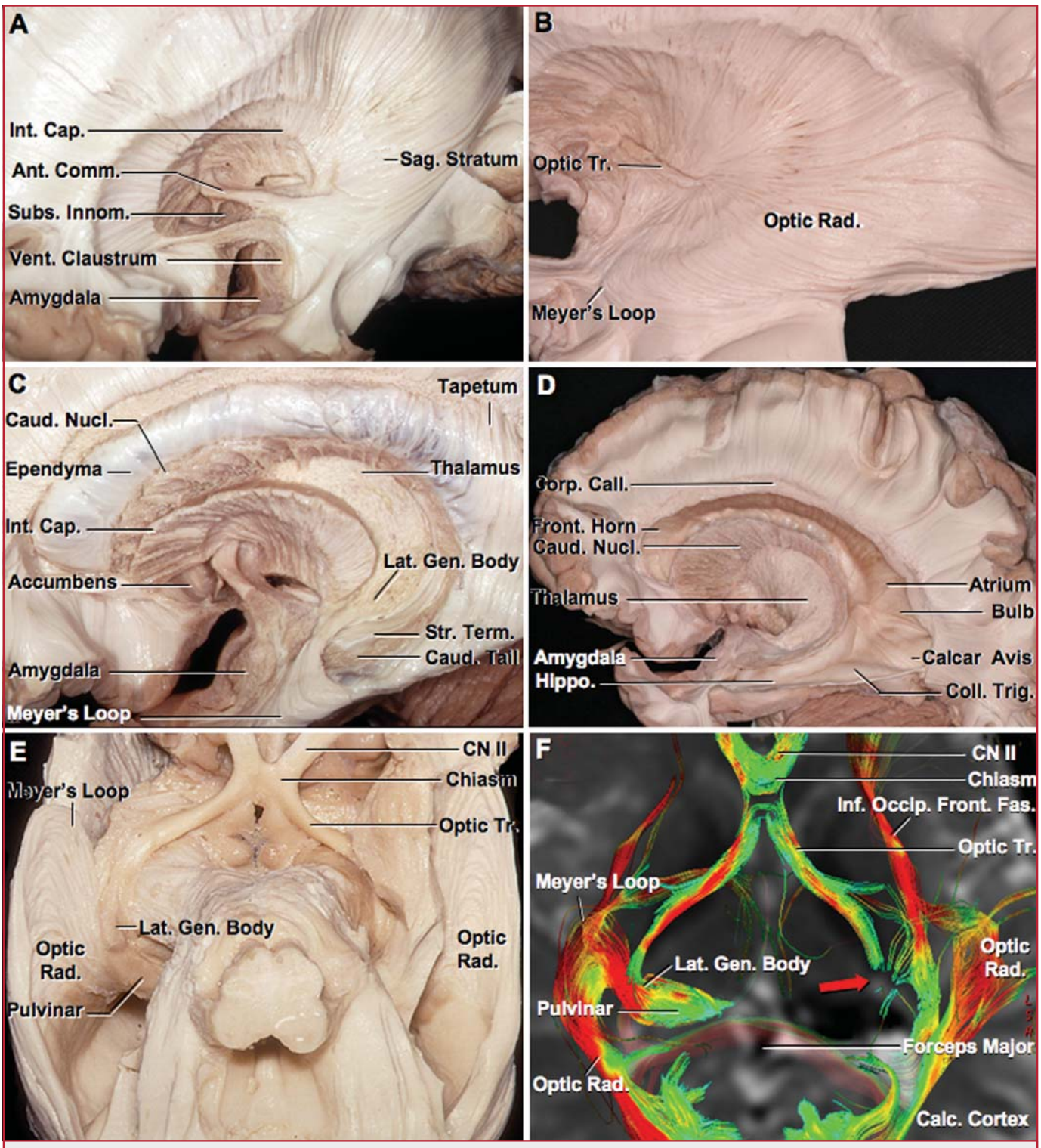

FIGURE 6. *Optic radiation.* **A**, *removal of the medial fibers of the uncinate fasciculus exposes the amygdala. The ventral claustrum blends into the amygdala and substantia innominata. A bundle of anterior commissure fibers courses within the sagittal stratum. A group of horizontal fibers in the lower part of the anterior temporal lobe belongs to the inferior longitudinal fasciculus, although posteriorly, its differentiation from the fibers of the sagittal stratum is not possible by the fiber-dissection technique.* **B**, *another specimen. Removal of the inferior occipitofrontal, inferior longitudinal, and uncinate fasciculi exposes Meyer's loop, the anterior component of the optic radiations. Meyer's loop passes anteriorly and laterally from the lateral geniculate body to reach the anterior edge of the roof of the temporal horn, where they curve posteriorly to join the middle and posterior part of the optic radiations passing toward the calcarine cortex. Meyer's loop is situated in the sublenticular portion of the internal capsule, and the remainder of the optic radiations is located at the retrolenticular portion.* **C**, *further dissection of the specimen shown in* **A**. *The fibers of the corona radiata and internal capsule have been removed and the caudal portion of the internal capsule preserved. The head of the caudate nucleus is situated medial to the (Continues)*

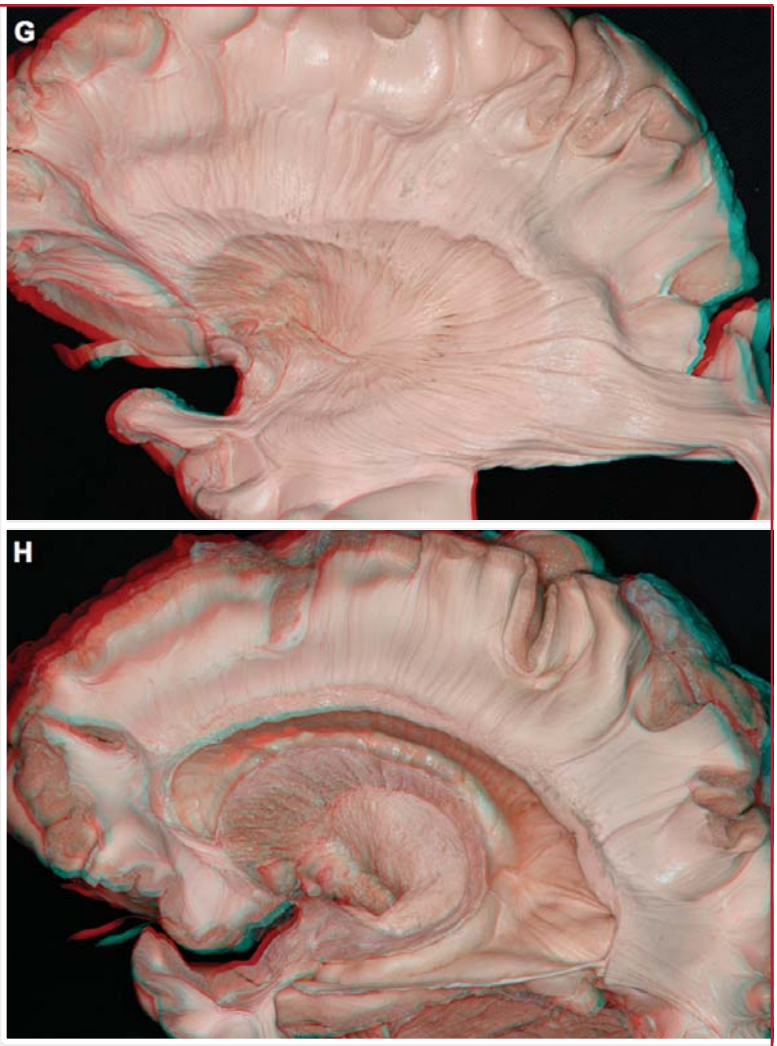

FIGURE 6. *(Continued) anterior limb of the internal capsule, and the thalamus is medial to the posterior limb and retrolenticular portion of the internal capsule. The most anterior fibers of Meyer's loop, which emerge from the lateral geniculate body and extend to the anterior limit of the temporal horn, have been preserved. The amygdala is located anterior and medial to Meyer's loop. The tapetum is composed of callosal fibers that course deep to the fibers of the internal capsule and sagittal stratum, and it forms part of the roof and lateral wall of the lateral ventricles. The ependyma is the deepest layer of the lateral wall of the lateral ventricles. The tail of the caudate nucleus, and the stria terminalis, an efferent white matter pathway arising from the amygdala and ending in the septal region, have been exposed in the roof of the temporal horn. The accumbens nucleus situated medial to the substantia innominata, below the head of the caudate nucleus, and adjacent to the septal region, has been removed.* **D**, *removal of the internal capsule, sagittal stratum, tapetum, and ependyma exposes the lateral ventricles. The caudate nucleus, with its characteristic C shape, has been exposed. The head of the caudate is positioned in the lateral wall of the frontal horn, the body in the lateral wall of the body of the lateral ventricle and atrium, and the tail of the caudate in the roof of the temporal horn. The thalamus is located within the C-shaped internal edge of the caudate nucleus. The anterior half of the thalamus is positioned in the floor of the body of the lateral ventricle, the posterior pole (pulvinar) of the thalamus in the anterior wall of the atrium, and the lower thalamic surface with the lateral geniculate nucleus is positioned medial to the roof of the temporal horn. The body of the corpus callosum forms the roof of the frontal horn, body, and atrium of the lateral ventricles. The medial wall of the atrium is formed by two prominences that are located one above the other. The upper prominence, called the bulb of the corpus callosum, overlies and is formed by the forceps major, and the lower prominence, the calcar avis, overlies the deepest part of the calcarine sulcus. The floor of the atrium is formed by the collateral trigone, a triangular area that bulges upward over the posterior part of the depth of the collateral sulcus. The floor of the temporal horn is formed medially by the hippocampus and laterally by the collateral eminence, an anterior extension of the collateral trigone that overlies the deep end of the collateral sulcus. The amygdala forms the anterior wall and anterosuperior part of the roof of the temporal horn.* **E**, *bilateral exposure of the visual pathway, formed by the optic nerve, optic chiasm, optic tract, lateral geniculate body, pulvinar, and optic radiations. Meyer's loop forms the anterior part of the optic radiation.* **F**, *tractographic reconstruction of the visual pathways in a patient with a left pulvinar arteriovenous malformation (AVM). The nasal (medial) fibers of the optic nerve decussate to the contralateral side in the optic chiasm, and the temporal (lateral) fibers remain in the ipsilateral side. The ipsilateral temporal and contralateral fibers form the optic tract, which ends at the lateral geniculate body. The optic radiation or geniculocalcarine tract arises from the lateral geniculate body, passes through the retrolenticular portion of the internal capsule and ends in the calcarine cortex located on the medial surface of the occipital lobe. The anterior component of the optic radiation, Meyer's loop, turns forward to the anterior edge of the roof and lateral wall of the temporal horn, and turns backward to reach the calcarine cortex. Fibers projecting from the pulvinar of the thalamus to the occipital cortex travel with the optic radiation. On the left side, a pulvinar AVM causes a decrease in the size of the thalamo-occipital fibers* (red arrow). *Tractography also shows some fibers of the inferior occipitofrontal fasciculus and the visual commissural fibers of the forceps major.* **G**, *3-D illustration. The 2-D illustration is labeled in* **B** *to facilitate understanding the same illustration in three dimensions.* **H**, *3-D illustration. The 2-D illustration is labeled in* **D** *to facilitate understanding the same illustration in three dimensions. The 3-D photograph should be viewed with red and blue anaglyph glasses.* **I** *and* **J**, *3-D (***I***) and 2-D (***J***) illustrations. The 2-D illustration is labeled to facilitate understanding the same illustration in three dimensions. Fiber dissection of the left mediobasal cerebral surface. The parahippocampal gyrus and hippocampal head and body have been removed to expose the roof and lateral wall of the temporal horn. The fibers of the tapetum, ependyma, caudate tail, and stria terminalis have been removed in the roof and lateral wall of the temporal horn to expose the optic radiations. Meyer's loop extends forward to the anterior tip of the temporal horn. The fibers forming Meyer's loop leave the lateral geniculate body, pursue a curved anterior course to the tip of the temporal horn, and turn backward along the roof and lateral wall of the temporal horn. The amygdala, which is located in the anterior uncal segment and anterior wall of the temporal horn, has been preserved.* Ant, *anterior;* Calc, *calcarine;* Call, *callosum;* Cap, *capsule;* Caud, *caudate;* CN, *cranial nerve;* Coll, *collateral;* Comm, *commissure;* Corp, *corpus;* Fas, *fasciculus;* Front, *frontal;* Gen, *geniculate;* Hippo, *hippocampus;* Inf, *inferior;* Innom, *innominate;* Int, *internal;* Lat, *lateral;* Nucl, *nucleus;* Occip, *occipito;* Rad, *radiations;* Sag, *sagittal;* Subs, *substantia;* Str, *stria;* Temp, *temporal;* Term, *terminalis;* Tr, *tract;* Trig, *trigone;* Vent, *ventral.*

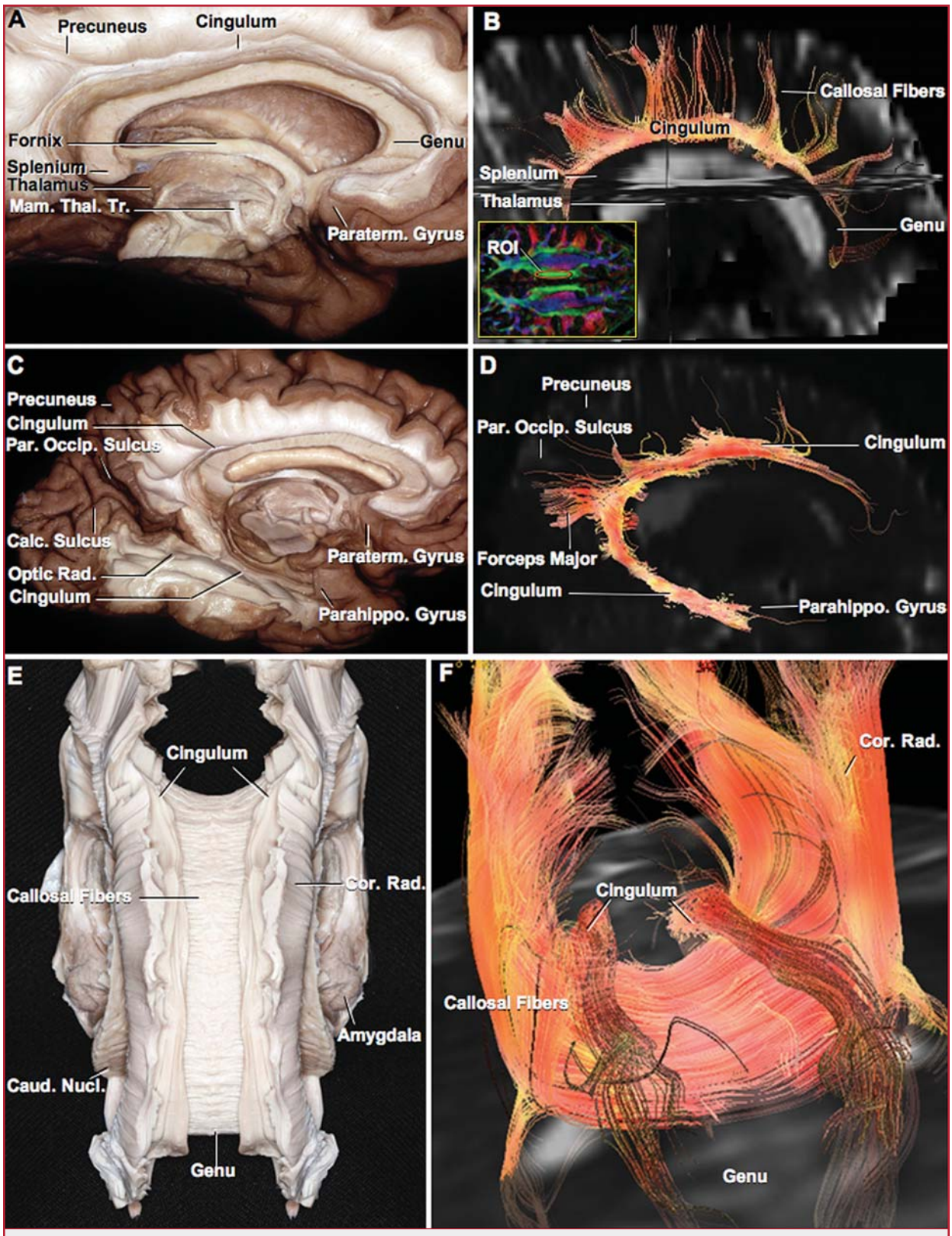

FIGURE 7. *Cingulum.* **A**, *medial view of the medial left hemispheric surface. The cortex and short fibers of the cingulate gyrus have been removed from the paraterminal gyrus to the isthmus of the cingulate gyrus, to expose the cingulum running (Continued) in a longitudinal direction, above the corpus callosum. An important contingent of fibers from the precuneus is observed becoming incorporated into the cingulum. The mammillothalamic tract courses between the mammillary body and the anterior nucleus of the thalamus.* **B**, *tractography of the cingulum coursing between the paraterminal gyrus and the isthmus. Some commissural fibers of the corpus callosum (Continues)*

FIGURE 7. *crossing below the cingulum are shown. The ROI* (orange) *is selected in the color-coded DTI axial map at the most medial fasciculus with an anteroposterior orientation* (green) *and at the deep level of the cingulate gyrus* (inset). **C**, *further fiber dissection of the left medial hemispheric surface. The cingulum narrows at the level of the isthmus of the cingulate gyrus where the commissural fibers of the forceps major cross in front of the fibers of the cingulum. Below this level, the cingulum courses near the optic radiations covering the inferior lip of the anterior part of the calcarine sulcus. The gray matter of the parahippocampal gyrus has been removed to expose the continuation of the cingulum toward the anterior parahippocampal region adjacent to the hippocampus. Multiple fibers from the precuneus are observed becoming incorporated into the cingulum.* **D**, *complete tractographic reconstruction of the cingulum, which travels from the medial temporal lobe to the medial parietal and frontal regions, and forms the so-called external limbic ring.* **E**, *superior view of fiber dissection of the cerebral hemispheres. The left and right cingulum course above the corpus callosum in an anteroposterior direction, and form the white matter of the cingulate gyrus. The fibers of the body of the corpus callosum cross to the opposite hemisphere and under the cingulum. The corona radiata is situated lateral to the cingulum and is intermingled with the callosal radiations.* **F**, *tractographic reconstruction of the left and right cingulum to be correlated with* **E**. Calc, *calcarine;* Caud, *caudate;* Cor, *corona;* Mam, *mammillo;* Nucl, *nucleus;* Occip, *occipital;* Parahippo, *parahippocampal;* Paraterm, *paraterminal;* Par, *parieto;* Rad, *radiata, radiations;* ROI, *region of interest;* Thal, *thalamic;* Tr, *tract.*

(*Fig. 5, D* and *F*). In addition, the ROI situated at the retrolenticular portion of the internal capsule revealed not only the parietooccipital fibers belonging to the sagittal stratum, but also the fibers of the inferior occipitofrontal fasciculus and inferior longitudinal fasciculus (*Fig. 5D*). As in the fiber dissections, differentiation of each independent fasciculus at this level is difficult.

The selection of successive ROIs along the visual pathway, optic nerve, chiasm, optic tract, lateral geniculate nucleus, and calcarine cortex provided a precise reconstruction of the visual pathway that accurately resembles its well-known anatomy (*Fig. 6, E* and *F*). Interestingly, the ROI situated in the calcarine cortex revealed not only the fibers of the optic radiation, but also the fibers of the inferior occipitofrontal fasciculus and the visual commissural fibers of the forceps major (*Fig. 6F*). Finally, another ROI was selected at the level of the anterior commissure, which is easily identifiable at the midline in the anterior wall of the third ventricle, and was displayed in the color-coded maps as a lateromedial (red) fasciculus. The tractographic reconstruction of the anterior commissure showed its relationship with the fibers of the internal capsule, the bifurcation of the anterior commissure in an anterior limb directed toward the temporal pole, and a posterior limb directed toward the posterior temporal and occipital regions, following the direction of the fibers of the sagittal stratum (*Fig. 5F*).

Cingulum and Fornix

Anatomic Study

Removing the cortex, subcortex, and short fibers of the cingulate gyrus exposes a group of fibers coursing in a longitudinal direction parallel and above the corpus callosum that forms the cingulum. Vertical fibers were observed to emerge from the superior frontal gyrus, paracentral lobule, and precuneus and become incorporated into the cingulum (*Fig. 7*). The vertical fibers originating in the precuneus are remarkably important for the enlargement of the cingulum, just as the fibers from the inferior parietal lobule are important for the superior longitudinal fasciculus. The dissection was continued anteriorly to expose the fibers of the cingulum curving inferiorly in front of the genu of the corpus callosum and ending in the subcallosal gyrus (or paraolfactory area of Broca) and paraterminal gyrus (*Fig. 7, A* and *C*). Dissection was then performed posteriorly, and we observed the narrowing of the cingulum at the level of the isthmus where the commissural fibers of the forceps major cross in front of the cingulum fibers. Below this level, the cingulum courses near the most anterior part of the optic radiations and covers the inferior lip of the anterior part of the calcarine sulcus (*Fig. 7C*). Removal of the gray matter of the parahippocampal gyrus exposes the continuation of the cingulum toward the anterior parahippocampal region, ending in the presubiculum and entorhinal cortex adjacent to the hippocampus (17). The complete dissection of the fibers of the cingulum exposes the most external cortical layer of the hippocampus. The fasciolar gyrus and its continuation, the subsplenial gyrus, form part of the hippocampal tail at the subsplenial level. The subsplenial gyrus surrounds the splenium and is continuous with the indusium griseum above the splenium. The indusium griseum runs along the superior surface of the corpus callosum to reach the subcallosal area. The lateral longitudinal stria courses on the indusium griseum and is considered to be aberrant fibers of the fornix, which, on leaving the fimbria, reach the superior surface of the corpus callosum to join the fornix again rostrally (*Fig. 8*) (42). The hippocampus forms the medial part of the floor of the temporal horn, and the amygdala forms the anterior wall. The dissection of the ependymal layer and the tapetum from the intraventricular side displayed the relationship of Meyer's loop with the temporal horn (*Fig. 6I*).

To expose the fornix, which is the main efferent hippocampal pathway, successive transverse and horizontal cuts were performed to reveal the lateral ventricles (113). The initial part of the fornix, the fimbria, arises in the floor of the temporal horn on the ventricular surface of the hippocampal formation and passes posteriorly to become the crus of the fornix. The crus wraps around the posterior surface of the pulvinar of the thalamus and arches superomedially toward the lower surface of the splenium of the corpus callosum. At the junction of the atrium and the body of the lateral ventricle, the paired crura meet to form the body of fornix, which courses forward along the superomedial border of the thalami in the medial wall of the body of the lateral ventricle. The body forms a gentle arch between the roof of the third ventricle and the floor of the body of each lateral ventricle. The body of fornix splits into two columns at the anterior margin of the openings of the foramen of Monro into the lateral ventricles (*Fig. 9*). Finally, the thalamus was removed from the medial

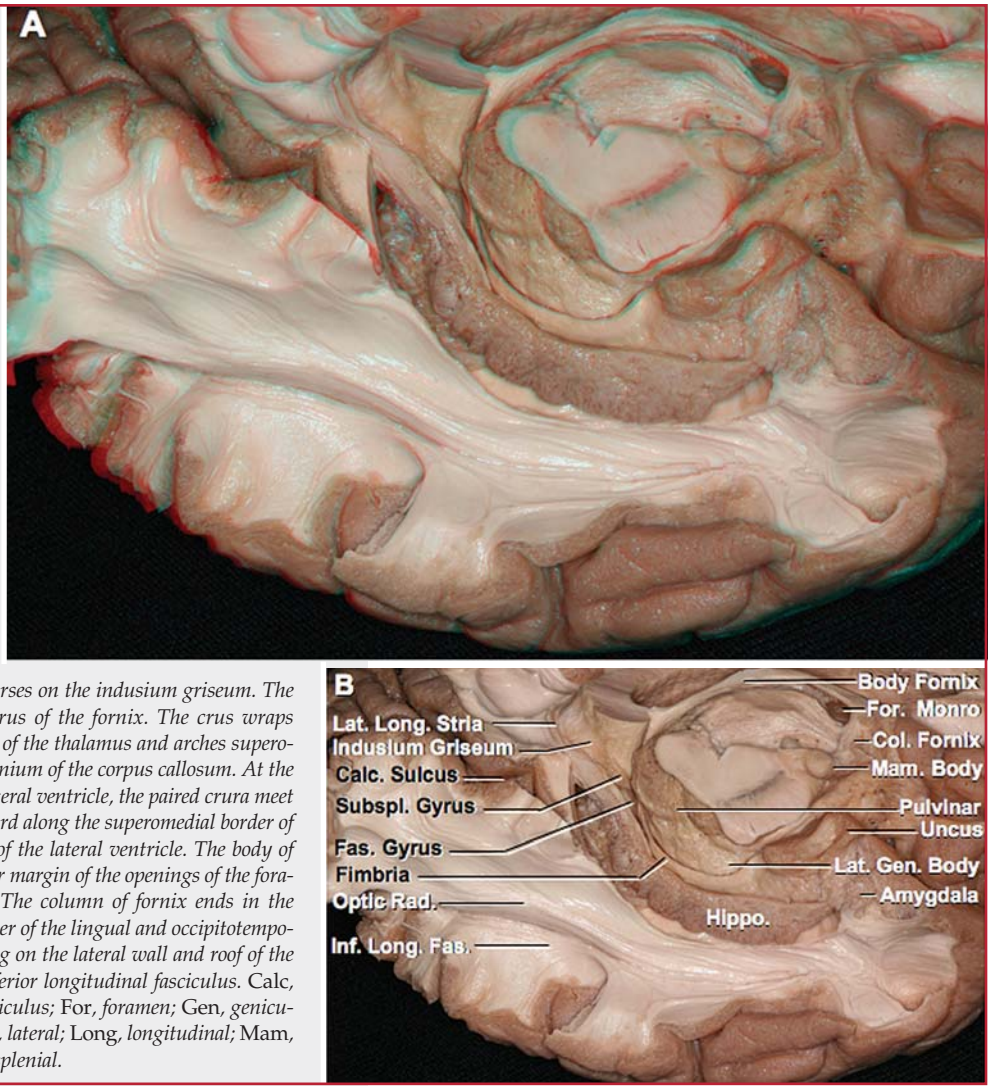

FIGURE 8. *Medial temporal lobe.* **A** *and* **B**, *3-D (*(**A**)*) and 2-D (*(**B**)*) illustrations. The 2-D illustration is labeled to facilitate understanding the same illustration in three dimensions. Fiber dissection of the left mediobasal cerebral surface. The cortical gray matter of the isthmus, and lingual, parahippocampal, and occipitotemporal gyri, have been removed. The uncus is divided into an anterior segment, which contains the amygdala, and a posterior segment, which contains the hippocampal head. The fibers of the cingulum traveling inside the isthmus and parahippocampal gyrus, and the fibers of the subiculum, have been removed to expose the most external cortical layer of the hippocampus. The fasciolar gyrus, and its continuation, the subsplenial gyrus, form part of the hippocampal tail at the subsplenial level. The subsplenial gyrus surrounds the splenium and is continued by the indusium griseum above the splenium. The indusium griseum runs along the superior surface of the corpus callosum to reach the subcallosal area. The lateral longitudinal stria courses on the indusium griseum. The fimbria passes posteriorly to become the crus of the fornix. The crus wraps around the posterior surface of the pulvinar of the thalamus and arches superomedially toward the lower surface of the splenium of the corpus callosum. At the junction of the atrium and the body of the lateral ventricle, the paired crura meet to form the body of fornix, which runs forward along the superomedial border of the thalami in the medial wall of the body of the lateral ventricle. The body of fornix splits into two columns at the anterior margin of the openings of the foramen of Monro into the lateral ventricles. The column of fornix ends in the mammillary body. Removal of the gray matter of the lingual and occipitotemporal gyri exposes the optic radiations coursing on the lateral wall and roof of the temporal horn and adjacent fibers of the inferior longitudinal fasciculus. Calc, *calcarine;* Col, *column;* Fas, *fascicular, fasciculus;* For, *foramen;* Gen, *geniculate;* Hippo, *hippocampus;* Inf, *inferior;* Lat, *lateral;* Long, *longitudinal;* Mam, *mammillary;* Rad, *radiations;* Subspl, *subsplenial.*

hemispheric side, which exposes the medial surface of the internal capsule, the subthalamic nucleus of Luys inferiorly, and the hypothalamic and septal nuclei anteriorly. The superior surface of the thalamus is crossed by two white-matter fasciculi: the stria medullaris thalami, which runs from the habenular region to the septohypothalamic region, and the fornix. A detailed dissection of the anterior column of the fornix revealed its bifurcation in a postcommissural portion directed toward the mammillary body and a precommissural portion that ends in the septal region. The mammillothalamic tract interconnects the mammillary bodies with the anterior nucleus of the thalamus (*Fig. 9, D* and *G*).

Tractographic Study

The selection of an ROI at the level of the cingulate gyrus (in the T2-weighted images) or at the level of the most medial anteroposterior fasciculus (in the color-coded maps) revealed a group of longitudinal fibers traveling between the subcallosal region and the isthmus of the cingulum (*Fig. 7, B* and *F*). The use of another ROI at the level of the parahippocampal gyrus displayed the mediotemporal fibers of the cingulum joining the supracallosal fibers; together these form the cingulum, which runs through the medial frontal, parietal, and temporal regions (*Fig. 7D*). Two ROIs, one at the level of the hippocampal body and another at the roof of the third ventricle, were selected to reconstruct the mammilohippocampal circuit, which is composed of the different portions of the fornix. As with the fiber dissection, the postcommissural fibers of the anterior column of the fornix coursing toward the mammillary body and the precommissural fibers ending at the septal region were identified (*Fig. 9F*). In addition, the relationship between the body and anterior columns of fornix and the anterior commissure was studied by selecting an additional ROI at the level of the anterior commissure (*Fig. 9E*).

Corpus Callosum

Anatomic Study

Removal of the cingulum exposes the corpus callosum from the genu and rostrum anteriorly to the splenium posteriorly. The dissection is performed in a transverse direction, following the orientation of the callosal fibers. Multiple transverse commissural fibers were observed interconnecting the precentral and parietal regions of both hemispheres (*Fig. 10*). At the level of the genu of the corpus callosum, the fibers take an anterior oblique direction, forming the forceps minor that interconnects the prefrontal and orbitofrontal regions (*Fig. 10C*). At the level of the splenium, the fibers take a posterior oblique direction, forming the forceps major, which interconnects the parieto-occipital and calcarine regions (*Fig. 10E*).

Tractographic Study

The corpus callosum is the fasciculus with the highest anisotropy (18). To reconstruct it completely, three different ROIs were selected at the level of the body, splenium, and genu of the corpus callosum, then clear images were obtained of the callosal radiations, forceps major, and forceps minor, interconnecting the regions already described by use of the fiber-dissection technique (*Fig. 10*).

Illustrative Cases

Patient 1

In a 29-year-old man, mild faciobrachial hemiparesis and moderate faciobrachial hemihypoesthesia resulted in the diagnosis of an intrinsic frontoparietal tumor. Preoperative DTI with selection of an ROI at the right cerebral peduncle depicted marked anteromedial displacement of the right pyramidal tract. The DTI aided in localizing the lesion at the postcentral gyrus and in planning surgical access. Total macroscopic resection without additional motor deficit was achieved. The definitive diagnosis was World Health Organization Grade IV glioblastoma. One month after surgery, the patient's motor deficit resolved, and DTI showed that the right pyramidal tract had returned to its normal position (*Fig. 11, A* and *B*). Three months after surgery, the patient's sensorial deficit resolved; 12 months after surgery, MRI showed no recurrence.

Patient 2

In a 9-year-old boy with moderate hemiparesis secondary to a thalamic pilocytic astrocytoma, a stereotactic biopsy through a coronal burr hole resulted in an unexpected worsening of motor function. Postbiopsy DTI revealed deformation and anterior displacement of the posterior limb of the right internal capsule and a small disruption of fibers at its upper level, presumably secondary to the stereotactic procedure. DTI helped to display the postbiopsy deficit. Subtotal resection was achieved using a transtemporal approach. The motor deficit markedly improved 1 month after surgery, and postoperative DTI revealed normalization in the shape of the corticospinal tract (*Fig. 11, C–E*).

Patient 3

A 47-year-old man presented with disorientation, confusion, emotional disturbance, and left hemiparesis. Anatomic MRI revealed an intrinsic tumoral lesion affecting the insular and basal ganglia regions and the anterior medial temporal lobe. DTI and tractographic reconstruction revealed partial disruption of the internal and external capsules with medial displacement of the internal capsule and lateral displacement of the external capsule (*Fig. 11F*). Thus, the lesion was located medial to the external capsule, thereby compromising the basal ganglia and amygdala. Stereotactic biopsy was performed that permitted the diagnosis of anaplastic astrocytoma. Radiotherapy and chemotherapy treatments were started. The patient experienced a progressive neurological deterioration and died 6 months later.

Patient 4

A 38-year-old woman experiencing severe, chronic, and treatment-refractory obsessive-compulsive disorder underwent bilateral anterior capsulotomy performed with thermocoagulation. One month after surgery, DTI revealed bilateral disruption of the anterior limb of the internal capsule (*Fig. 11G*). Significant reduction in her obsessive-compulsive disorder symptoms was noted, and 1 year after surgery, her score on the Yale-Brown Obsessive-Compulsive Scale decreased from 33 to 19. No surgery-related side effects were reported, although global functioning did not return to normal after surgery.

DISCUSSION

In this study, we expose the complex architecture of the white matter of the brain using the fiber-dissection technique and DTI-based tractography. Several articles regarding the anatomy of the white matter have been published in recent years (21, 43, 44, 68, 107, 113, 117, 120, 137–139). Some of these articles offered a general overview of the anatomy of the white matter tracts (113, 138), and others provided a detailed study of a particular anatomic region including the insular region (137), the medial hemispheric surface (139), the frontotemporal region (44, 68, 107), and the temporo-occipital region (21, 43, 117, 120). None of these works used DTI-based tractography to complement the anatomic investigations, and only one (117) used three-dimensional reconstruction of the anatomic images to improve understanding of the spatial arrangement of white fiber tracts. On the other hand, numerous recent publications on DTI-based tractography have reported examinations of the white matter anatomy in general (18, 74, 75, 81, 89, 108), and in specific tracts (19, 20, 76, 77, 80). Most have validated their results by comparing them to classical anatomic descriptions rather than contemporary fiber dissections (24, 26, 95).

Comparison between the Fiber-dissection Technique and DTI-based Tractography

The main goal of both techniques is the same, namely, to expose the anatomy of the white fiber tracts. However, the means are different. The fiber-dissection technique requires a good anatomic specimen, appropriate preparation (including the freezing process), a surgical microscope, and many hours of careful study in the microsurgical laboratory. At the beginning, results might not be completely satisfactory, but meticulous practice leads to beautiful dissections. Inevitably, the last consequence of this manual and intellectual exercise is the acquisition of a unique three-dimensional anatomic knowledge of the white matter of the brain.

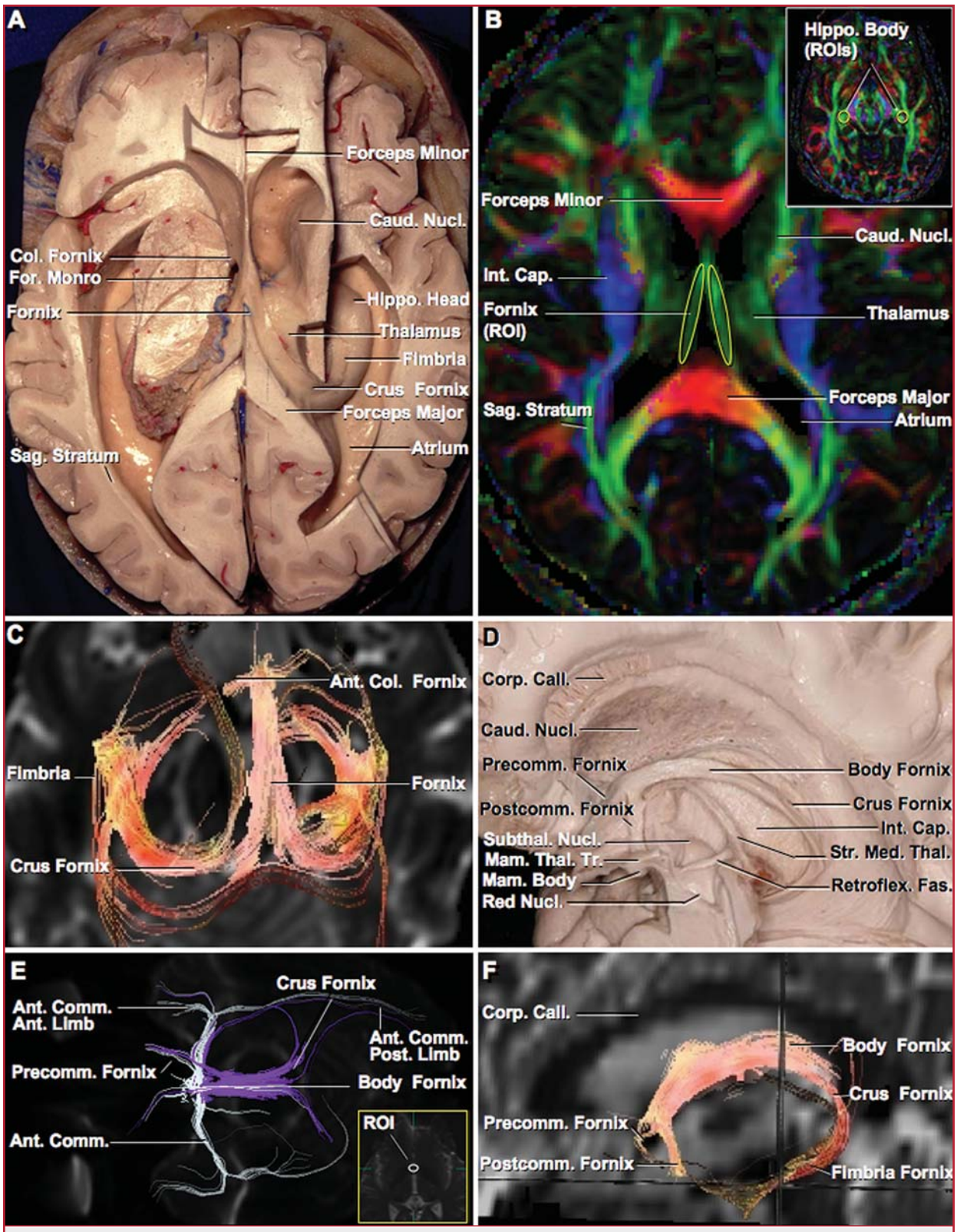

FIGURE 9. *Fornix.* **A**, *successive transverse and horizontal cuts have been made to expose the lateral ventricles. The initial part of the fornix, the fimbria, arises in the floor of the temporal horn on the ventricular surface of the hippocampal formation and passes posteriorly to become the crus of the fornix. The crus wraps around the posterior surface of the pulvinar of the thalamus and arches superomedial toward the lower surface of the splenium of the corpus callosum. At the junction of the atrium and the body of the lateral ventricle, the paired crura meet to form the body of fornix, which runs forward along the superomedial border of the thalami in the* (Continues)

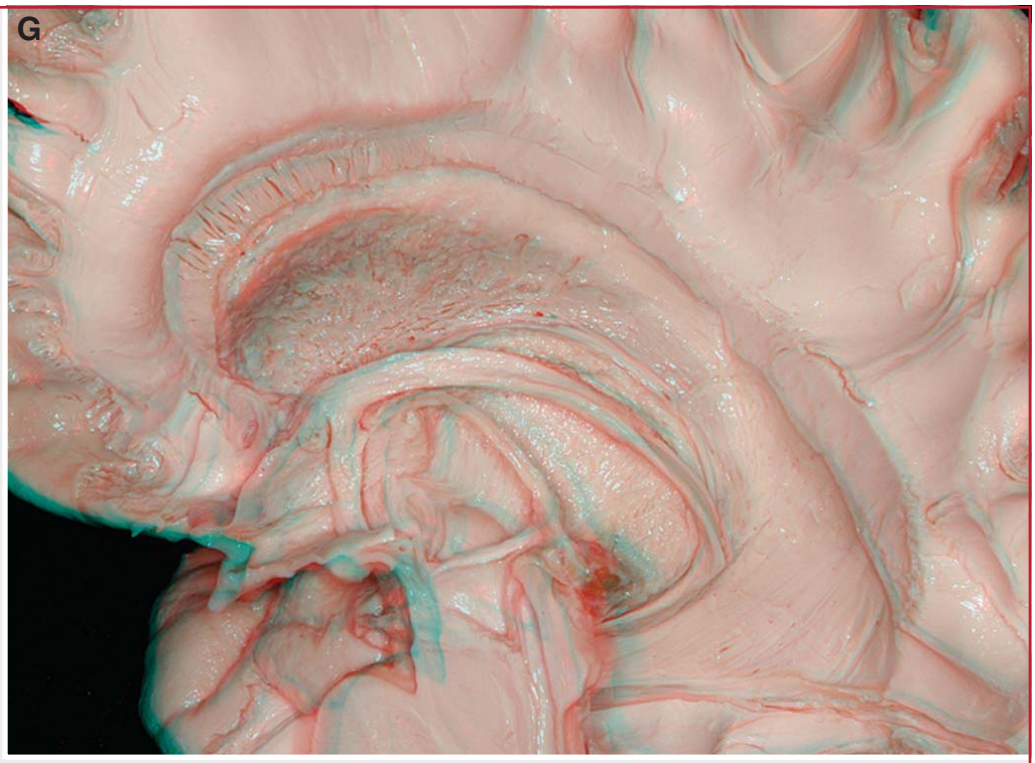

FIGURE 9. *(Continued) medial wall of the body of the lateral ventricle. The body forms a gentle arch located between the roof of the third ventricle and the floor of the body of each lateral ventricle. The body of fornix splits into two columns to form the anterior margin of the openings of the foramen of Monro into the lateral ventricles.* **B**, *color-coded DTI map of an axial plane at the level of the fornix to be correlated with* **A**. *Several white matter tracts are identified by virtue of their anatomic location and color-coded orientation. The fornix is a tract with longitudinal orientation* (green), *which courses on the roof of the third ventricle under the body of the corpus callosum. An ROI* (yellow) *is selected at each fornix for tractographic reconstruction (*C, E, *and* F*). The forceps minor and major of the corpus callosum are formed by lateromedial commissural fibers* (red), *the sagittal stratum have a partially oblique but predominantly antero-posterior orientation* (green), *and the internal capsule at this level has a predominant vertical orientation* (blue). *The* inset *shows a color-coded DTI axial map at the level of the cerebral peduncles used for the selection of additional ROIs* (yellow) *to complete the reconstruction of the fornix; the fimbria is identified as an anteroposterior tract* (green) *situated lateral to the posterior third of the cerebral peduncle* (yellow circles). **C**, *bilateral tractographic reconstruction of the fornix, axial view. The fornices travel from the hippocampal formation to the mammillary bodies and septal region and form the so-called internal limbic circuit.* **D**, *the thalamus, which faces the medial surface of the posterior limb of the internal capsule, has been removed. Two white matter bundles cross the superior surface of the thalamus: the stria medullaris thalami, which runs from the habenular region to the septohypothalamic region, and the fornix with its different portions. The column of the fornix splits in a postcommissural portion, directed toward the mammillary body, and a precommissural portion, which ends in the septal region. The mammillothalamic tract, which interconnects the mammillary bodies with the anterior nucleus of the thalamus, has been divided above the mammillary body and removed. The subthalamic nucleus of Luys is exposed below the thalamus, at the lower margin of the internal capsule. The red nucleus is located in the mesencephalic tegmentum. The fasciculus retroflexus or habenulo-interpeduncular tract runs from the habenular ganglium to the interpeduncular nucleus.* **E**, *simultaneous tractographic reconstruction of the fornix and anterior commissure. Precommisural and postcommisural forniceal fibers* (magenta) *pass around the anterior commissure* (white), *which bifurcates in an anterior and posterior limb. The* inset *shows the location of the ROI* (white) *used for the reconstruction of the anterior commissure.* **F**, *sagittal view of tractographic reconstruction of the fornix (to be correlated with* **D**) *showing the fimbria, crus, body of fornix, and bifurcation of the anterior column in pre- and postcommissural fibers.* **G**, *3-D illustration. The 2-D illustration is labeled in* **D** *to facilitate understanding the same illustration in three dimensions.* Ant, *anterior;* Call, *callosum;* Cap, *capsule;* Caud, *caudate;* Col, *column;* Comm, *commissure;* Corp, *corpus;* Fas, *fasciculus;* For, *foramen;* Hippo, *hippocampal;* Int, *internal;* Mam, *mammillary, mammillo;* Med, *medullaris;* Nucl, *nucleus;* Postcomm, *postcommissural;* Post, *posterior;* Precomm, *precommissural;* Retroflex, *retroflexus;* ROI, *region of interest;* Sag, *sagittal;* Str, *stria;* Subthal, *subthalamic;* Thal, *thalami, thalamic;* Tr, *tract.*

DTI-based tractography, on the other hand, represents one of the most exciting radiological advances in recent decades. The possibility to not only study the intrinsic structure of the brain in vivo in several minutes, but to also observe the manner in which intracerebral lesions affect the fiber tracts, is now a reality. These studies require an MRI system that is capable of creating diffusion-tensor images and the software for three-dimensional tractographic reconstruction. The exercise of "radiologically" investigating and dissecting the interior of the normal and pathological human brain in vivo has opened a completely new perspective in the practice of the neurosurgeon.

The combination enriches both techniques reciprocally because one solves the limitations of the other. The fiber-dissection technique is limited because of the complex relationships of the fiber systems, so the demonstration of one fiber system often results in the destruction of other fiber systems (138). This destruction is avoided with the use of DTI-based tractography, which can reveal the complex relationships among the fiber systems at the same time (*Fig. 12*). On the other hand, the main limitation of tractography occurs when the axons are not oriented in a coherent fashion. In these situations, the voxel-averaged estimate of orientation cannot sum-

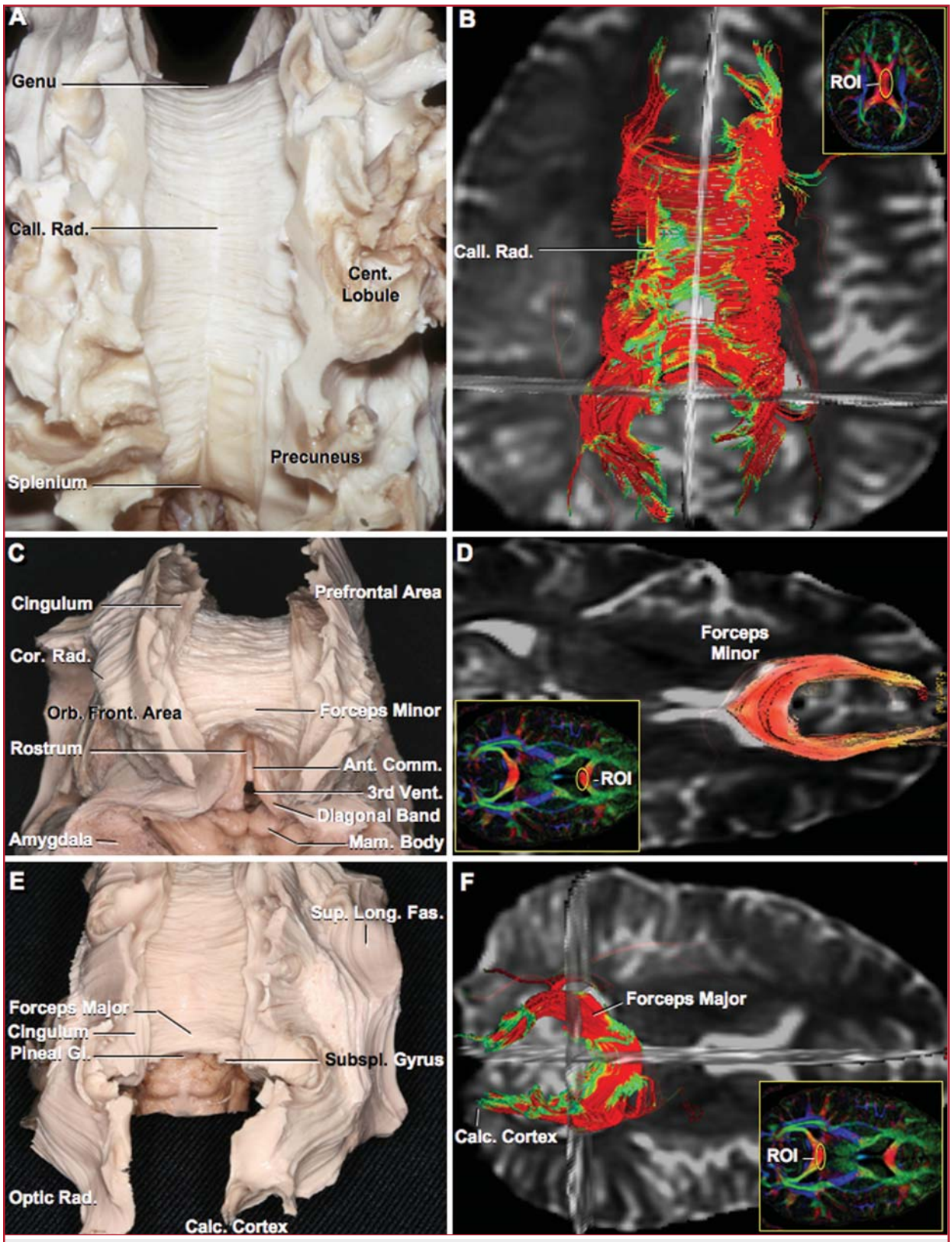

FIGURE 10. *Corpus callosum.* **A**, *superior view of both hemispheres. The left and right cingulum have been removed to expose the body of the corpus callosum. Multiple transverse commissural fibers interconnect the paracentral and parietal regions of the hemispheres.* **B**, *tractographic reconstruction of the body of the corpus callosum. The* inset *shows the color-coded DTI axial map used for the selection of the correspondent ROI* (yellow). **C**, *anterior view, fiber dissection of the genu and rostrum of the corpus callosum. (Continues)*

FIGURE 10. *(Continued) The genu contains the commissural fibers that connect the prefrontal and orbitofrontal regions to form the forceps minor. The lamina terminalis, which fills the interval between the optic chiasm and the rostrum of the corpus callosum, has been removed to expose the third ventricle. The upper part of the anterior wall of the third ventricle is hidden posterior to the rostrum of the corpus callosum. The columns of the fornix, which end in the mammillary bodies, and the anterior commissure form part of the anterior wall of the third ventricle. The diagonal band of Broca is identified coursing between the septal region and the amygdala.* **D**, *tractographic reconstruction of the forceps minor of the corpus callosum. The* inset *shows the color-coded DTI axial map used for the selection of the correspondent ROI* (yellow). **E**, *posterior view, fiber dissection of the splenium of the corpus callosum. The splenium contains the commissural fibers that connect the parieto-occipital and calcarine regions to form the forceps major, which courses under the cingulum.* **F**, *tractographic reconstruction of the forceps major of the corpus callosum, formed by the commissural fibers passing through the splenium and interconnecting the parieto-occipital and calcarine regions. The* inset *shows the color-coded DTI axial map used for the selection of the correspondent ROI* (yellow). Ant, *anterior;* Calc, *calcarine;* Call, *callosal;* Cent, *central;* Comm, *commissure;* Cor, *corona;* Fas, *fasciculus;* Front, *frontal;* Gl, *gland;* Long, *longitudinal;* Mam, *mammillary;* Orb, *orbito;* Rad, *radiata, radiations;* ROI, *region of interest;* Subspl, *subsplenial;* Sup, *superior;* Vent, *ventricle.*

marize the orientation of the underlying fibers accurately (18), and it, thus, introduces continuity between the fibers where there is none (118). Avoiding this problem requires the development of new techniques to analyze voxels containing multi-oriented fiber populations (50) and obtain an accurate knowledge of the anatomy of the fiber systems acquired by means of the fiber-dissection technique. A source of variability and inaccuracy in tractographic studies is manual selection of the seed points. In addition, small changes in the ROI placement can significantly affect the reconstructed fiber bundles. For example, during selection of an ROI at the deep white matter of the middle frontal gyrus for reconstructing the frontoparietal segment of the superior longitudinal fasciculus, a small medial displacement of the ROI will also reconstruct part of the dorsal external capsule. Similarly, at the uncinate fasciculus, a slight posterior displacement of the ROI will also reconstruct the entire ventral external capsule, formed by the inferior occipitofrontal fasciculus, and even part of the dorsal external capsule (*Fig. 5B*). As a consequence, a precise understanding of the three-dimensional anatomy of the white tracts on the basis of fiber dissections increases the accuracy of the seed-point selection process. Therefore, we think the combination of both techniques should be used not only in neurosurgical training and operative planning, but also as alternative and complementary methods of neuroanatomic research.

Finally, both techniques share a common problem. The extraordinarily complex intracerebral organization, integrated by thousands of millions of micrometric axons circulating in the three spatial planes, makes it impossible for either technique to reach the neuroanatomic precision of the histological techniques, especially the autoradiographic technique. The main limitation of the latter is that it can be used only in experimental animals (118). Thus, the fiber-dissection technique and tractography reveal the macroscopic and topographic anatomy of the main stem of the fiber tracts, but not the precise origin and termination of the fibers that compose each fasciculus. Although the former is important for neurosurgical practice (113, 148, 149), the latter is essential for complete knowledge of brain anatomy and function (86, 111).

Anatomofunctional Correlation of the White Matter Tracts

Since Paul Broca's studies, specialization of cortical regions in specific functions has become well established. The neurosurgeon has available a well-developed map of the functions of multiple cortical areas that, although not constant, bears only limited variability. However, the functional significance of the various white matter pathways, and especially the associative tracts, is largely unknown. The combination of the topographical anatomy of the human cerebral tracts (acquired by means of the fiber-dissection technique, DTI-based tractography, and extrapolation of experimental studies in nonhuman primates) and the data obtained from clinical observation and radiological diagnosis of human white matter lesions, and especially from intraoperative subcortical electric-stimulation studies, can establish the possible functional relevance of the white matter tracts (*Tables 2* and *3*).

Superior Longitudinal Association System

This fiber system provides the interconnection of distant functional cortical areas such as the motor, somatosensory, associative, auditory, and visual areas. We postulate that the superior longitudinal association system is a high-order multisensory associative system that coordinates different inputs as required in higher human brain functions, such as spatial awareness in the nondominant hemisphere and language in the dominant hemisphere (*Fig. 3, E* and *F*).

In this study, we describe the segmentation of the superior longitudinal fasciculus, which was recently reported in two DTI studies (20, 80) but has not been reported in a human fiber-dissection study. Several investigations of nonhuman primates (103, 106, 118) revealed a pattern of segmentation in the superior longitudinal fasciculus that is partially different from the human segmentation described in this study. The main difference is that the detailed experimental studies in nonhuman primates revealed three different frontoparietal pathways, whereas our study described only one.

The frontoparietal segment of the superior longitudinal fasciculus interconnects the prefrontal region with the inferior parietal lobule. The latter is a high-order association cortex involved in the integration of inputs from multiple modalities, which plays a major role in spatial function in the nondominant hemisphere (9, 20, 84). The nondominant prefrontal region has an important role in the regulation of visual attention within different parts of space (104). Thus, the nondominant frontoparietal segment may serve as the conduit that subserves visuospatial awareness (118). This assertion is in

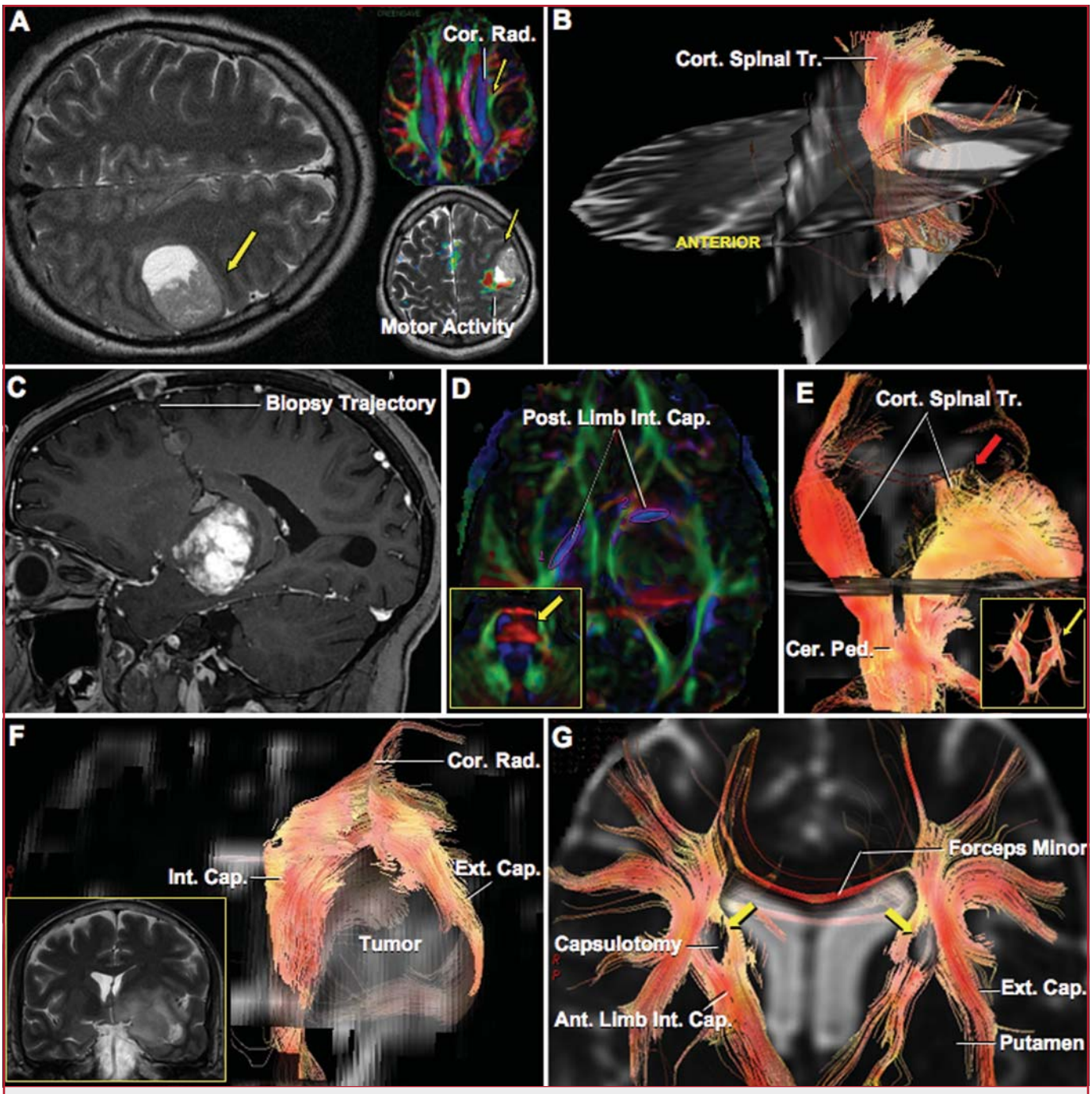

FIGURE 11. *Illustrative cases.* **A** *and* **B**, *Patient 1.* **A**, *axial T2-weighted MRI scan showing a frontoparietal intrinsic tumor suggestive of a high-grade glioma in a patient with faciobrachial hemiparesis and hemihypoesthesia. The lesion is located into the postcentral gyrus, with anterior displacement of the precentral gyrus (*yellow arrow*). However, the functional MRI study shows motor activation medial and posterior to the lesion (*inset at right lower corner*).* Inset at right upper corner *shows the preoperative DTI color-coded map displaying the medial displacement of the corona radiata (*blue*).* **B**, *tractographic reconstruction of the corticospinal tract after selection of an ROI at the level of the cerebral peduncle. The corticospinal tract is displaced anteriorly and medially. In this case, tractography solved the controversy between anatomic and functional MRI and aided in planning the surgical strategy.* **C**, **D**, *and* **E**, *Patient 2.* **C**, *sagittal T1-weighted MRI scan showing a thalamic tumor compatible with a pilocytic astrocytoma and the trajectory of the stereotactic biopsy, which resulted in unexpected motor worsening.* **D**, *postbiopsy DTI color-coded map revealing a marked anterior displacement of the posterior limb of the right internal capsule (*blue*). An ROI at the level of the posterior limb of the internal capsule on both sides has been selected for the tractographic reconstruction. The* inset *shows a DTI color-coded map at the level of the pons. The blue signal correspondent to the right corticospinal tract (*yellow arrow*) is reduced in size in comparison to the left corticospinal tract, in relation with the compression of the corticospinal tract at the level of the internal capsule.* **E**, *tractographic reconstruction showing an important deformation and anterior displacement of the right corticospinal tract at the level of the internal capsule. A small disruption of fibers at its upper level, presumably secondary to the stereotactic procedure, is also displayed (*red arrow*). DTI helped in understanding the postbiopsy deficit and planning the surgical approach. The* inset *contains (Continues)*

FIGURE 11. *(Continued) a postoperative tractographic reconstruction showing the normalization in the shape of the right corticospinal tract* (yellow arrow)*, which accompanies the clinical improvement obtained after surgery.* **F**, *Patient 3. Coronal T1-weighted MRI scan showing an intrinsic tumoral lesion affecting the insular and basal ganglia region and the anterior medial temporal lobe* (inset, left lower corner)*. Tractographic reconstruction showed partial disruption in the internal and external capsules, with medial displacement of the internal capsule and lateral displacement of the external capsule. Tractography aided in localizing the lesion and in deciding the treatment.* **G**, *Patient 4. Postoperative tractographic reconstruction showing bilateral disruption of the anterior limb of the internal capsule* (yellow arrows) *secondary to bilateral anterior capsulotomy performed with thermocoagulation.* Ant, *anterior;* Cap, *capsule;* Cer, *cerebral;* Cor, *corona;* Cort, *cortico;* Ext, *external;* Int, *internal;* Ped, *peduncle;* Post, *posterior;* Rad, *radiata;* Tr, *tract.*

TABLE 2. Classification of the white matter fasciculi according to predominant fiber type and interconnected regions

Type of fasciculus	Name	Interconnected regions
Association	Superior longitudinal fasciculus	Lateral frontoparietotemporal
	Inferior longitudinal fasciculus	Temporo-occipital
	Uncinate fasciculus	Fronto-orbital/temporomesial
	Inferior occipitofrontal fasciculus (ventral extreme-external capsule)	Frontotemporal-(?) occipital
	Cingulum	Medial frontoparietotemporal
Projection	Internal capsule	Corticopontospinal and thalamocortical
	Sagittal stratum	Thalamotemporoparieto-occipital
	Dorsal external capsule	Claustrocortical
Commissural	Anterior commissure	Inferotemporal and occipital bilateral
	Corpus callosum—body, forceps major and minor	Frontoparietotemporo-occipital bilateral

TABLE 3. Potential functional role of different fasciculi and associated disconnection syndromes

Fasciculus	Functional role	Disconnection syndrome
Superior longitudinal fasciculus	Nondominant: spatial awareness Dominant: language	
Frontoparietal segment	Visuospatial processing Dorsal phonological pathway (motor language)	Left spatial hemineglect Phonological apraxia
Temporoparietal segment	Audiospatial processing Sensitive language (auditory comprehension)	Vestibular symptoms Sensitive aphasia
Frontotemporal or arcuate segment	Visu-audiospatial (?) Repetition	Vestibular symptoms (?) Conductive aphasia
Inferior longitudinal fasciculus	Object identification, discrimination, and recognition	Visual agnosia, prosopagnosia (bilateral)
Uncinate fasciculus	Ventral limbic pathway	Behavioral disturbances (?)
Inferior occipitofrontal fasciculus (ventral extreme-external capsule)	Ventral semantic pathway	Conductive aphasia
Cingulate fasciculus	Dorsal limbic pathway	Behavioral disturbances (?)
Claustrocortical system (dorsal external capsule)	Integration of visual, somatosensory, and motor information	Unilateral: absent cortical somatosensory evoked potentials Bilateral: severe encephalopathy
Internal capsule	Genu and posterior limb—motor/sensation Anterior limb—behavior	Motor/sensory deficits Behavioral syndromes
Sagittal stratum	Visual processing	Visual field defects
Anterior commissure	Complementary visual processing (?)	None (?)
Corpus callosum	Contralateral control	Unilateral tactile anomia Left hemialexia Unilateral apraxia Transitory mutism

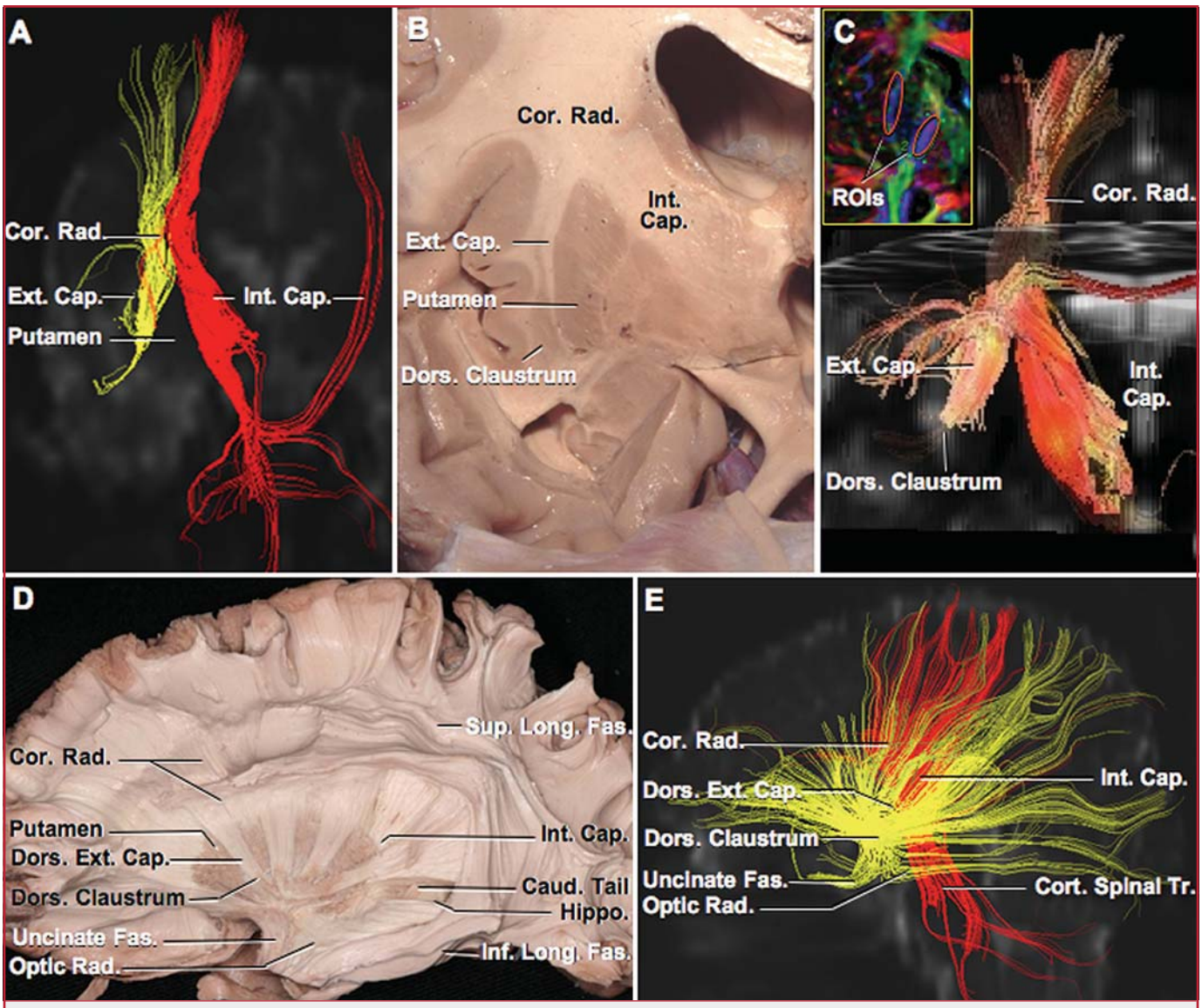

FIGURE 12. *Anatomicoradiological correlations between the tractographic and fiber-dissection studies of the external and internal capsules.* **A**, *coronal view of DTI-based tractography obtained with two ROIs, one at the external capsule, and the other at the posterior limb of the internal capsule. The* yellow tract *corresponds to the external capsule, and the* red tract *to the internal capsule. The putamen is located below and between where the fibers converge. The fibers of the external capsule join the fibers of the internal capsule at the superior edge of the putamen to form together the corona radiata. The fibers of the external and internal capsule do not join at the lower edge of the putamen.* **B**, *coronal section of the right hemisphere 5 mm behind the anterior commissure. As shown with the tractography* (Fig. 10A), *the external capsule joins the internal capsule at the superior edge of the putamen to form the corona radiata. The external capsule is wider at the superior edge of the claustrum, and narrows as it descends along the medial edge of the claustrum leaving only a thin layer of fibers at the inferior edge of the putamen.* **C**, *coronal view of a different tractographic study of the external and internal capsules. The fibers of the dorsal external capsule converge in the dorsal claustrum, the presumed site of the gray matter and nerve cells giving rise to the fibers. The* inset *shows the color-coded DTI axial map used for the selection of the correspondent ROIs* (orange) *at the level of the external and internal capsules.* **D**, *fiber dissection of the left hemisphere. The dorsal external capsule has been partially removed to expose the relationship between the dorsal claustrum and external capsule, the putamen, and the corona radiata. The internal capsule is situated deep to the putamen. The superior longitudinal fasciculus is situated above the external capsule and lateral to the corona radiata. The optic radiations, which form part of the sagittal stratum, have been exposed in the sublenticular and retrolenticular portion of the internal capsule. A small window has been opened in the sagittal stratum to expose the lateral ventricle at the level of the confluence between the temporal horn and atrium. The choroid plexus has been removed to expose the posterior part of the body of hippocampus in the floor of the ventricle, and the tail of the caudate nucleus in the roof. The inferior longitudinal fasciculus, which runs from the anterobasal temporal region to the occipital lobe, has been exposed deep to the inferotemporal and temporo-occipital gyrus. The uncinate (Continues)*

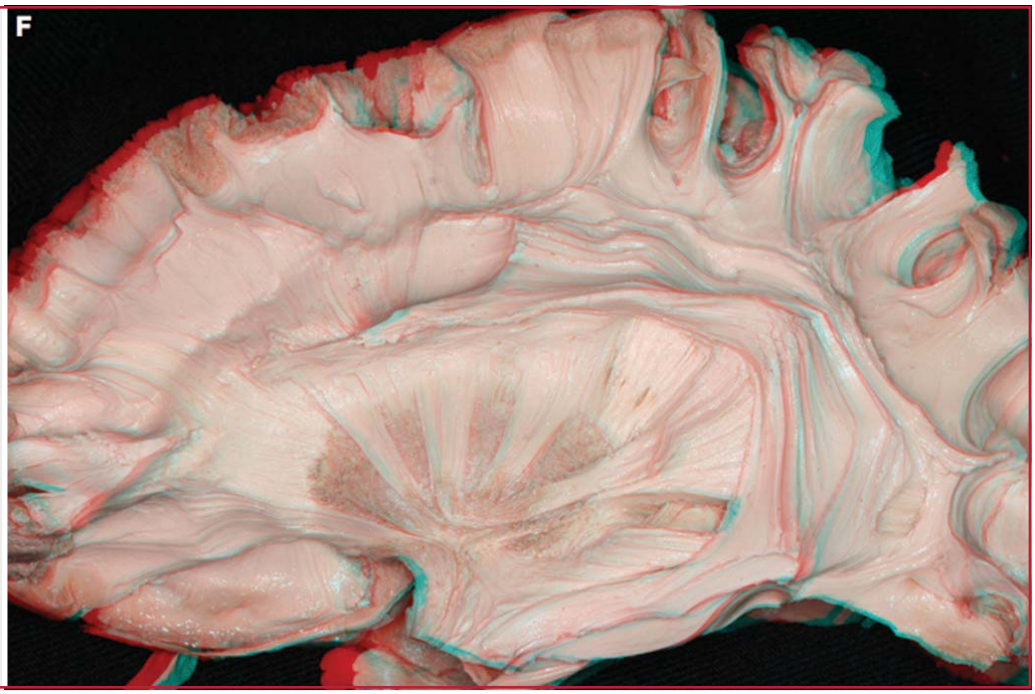

FIGURE 12. *(Continued) fasciculus has been cut at the level of the anterior margin of the amygdala.* **E**, *left sagittal view of the tractrographic study shown in* **A**. *Anatomicoradiological correlation with* **D**. *Tractography permits the visualization of the internal and external capsules, at different depths.* **F**, *3-D illustration. The 2-D illustration is labeled in* **E** *to facilitate understanding the same illustration in three dimensions.* Cap, *capsule;* Caud, *caudate;* Cor, *corona;* Cort, *cortico;* Dors, *dorsal;* Ext, *external;* Fas, *fasciculus;* Hippo, *hippocampus;* Inf, *inferior;* Int, *internal;* Long, *longitudinal;* Rad, *radiata, radiations;* ROI, *region of interest;* Sup, *superior;* Tr, *tract.*

agreement with clinical observations of patients with symptoms of left spatial hemineglect caused by injury in the nondominant supramarginal gyrus (rostral inferior parietal lobule) or underlying frontoparietal white matter (3, 29). Interestingly, the spatial hemineglect caused by subcortical lesions results in more enduring and generalized dysfunction and is more severe than that associated with cortical lesions (29). Even more eloquent is the recent article by Thiebaut de Schotten et al. (134), wherein they reported bisection of straight lines (the clinical test of spatial hemineglect) during direct intraoperative cortical and subcortical stimulation. They observed that greater dysfunction in the bisection test was elicited by stimulation of the white matter located deep to the nondominant inferior parietal lobule. However, as the authors later recognized (P. Bartolomeo, personal communication, 2006), they incorrectly concluded that the fasciculus responsible for the symptoms was the superior occipitofrontal fasciculus (which is known to be related with the medial parieto-occipital region and not with the inferior parietal lobule [118]) instead of the frontoparietal segment of the superior longitudinal fasciculus, as demonstrated in our study. Thus, the more severe effect of subcortical inactivation on spatial function in comparison with cortical inactivation offers direct evidence of the existence of a neuronal network related to the spatial awareness anatomically represented by the frontoparietal segment of the superior longitudinal fasciculus.

The temporoparietal segment of the superior longitudinal fasciculus interconnects the inferior parietal lobule with the superior temporal gyrus. The latter has been related to the processing of auditory information. Thus, the nondominant temporoparietal (indirect pathway) and the arcuate (frontotemporal, direct pathway) segments of the superior longitudinal fasciculus may process audiospatial and audiovisuospatial information, respectively (118). Interestingly, Kahane et al. (61) and Spena et al. (121) elicited vestibular symptoms (nystagmus, vertigo) after intraoperative direct stimulation of the temporoparietal perisylvian white matter in the nondominant hemisphere. In summary, the nondominant superior longitudinal association system may serve spatial awareness by integrating the visuospatial information from the indirect frontoparietal pathway with the audiospatial information from the temporoparietal pathway.

In the dominant hemisphere, the inferior parietal lobule is involved in the integration of inputs from multiple modalities, which plays a major role in language function (20). The dominant prefrontal cortex and frontal operculum (Broca's territory) are related to the motor aspect of language, and the dominant frontoparietal segment of the superior longitudinal association system may be involved in the vocalization of semantic content (20). In this line, the clinical syndromes of ideomotor and buccofacial apraxia result from lesions of the rostral inferior parietal lobule or underlying white matter and from the premotor cortices in the frontal lobe (66, 118). In addition, direct intraoperative stimulation of the white matter located between the frontal operculum and inferior parietal lobule elicited phonological apraxia (38). Thus, Duffau et al. (38) have designated this pathway as the dorsal phonological pathway, which is the anatomic equivalent to the frontoparietal segment of the dominant superior longitudinal association system.

The dominant posterosuperior temporal sulcus and gyrus, also known as Wernicke's territory, are related to the auditory comprehension of language. The temporoparietal segment of

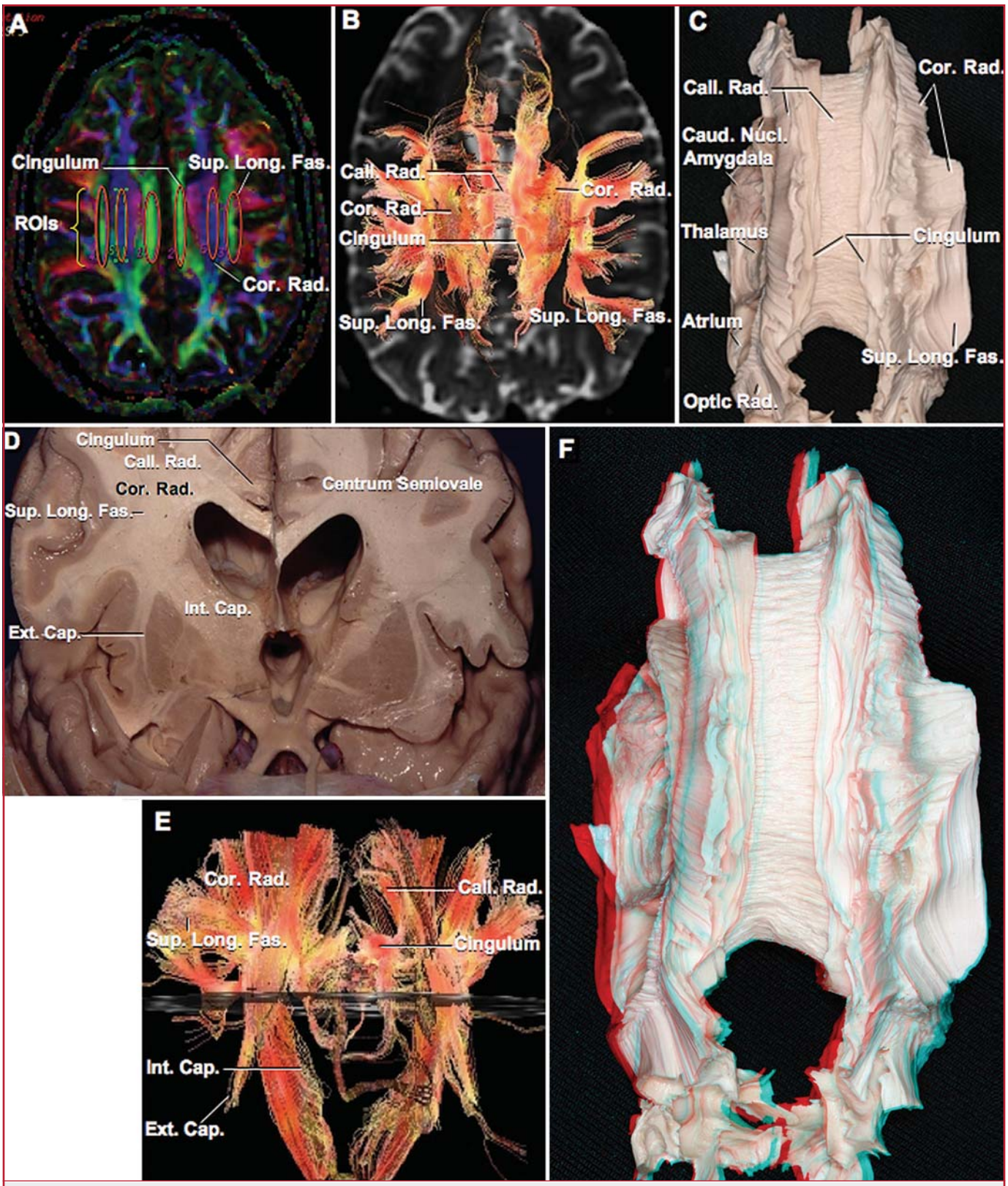

FIGURE 13. *Centrum semiovale.* **A**, *color-coded DTI axial map at the level of the centrum semiovale, which is defined as the common central mass of white matter with an oval appearance in horizontal sections of the brain. From lateral to medial, the superior longitudinal fasciculus (anteroposterior orientation,* green*), corona radiata (craniocaudal orientation,* blue*), and cingulum (anteroposterior orientation,* green*), are displayed. The different ROIs* (orange) *selected for the tractographic reconstruction of the centrum semiovale are shown.* **B**, *tractographic reconstruction of the superior longitudinal fasciculus (horizontal or frontoparietal segment) laterally, the cingulum medially, and the corona* (Continues)

FIGURE 13. (*Continued) radiata between the superior longitudinal fasciculus and cingulum. Some commissural callosal fibers are shown crossing under the cingulum and radiating between the cingulum and the corona radiata. All these fasciculi form the complex white matter structure of the centrum semiovale.* **C**, *superior view, fiber dissection of the centrum semiovale. The fibers of the corpus callosum cross to the opposite hemisphere under the cingulum. The superior longitudinal fasciculus forms the most lateral part of the centrum semiovale. The corona radiata is situated between the cingulum and superior longitudinal fasciculus, and is intermingled with the callosal radiations. The corona radiata and superior longitudinal fasciculus have been removed on the left side to expose the lateral ventricle, the caudate nucleus, and the thalamus.* **D**, *coronal section at the level of the foramen of Monro on the right side, and at the level of the anterior commissure in the left side. The white matter extends from the cortex to the basal ganglia and ventricular system. The common central mass of white matter with an oval appearance in horizontal sections of the brain is termed the* centrum semiovale. *It is located above the lateral ventricles and is formed by the superior longitudinal fasciculus, corona radiata, cingulum, and callosal fibers.* **E**, *coronal view of the tractographic reconstruction shown in* **B**. *The corona radiata is formed by the internal and external capsule fibers. Correlation with the anatomic specimen shown in* **D**. **F**, *3-D illustration. The 2-D illustration is labeled in* **C** *to facilitate understanding the same illustration in three dimensions.* Call, *callosal;* Cap, *capsule;* Caud, *caudate;* Cor, *corona;* Ext, *external;* Fas, *fasciculus;* Int, *internal;* Long, *longitudinal;* Nucl, *nucleus;* Rad, *radiata, radiations;* ROIs, *regions of interest;* Sup, *superior.*

the superior longitudinal association system may be involved in the auditory comprehension of semantic content (20), and lesions in it may cause impaired comprehension or Wernicke's aphasia. The direct or frontotemporal (arcuate) segment of the superior longitudinal association system has been involved in phonological function such as repetition. It is generally accepted that the disruption of the arcuate fasciculus (or segment) causes transcortical or conductive aphasia, characterized by paraphasic errors and repetition disorders (151). However, several connectional studies in experimental animals concluded that the arcuate fasciculus is not related to language (105, 118). To solve this controversy, human intraoperative direct stimulation of the white matter deep to Broca's territory, supramarginal gyrus (rostral inferior parietal lobule), and Wernicke's territory elicited phonemic paraphasias and repetition disorders caused by inactivation of the arcuate or frontotemporal segment of the superior longitudinal association system (37). A recent study in which the arcuate fasciculus was visualized by tractography (after the ROIs were selected with functional MRI and magnetoencephalography) demonstrated the close relationship between language and the arcuate fasciculus (63). The discrepancy between animal and the human experimental studies suggests that extrapolation of neuroanatomic data from experimental animals should be undertaken carefully, especially when the study concerns specific human brain functions such as language and overdeveloped human brain regions such as the inferior parietal lobule or the prefrontal region.

Thus, each segment of the dominant superior longitudinal association system may be related with a specific disorder: the frontoparietal segment with nonfluent aphasia, the temporoparietal segment with comprehension aphasia, and the frontotemporal or arcuate segments with conductive aphasia. The frequent combination of white matter lesions, particularly combinations of indirect and direct segment lesions, would produce a combination of aphasic disorders.

Inferior Longitudinal Association System

Both fiber-dissection and tractographic studies reveal a group of temporo-occipital fibers that comprise the inferior longitudinal fasciculus, which has a close anatomic relationship with the optic radiations. Interestingly, a recent tractographic study reveals that the inferior longitudinal fasciculus connects the prestriate occipital cortex with the medial temporal structures (hippocampus, parahippocampal gyrus, and amygdala) (19), and by virtue of the microscopic connectional details of the inferior longitudinal fasciculus provided by experimental material obtained in monkeys, this fasciculus has been related to object identification, discrimination, and recognition (118). Supporting these ideas, Geschwind (53) related visual agnosia with damage not only to the occipitotemporal association cortices but also to the underlying white matter, and Damasio et al. (25) discussed prosopagnosia (loss of the ability to recognize faces) as secondary to bilateral lesion of the fusiform gyrus and underlying fiber system.

Claustrocortical Integration System

In this study, we demonstrate that the dorsal (posterosuperior) external capsule in humans is mainly composed of claustrocortical fibers (cortical fibers merging into the dorsal claustrum), as we have recently described (48), and as it has been described in experimental animal studies (16, 31–34, 67, 92–94, 102, 118). Although their work dates from more than a century ago, Dejerine (26) and Trolard (136) stated that the external capsule in humans contains fibers from the claustrum. Recent studies of the white fiber tracts via the fiber-dissection technique (107, 120, 137, 138) or DTI-based tractography (18, 20, 74, 75, 81, 89, 108, 142) have neglected this important fact, as have current neuroanatomic texts (17, 95, 127, 151). In addition, our tractographic studies suggest a topographical organization in the dorsal claustrum and external capsule, where posterior cortical areas connect with the posterior part of the dorsal claustrum, and more anterior cortical areas converge in the anterior part, as we recently reported (48), and as suggested in humans by Morys et al. (90) and demonstrated in experimental animal studies by Pearson et al. (102).

Although the claustrocortical system in mammals has been related to the integration of visual, somatosensory, and motor information (102), its functional significance in the human brain is unknown (45, 127, 148). Recently, Francis Crick, who devoted more than 20 years to the problem of consciousness (128), suggested that the claustrum is critical in integrating information in the fast timescale, as is essential for consciousness (23). Supporting Crick's hypothesis, a positron-emission

tomography study (55) revealed involvement of the claustrum in cross-model matching, in tasks that require the simultaneous evaluation of information from more than one sensory domain (visuotactile, audiovisual, and so on), and a functional MRI study (14) detected claustral activation specifically during unimodal phases of the bimodal–unimodal contrasts. In this study, given the anatomic separation and lack of direct connections between the auditory and visual cortices, and the absence of any additional contribution from a possible intersensory region during the bimodal condition, the question arose as to how the auditory and visual signals were combined (14). Ettlinger and Wilson (47) suggested a system whereby the senses could access one another directly via an interconnecting structure such as the claustrum. In this study, we show the anatomic and radiological characteristics of what we describe as the claustrocortical integration system.

Concerning the clinical repercussions of claustral lesions, Moryś et al. (91) reported that in all of the patients in their study with unilateral vascular lesions of the dorsal claustrum, the cortical somatosensory evoked potentials were absent contralaterally to the side of the lesion and ipsilaterally to the stimulated nerve. On the contrary, Duffau et al. (41) reported the absence of permanent sensorimotor or cognitive disorders after unilateral resection of the claustrum in patients with insular glioma, thus demonstrating that its functional role can be compensated after unilateral lesions, and supporting a connectionist view of the claustrum as part of a large-scale network rather than as an essential epicenter. On the other hand, selective bilateral lesions of the claustrum and external capsule have been associated with herpes simplex encephalitis (69), sugihiratake (angel's wings) mushroom ingestion (99), and unknown cause (123). Patients in all of the reported cases developed severe encephalopathy with disturbance of consciousness, seizures, and psychotic symptoms. The reversibility of both neurological symptoms and radiological signs in one patient indicated a close association of epilepsy, behavior, and the claustrocortical system (123).

Uncinate Fasciculus

This fasciculus interconnects the anterotemporal lobe with the orbitofrontal area. The anterotemporal lobe is involved in processing modality-specific information, as auditory (rostral superotemporal gyrus), visual (rostral inferotemporal region), somatosensory and gustatory (rostral insular opercular cortex), mnemonic (parahippocampal gyrus), and emotional information (amygdala) (118). The orbitofrontal area is implicated in the regulation of behaviors and emotions (118), decision making (6), and self regulation (129). The uncinate fasciculus acts as a link between emotion and cognition and is conceived by Schmahmann and Pandya (118) as the ventral limbic pathway, in contraposition to the cingulum or dorsal limbic pathway.

Clinically, the implication of the uncinate fasciculus in neuropsychiatric disorders such as schizophrenia is being extensively investigated with DTI technology to assess its morphometry, although definitive results are not yet available (71, 72). On the other hand, disruption of the uncinate fasciculus during anteromedial temporal lobectomy or transsylvian transinsular selective amygdalohippocampectomy for medial intractable temporal lobe epilepsy (15, 21) may be associated with the psychosocial clinical improvement observed after surgery, perhaps because the uncinate fasciculus can no longer convey pathological information from the temporal lobe to the decision-making regions of the orbitofrontal cortex (118).

Inferior Occipitofrontal Fasciculus

In their monumental and extraordinary work, Schmahmann and Pandya (118) stated that the inferior occipitofrontal fasciculus corresponds to the extreme capsule, and they concluded that the latter, by virtue of its connections in nonhuman primates, may have a role in humans in nonarticulatory control of linguistic functions such as syntax and grammar.

Recent observations from intraoperative stimulation during insular glioma surgery implicated the dominant ventral (anteroinferior) insular cortex in planning for motor speech (35, 36), as previously suggested by study of patients with insular ischemic lesions (30). At the subcortical level, direct intraoperative stimulation of the ventral external (and extreme) capsule elicited paraphasic errors and repetition disorders characteristic of conductive aphasia (35, 39), as also happens with the arcuate segment of the superior longitudinal fasciculus. In our study, we demonstrate that the inferior occipitofrontal fasciculus forms part of the ventral extreme and external capsule and travels under the ventral insular cortex from the prefrontal to the posterotemporal regions. This fasciculus is the anatomic substrate of the ventral semantic pathway described by Duffau et al. (39), in contraposition to the dorsal phonological pathway mentioned previously, and in agreement with the work of Schmahmann and Pandya (118).

Internal Capsule

The tractographic examinations in this study display the various components of the internal capsule. Current intraoperative subcortical stimulation techniques can identify the motor fibers of the posterior limb of the internal capsule for safer surgical resection (35). On the other hand, lesions of the anterior limb of the internal capsule resulting in complex behavioral syndromes (abulia, apathy, inattention, psychomotor retardation) secondary to the disruption of thalamoprefrontal fibers have been recognized (118). Interestingly, a DTI study revealed that patients with schizophrenia had smaller-than-normal size anterior limbs of the internal capsules (12).

Talairach (132) and Leksell et al. (78) pioneered the first stereotactic bilateral anterior capsulotomies. This procedure has become established for the management of otherwise-intractable anxiety neurosis and obsessive-compulsive disorders, with a reported success rate of 70% in various series (126).

Cingulum and Fornix

In 1937, James Papez (101) described an anatomic circuit for the processing of emotions, which has subsequently been proven to be critical for memory function. As we show in this

study, the cingulum forms the external ring of Papez's limbic circuit, interconnecting the cingulate cortex with the parahippocampal gyrus, and the fornix forms the internal ring, interconnecting the hippocampus with the mammillary bodies. The latter are connected by the mammillothalamic tract to the anterior nucleus of the thalamus and from there to the cingulate gyrus (*Fig. 7, A* and *C*).

Modern neuroanatomic studies in monkeys have revealed that the cingulum conveys fibers from the cingulate cortex to isocortical areas (high-order association areas in the frontal, temporal, and parietal cortices), paralimbic cortices (parahippocampal gyrus), and limbic cortices (presubiculum and entorhinal cortex) (118). A recent study used DTI to evaluate diffusion in the cingulum in patients with schizophrenia and showed decreased fractional anisotropy in the cingulum of patients versus control subjects. This provides strong evidence for cingulum disruption in schizophrenia, which may be connected to disease-related attention and working-memory abnormalities (73). In addition, preliminary reports provide evidence of an abnormality that involves the cingulum in the pathogenesis of obsessive-compulsive disorder (131).

Psychosurgery was initiated with the introduction of cingulotomy as a treatment for depression and psychosis by Egaz Moniz (88) and Freeman and Watts (51). In 1961, Tooth and Newton (135) published a large report of psychosurgery, reporting that patients with schizophrenia fared poorly, and throughout the 1960s, psychosurgical procedures became less popular. Today, the primary indication for bilateral stereotactic cingulotomy is medically intractable obsessive-compulsive disorder (60), and in selected patients with chronic pain syndromes and refractory depression (150).

Van der Werf et al. (140) observed an episodic deficit of long-term memory with relative sparing of intellectual capacity and short-term memory when the mammillothalamic tract is damaged, and the mammillary bodies are hemorrhagic or involuted in patients with Wernicke-Korsakoff syndrome (46). However, review of the literature related to the role of the fornix in memory processes provides contradictory opinions (2). In any case, when approaching third ventricle lesions, forniceal damage should be avoided if at all possible because we cannot predict whether it will cause memory disturbance. The transforaminal transchoroidal approach described by Wen et al. (143) provides wide exposure of the third ventricle while minimizing risk to the fornix. In this study, we demonstrate the anatomic relationship between the fornix and the anterior commissure, which is an important relationship in performing the anterior transforniceal approach described by Rosenfeld et al. (116).

Anterior Commissure

Our tractographic studies reveal that the anterior commissure is composed of two sets of fibers that form anterior and posterior components. It is thought that fibers from the anterior olfactory nucleus contribute to the smaller anterior component, whereas neocortical fibers from at least the inferotemporal and occipital cortices contribute to the larger posterior limb (28). Little is known regarding the function of the anterior commissure, although it may compensate the integration of interhemispheric visual information for a congenitally absent corpus callosum (22). Schmahmann and Pandya (118) affirm that the splenium of the corpus callosum and the anterior commissure seem to have complementary roles in visual processing. From the clinical perspective, it has been suggested that seizure activity emerging from anterior paralimbic regions can propagate rapidly to the contralateral medial temporal lobe via the anterior commissure (1), so its division is part of the hemispherotomy or functional hemispherectomy for control of intractable seizures (141, 146).

Corpus Callosum

Several tracing studies have established a topographical distribution of the fiber connections to the cortex in midsagittal cross sections of the corpus callosum. The most prominent example is Witelson's scheme, which defines five vertical partitions mainly based on primate data (prefrontal, premotor, motor, sensory, and parietotemporo-occipital) (147). A recent study of DTI-based tractography has recognized striking differences to Witelson's classification in the human corpus callosum. In particular, callosal motor fibers bundles were determined to cross the corpus callosum in a more posterior location than previously indicated (57).

In 1892, Dejerine (27) reported the first clinical case of alexia without agraphi, or pure alexia, caused by a lesion in the dominant occipital lobe that prevented visual information from accessing the language area in the dominant angular gyrus, and a lesion of the splenium of the corpus callosum, which prevented visual input from the intact nondominant occipital lobe from reaching the language area in the dominant angular gyrus (20, 118). In contrast, Liepmann described that a lesion of the anterior portion of the corpus callosum disconnected the right hemisphere from the left, which led to unilateral left-hand apraxia (54). The use of callosotomy for intractable epilepsy has provided a unique opportunity to study the effects of disconnection of the hemispheres (118), as it has revealed that the corpus callosum is responsible for transferring information concerning specific sensory modalities (52) and provided new insights into the functional specialization of the hemispheres (125). Sperry (124) stated that the left hemisphere is engaged in linguistic and analytical tasks, and the right hemisphere is involved in spatial and imagistic thinking. The typical disconnection syndrome after callosotomy includes unilateral tactile anomia, left hemialexia, unilateral apraxia, and even transitory mutism, but when the callosotomy spares the splenium, very little of that syndrome is observed (10). However, Duffau et al. (40) reported that no functional responses were elicited by the intraoperative stimulation of the corpus callosum; low-grade gliomas involving this structure were resected without any consequence on the patient's quality of life, regardless of the callosectomy location.

Recent advances in neuroanatomic studies in experimental animals, development of DTI-based tractography, and evolution of intraoperative corticosubcortical electrical mapping

have shifted the view of the neural basis of cognition from Broca's localizationist model and Wernicke's and Geschwind's associationist views toward Mesulam's connectionist model (85, 84). Rather than maintaining that information is processed by localized cortical regions with passage of information between regions through white matter tracts, Mesulam's model is conceived as resulting from parallel distributed processing performed by multiple groups of connected neurons (large-scale neural networks) rather than individual centers (31, 85).

Importance of White Matter Tracts in Neurosurgery

It is important for neurosurgeons to improve their knowledge of the anatomofunctional connectivity of the white matter tracts (*Table 3*) (35, 148, 149). Every intracerebral lesion affects, to some degree, the white matter structure of the brain, and lessons from stroke studies have taught us that lesions of the white matter elicit more severe and more permanent neurological deficits than cortical damages (35).

The interpretation of pre- and postsurgical neurological symptoms and syndromes may be enriched by a precise knowledge of the anatomofunctional fasciculi of white matter and the associated disconnection syndromes (*Table 3*). Equally, neuroradiological analysis of computed tomographic and MRI scans may improve with understanding of the three-dimensional arrangement of the white matter tracts. Old neuroanatomic terms that are based on macroscopic descriptions, such as *corona radiata* or *centrum semiovale*, are now understood as the group of different fasciculi that integrates those structures (*Figs. 12* and *13*).

The anatomy of white matter tracts is particularly relevant in the surgical treatment of cerebral gliomas; first, because gliomas involve both cortical and subcortical structures, and thus may alter the connectivity (35); and second, because diffusion of gliomas occurs along white matter tracts (7, 13, 82, 138, 148, 149). As recently modeled (130), tumoral growth results from two underlying mechanisms: proliferation and diffusion. When proliferation is the major phenomenon, the tumor is grossly bulky, and it is reasonable to describe its location by naming the pathological lobe or gyrus. A predominantly diffuse tumor has a complex shape with digitations along the white matter (82). In this case, it could be informative to complete the description of the main location by identifying the invaded white matter tracts (82). Mandonnet et al. (82) stated that this additional classification on the basis of white matter invasion patterns could be helpful during surgical planning, and it might be possible to better estimate preoperatively the maximal extent of resection with preservation of function. In modern glioma surgery, the limits of surgical resection can now be defined in terms of the anatomofunctional white matter tracts (35).

DTI-based tractography allows the study of the spatial relationships of intracerebral lesions with the white matter tracts. Several authors have reported the usefulness of integrating this technique into the neuronavigation system to localize the pyramidal tract (8, 62, 96–98), primary motor area (64), optic radiations (65, 96), and language pathways (56) during the surgical procedure. Its combination with mapping techniques may improve preservation of eloquent regions during surgery by providing access to direct connectivity information between functional regions of the brain (56).

In several neurosurgical procedures, such as bilateral cingulectomy or anterior capsulotomy, the main goal is disruption of a particular white matter tract. In addition, the different variants of amygdalohippocampectomy need to traverse the temporal white matter in the approach to the temporal horn. In the case of Spencer's anteromedial temporal lobectomy (122), the lateral approach to the temporal horn disrupts the temporal extension of the uncinate fasciculus and anterior commissure and may damage the most anterior extension of the inferior longitudinal fasciculus, temporoparietal segment of the superior longitudinal fasciculus, and Meyer's loop (4, 15). On the contrary, in Yaşargil's selective amygdalohippocampectomy (145), the temporal horn is approached through the limen insula and the anterior 10 to 15 mm of the inferior insular sulcus, thus disrupting the main stem of the uncinate fasciculus and anterior commissure but preserving the inferior longitudinal fasciculus, the temporoparietal segment of the superior longitudinal fasciculus, and Meyer's loop (21). Better neuropsychological outcomes have been reported with the latter than with the former procedure (144), but these findings remain controversial (112). A third variant, selective subtemporal amygdalohippocampectomy (58), approaches the temporal horn through the collateral sulcus after removal of the medial half of the fusiform gyrus, thereby resulting in partial preservation of the uncinate fasciculus and Meyer's loop, but cause damage to the inferior longitudinal fasciculus. Although Wieser (144) stressed the importance of the interruption of the uncinate fasciculus to obtain a good postoperative seizure control, Hori et al. (59) demonstrated that preserving the lateral portion of the uncinate fasciculus (related to the temporal neocortex) produces better results in verbal memory and similar results in seizure control.

Finally, the knowledge of not only the location, trajectory, and function but also the orientation of the white matter fibers may have surgical implications. Disruption of a fasciculus parallel to the orientation of its fibers would be less damaging than its incision in a perpendicular direction. The benefit of this surgical technique has already been shown by Mazza et al. (83), who demonstrated improved neuropsychological results by performing transversal instead of longitudinal callosotomy while approaching third ventricle lesions. This strategy, although useful in specific anatomic regions, is challenging because of the superposition of white matter tracts with different orientations.

CONCLUSION

A comprehensive understanding of the microsurgical anatomy of the white matter tracts is important for treating a wide spectrum of neurosurgical lesions. For the neurosurgeon, performing the fiber-dissection technique is the best method for learning the three-dimensional anatomy of the white matter of the brain. DTI-based tractography provides a reliable representation of the white matter tracts in normal human brain and the

spatial relationship of the tracts with intracerebral lesions. Combined application of both techniques for the study of human white matter anatomy is reciprocally enriched because the anatomic knowledge acquired by fiber dissection aids in proper interpretation and analysis of the new tractographic studies and because the tractographic studies can reveal, at the same time, the complex relationships between the fiber systems.

The combination of topographical anatomy of the human cerebral tracts with data obtained from the neuroanatomic studies in primates, clinical and radiological diagnosis of human white matter lesions, and intraoperative subcortical electric-stimulation studies aids in understanding the possible functional role of the white matter tracts. Thus, anatomic and radiological knowledge of the anatomofunctional fiber tracts helps to explain pre-, intra-, and postoperative clinical "disconnection" syndromes and white matter tumoral invasion patterns, and may improve presurgical planning and surgical strategy, thereby potentially decreasing surgical morbidity.

REFERENCES

1. Adam C: How do the temporal lobes communicate in medial temporal lobe seizures? [in French]. **Rev Neurol (Paris)** 162:813–818, 2006.
2. Apuzzo MLJ, Giannotta SL: Transcallosal interforniceal approach, in Apuzzo MLJ (ed): *Surgery of the Third Ventricle*. Baltimore, Williams & Wilkins, 1987, pp 357–358.
3. Bartolomeo P: The relationship between visual perception and visual mental imagery: A reappraisal of the neuropsychological evidence. **Cortex** 38:357–378, 2002.
4. Barton JJ, Hefter R, Chang B, Schomer D, Drislane F: The field defects of anterior temporal lobectomy: A quantitative reassessment of Meyer's loop. **Brain** 128:2123–2133, 2005.
5. Basser PJ, Pierpaoli C: Microstructural and physiological features of tissues elucidated by quantitative-diffusion-tensor MRI. **J Magn Reson B** 111:209–219, 1996.
6. Bechara A: The role of emotion in decision-making: Evidence from neurological patients with orbitofrontal damage. **Brain Cogn** 55:30–40, 2004.
7. Berger M: Fiber dissection technique: Lateral aspect of the brain. **Neurosurgery** 47:417–427, 2000 (comment).
8. Berman JI, Berger MS, Mukherjee P, Henry RG: Diffusion-tensor imaging-guided tracking of fibers of the pyramidal tract combined with intraoperative cortical stimulation mapping in patients with gliomas. **J Neurosurg** 101:66–72, 2004.
9. Bisley JW, Goldberg ME: Neuronal activity in the lateral intraparietal area and spatial attention. **Science** 299:81–86, 2003.
10. Bogen JE: Physiological consequences of complete or partial commissural section, in Apuzzo MLJ (ed): *Surgery of the Third Ventricle*. Baltimore, Williams and Wilkins, 1987, pp 175–191.
11. Brand S: A serial section Golgi analysis of the primate claustrum. **Anat Embryol (Berl)** 162:475–488, 1981.
12. Buchsbaum MS, Schoenknecht P, Torosjan Y, Newmark R, Chu KW, Mitelman S, Brickman AM, Shihabuddin L, Haznedar MM, Hazlett EA, Ahmed S, Tang C: Diffusion tensor imaging of frontal lobe white matter tracts in schizophrenia. **Ann Gen Psychiatry** 5:19, 2006.
13. Burger PC, Heinz ER, Shibata T, Kleihues P: Topographic anatomy and CT correlations in the untreated glioblastoma multiforme. **J Neurosurg** 68:698–704, 1988.
14. Calvert GA, Brammer MJ, Bullmore ET, Campbell R, Iversen SD, David AS: Response amplification in sensory-specific cortices during crossmodal binding. **Neuroreport** 10:2619–2623, 1999.
15. Campero A, Tróccoli G, Martins C, Fernandez-Miranda JC, Yasuda A, Rhoton AL Jr: Microsurgical approaches to the medial temporal region: An anatomical study. **Neurosurgery** 59 [Suppl 2]:ONS279–ONS308, 2006.
16. Carman JB, Cowan WM, Powell TP: The cortical projection upon the claustrum. **J Neurol Neurosurg Psychiatry** 2:46–51, 1964.
17. Carpenter MB, Sutin J: *Human Neuroanatomy*. Baltimore, Williams & Wilkins, 1983, ed 8, pp. 35–45, 552–564, 586, 612–642.
18. Catani M, Howard RJ, Pajevic S, Jones DK: Virtual in vivo interactive dissection of white matter fasciculi in the human brain. **Neuroimage** 17:77–94, 2002.
19. Catani M, Jones DK, Donato R, Ffytche DH: Occipito-temporal connections in the human brain. **Brain** 126:2093–2107, 2003.
20. Catani M, Jones DK, ffytche DH: Perisylvian language networks of the human brain. **Ann Neurol** 57:8–16, 2005.
21. Choi C, Rubino PA, Fernandez-Miranda JC, Abe H, Rhoton AL Jr: Meyer's loop and the optic radiations in the transsylvian approach to the mediobasal temporal lobe. **Neurosurgery** 59 [Suppl 2]:ONS228–ONS236, 2006.
22. Corballis MC, Finlay DC: Interhemispheric visual integration in three cases of familial callosal agenesis. **Neuropsychology** 14:60–70, 2000.
23. Crick FC, Koch C: What is the function of the claustrum? **Philos Trans R Soc Lond B Biol Sci** 360:1271–1279, 2005.
24. Crosby EC, Humphrey T, and Lauer EW: *Correlative Anatomy of the Nervous System*. New York, Macmillan, 1962.
25. Damasio AR, Damasio H, Van Hoesen GW: Prosopagnosia: Anatomic basis and behavioral mechanisms. **Neurology** 32:331–341, 1982.
26. Dejerine J: *Anatomy of the Nervous Centers* [in French]. Paris, Rueff & Cie, 1895, vol 1.
27. Dejerine J: Contribution to the anatomopathologic and clinical study of the different forms of aphasia [in French]. **Mem Soc Biol** 4:61–90, 1892.
28. Di Virgilio G, Clarke S, Pizzolato G, Schaffner T: Cortical regions contributing to the anterior commissure in man. **Exp Brain Res** 124:1–7, 1999.
29. Doricchi F, Tomaiuolo F: The anatomy of neglect without hemianopia: A key role for parietal-frontal disconnection? **Neuroreport** 14:2239–2243, 2003.
30. Dronkers NF: A new brain region for coordinating speech articulation. **Nature** 384:159–161, 1996.
31. Druga R: Claustro-neocortical in the cat and rat demonstrated by HRP tracing technique. **J Hirnforsch** 23:191–202, 1982.
32. Druga R: Cortico-claustral connections. I. Fronto-claustral connections. **Folia Morphol (Praha)** 14:391–399, 1966.
33. Druga R: Cortico-claustral connections. II. Connections from the parietal, temporal, and occipital cortex to the claustrum. **Folia Morphol (Praha)** 16:142–149, 1968.
34. Druga R: Efferent projections from the claustrum (an experimental study using Nauta's method). **Folia Morphol (Praha)** 20:163–165, 1972.
35. Duffau H: New concepts in surgery of WHO grade II gliomas: Functional brain mapping, connectionism and plasticity—a review. **J Neurooncol** 79:77–115, 2006.
36. Duffau H, Capelle L, Lopes M, Faillot T, Sichez JP, Fohanno D: The insular lobe: Physiopathological and surgical considerations. **Neurosurgery** 47:801–811, 2000.
37. Duffau H, Capelle L, Sichez N, Denvil D, Lopes M, Sichez JP, Bitar A, Fohanno D: Intraoperative mapping of the subcortical language pathways using direct stimulations. An anatomo-functional study. **Brain** 125:199–214, 2002.
38. Duffau H, Gatignol P, Denvil D, Lopes M, Capelle L: The articulatory loop: Study of the subcortical connectivity by electrostimulation. **Neuroreport** 14:2005–2008, 2003.
39. Duffau H, Gatignol P, Mandonnet E, Peruzzi P, Tzourio-Mazoyer N, Capelle L: New insights into the anatomo-functional connectivity of the semantic system: A study using cortico-subcortical electrostimulations. **Brain** 128:797–810, 2005.
40. Duffau H, Khalil I, Gatignol P, Denvil D, Capelle L: Surgical removal of corpus callosum infiltrated by low-grade glioma: Functional outcome and oncological considerations. **J Neurosurg** 100:431–437, 2004.
41. Duffau H, Mandonnet E, Gatignol P, Capelle L: Functional compensation of the claustrum: Lessons from low-grade glioma surgery. **J Neurooncol** 81:327–329, 2007.

42. Duvernoy HM: *The Human Hippocampus*. New York, Springer-Verlag, 2005, p 44.
43. Ebeling U, Reulen HJ: Neurosurgical topography of the optic radiation in the temporal lobe. **Acta Neurochir (Wien)** 92:29–36, 1988.
44. Ebeling U, von Cramon D: Topography of the uncinate fascicle and adjacent temporal fiber tracts. **Acta Neurochir (Wien)** 115:143–148, 1992.
45. Edelstein LR, Denaro FJ: The claustrum: A historical review of its anatomy, physiology, cytochemistry and functional significance. **Cell Mol Biol (Noisy-le-grand)** 50:675–702, 2004.
46. Ehni G, Ehni B: Considerations in transforaminal entry, in Apuzzo MLJ (ed): *Surgery of the Third Ventricle*. Baltimore, Williams & Wilkins, 1987, pp 346–347.
47. Ettlinger G, Wilson WA: Cross-modal performance: Behavioural processes, phylogenetic considerations and neural mechanisms. **Behav Brain Res** 40:169–192, 1990.
48. Fernandez-Miranda JC, Rhoton AL Jr, Kakizawa Y, Choi C, Alvarez-Linera J: The claustrum and its projection system in the human brain: A microsurgical and tractographic anatomical study. **J Neurosurg** (in press).
49. Filimonoff IN: The claustrum, its origin and development. **J Hirnforsch** 8:503–528, 1966.
50. Frank LR: Anisotropy in high angular resolution diffusion-weighted MRI. **Magn Reson Med** 45:935–939, 2001.
51. Freeman W, Watts J: *Psychosurgery: Intelligence, Emotion and Social Behavior Following Prefrontal Lobotomy for Mental Disorders*. Springfield, Charles C. Thomas, 1942.
52. Gazzaniga MS, Risse GL, Springer SP, Clark DE, Wilson DH: Psychologic and neurologic consequences of partial and complete cerebral commissurotomy. **Neurology** 25:10–15, 1975.
53. Geschwind N: Disconnection syndromes in animals and man. I. **Brain** 88:237–294, 1965.
54. Goldenberg G: Apraxia and beyond: Life and work of Hugo Liepmann. **Cortex** 39:509–524, 2003.
55. Hadjikhani N, Roland PE: Cross-modal transfer of information between the tactile and the visual representations in the human brain: A positron emission tomographic study. **J Neurosci** 18:1072–1084, 1998.
56. Henry RG, Berman JI, Nagarajan SS, Mukherjee P, Berger MS: Subcortical pathways serving cortical languages sites: Initial experience with diffusion tensor imaging fiber tracking combined with intraoperative language mapping. **Neuroimage** 21:616–622, 2004.
57. Hofer S, Frahm J: Topography of the human corpus callosum revisited—comprehensive fiber tractography using diffusion tensor magnetic resonance imaging. **Neuroimage** 32:989–994, 2006.
58. Hori T, Tabuchi S, Kurosaki M, Kondo S, Takenobu A, Watanabe T: Subtemporal amygdalohippocampectomy for treating medically intractable temporal lobe epilepsy. **Neurosurgery** 33:50–57, 1993.
59. Hori T, Yamane F, Ochiai T, Kondo S, Shimizu S, Ishii K, Miyata H: Selective subtemporal amygdalohippocampectomy for refractory temporal lobe epilepsy: Operative and neuropsychological outcomes. **J Neurosurg** 106:134–141, 2007.
60. Jung HH, Kim CH, Chang JH, Park YG, Chung SS, Chang JW: Bilateral anterior cingulotomy for refractory obsessive-compulsive disorder: Long-term follow-up results. **Stereotact Funct Neurosurg** 84:184–189, 2006.
61. Kahane P, Hoffmann D, Minotti L, Berthoz A: Reappraisal of the human vestibular cortex by cortical electrical stimulation study. **Ann Neurol** 54:615–624, 2003.
62. Kamada K, Sawamura Y, Takeuchi F, Kawaguchi H, Kuriku S, Todo T, Morita A, Masutani Y, Aoki S, Kirino T: Functional identification of the primary motor area by corticospinal tractography. **Neurosurgery** 56 [Suppl 1]:98–109, 2005.
63. Kamada K, Todo T, Masutani Y, Aoki S, Ino K, Morita A, Saito N: Visualization of the frontotemporal language fibers by tractography combined with functional magnetic resonance imaging and magnetoencephalography. **J Neurosurg** 106:90–98, 2007.
64. Kamada K, Todo T, Masutani Y, Aoki S, Ino K, Takano T, Kirino T, Kawahara N, Morita A: Combined use of tractography-integrated functional neuronavigation and direct fiber stimulation. **J Neurosurg** 102:664–672, 2005.
65. Kamada K, Todo T, Morita A, Masutani Y, Aoki S, Ino K, Hawai K, Kirino T: Functional monitoring for visual pathway using real-time visual evoked potentials and optic-radiation tractography. **Neurosurgery** 57 [Suppl 1]:121–127, 2005.
66. Kareken DA, Mosnik DM, Doty RL, Dzemidzic M, Hutchins GD: Functional anatomy of human odor sensation, discrimination, and identification in health and aging. **Neuropsychology** 17:482–495, 2003.
67. Kemp JM, Powell TP: The cortico-striate projection in the monkey. **Brain** 93:525–546, 1970.
68. Kier EL, Staib LH, Davis LM, Bronen RA: MR imaging of the temporal stem: Anatomic dissection tractography of the uncinate fasciculus, inferior occipitofrontal fasciculus, and Meyer's loop of the optic radiation **AJNR Am J Neuroradiol** 25:677–691, 2004.
69. Kimura S, Nezu A, Osaka H, Saito K: Symmetrical external capsule lesions in a patient with herpes simplex encephalitis. **Neuropediatrics** 25:162–164, 1994.
70. Klinger J, Gloor P: The connections of the amygdala and of the anterior temporal cortex in the human brain. **J Comp Neurol** 115:333–369, 1960.
71. Kubicki M, Park H, Westin CF, Nestor PG, Mulkern RV, Maier SE, Niznikiewicz M, Connor EE, Levitt JJ, Frumin M, Kikinis R, Jolesz FA, McCarley RW, Shenton ME: DTI and MTR abnormalities in schizophrenia: Analysis of white matter integrity. **Neuroimage** 26:1109–1118, 2005.
72. Kubicki M, Westin CF, Maier SE, Maier SE, Frumin M, Nestor PG, Kikinis R, Jolesz FA, McCarley RW, Shenton ME: Uncinate fasciculus findings in schizophrenia: A magnetic resonance diffusion tensor imaging study. **Am J Psychiatry** 159:813–820, 2002.
73. Kubicki M, Westin CF, Nestor PG, Wible CG, Frumin M, Maier SE, Kikinis R, Jolesz FA, McCarley RW, Shenton ME: Cingulate fasciculus integrity disruption in schizophrenia: A magnetic resonance diffusion tensor imaging study. **Biol Psychiatry** 54:1171–1180, 2003.
74. Lazar M, Weinstein DM, Tsuruda JS, Hasan KM, Arfanakis K, Meyerand ME, Badie B, Rowley HA, Haughton V, Field A, Alexander AL: White matter tractography using diffusion tensor deflection. **Hum Brain Mapp** 18:306–321, 2003.
75. Le Bihan D: Looking into the functional architecture of the brain with diffusion MRI. **Nat Rev Neurosci** 4:469–480, 2003.
76. Lehéricy S, Ducros M, Krainik A, Francois C, Van de Moortele PF, Ugurbil K, Kim DS: 3-D diffusion tensor axonal tracking shows distinct SMA and pre-SMA projections to the human striatum. **Cereb Cortex** 14:1302–1309, 2004.
77. Lehéricy S, Ducros M, Van de Moortele PF, Francois C, Thivard L, Poupon C, Swindale N, Ugurbil K, Kim DS: Diffusion tensor fiber tracking shows distinct corticostriatal circuits in humans. **Ann Neurol** 55:522–529, 2004.
78. Leksell L, Herner T, Lidén K: Stereotaxic radiosurgery of the brain. **Kungliga Fysiografiska Sällskapet i Lund Förhandlingar** 25:1–10, 1955.
79. Ludwig E, Klingler J: *Atlas Cerebri Humani*. Basel, S. Karger, 1956.
80. Makris N, Kennedy DN, McInerney S, Sorensen AG, Wang R, Caviness VS Jr, Pandya DN: Segmentation of subcomponents within the superior longitudinal fasciculus: A quantitative, in vivo, DT-MRI study. **Cereb Cortex** 15:854–869, 2005.
81. Mamata H, Mamata Y, Westin CF, Shenton ME, Kikinis R, Jolesz FA, Maier SE: High-resolution line scan diffusion tensor MR imaging of white matter fiber tract anatomy. **AJNR Am J Neuroradiol** 23:67–75, 2002.
82. Mandonnet E, Capelle L, Duffau H: Extension of paralimbic low grade gliomas: Toward an anatomical classification based on white matter invasion patterns. **J Neurooncol** 78:179–185, 2006.
83. Mazza M, Di Rienzo A, Costagliola C, Roncone R, Casacchia M, Ricci A, Galzio RJ: The interhemispheric transcallosal-transversal approach to the lesions of the anterior and middle third ventricle: Surgical validity and neuropsychological evaluation of the outcome. **Brain Cogn** 55:525–534, 2004.
84. Mesulam MM: From sensation to cognition. **Brain** 121:1013–1052, 1998.
85. Mesulam MM: Large-scale neurocognitive networks and distributed processing for attention, language, and memory. **Ann Neurol** 28:597–613, 1990.
86. Mesulam MM: Spatial attention and neglect: Parietal, frontal and cingulate contributions to the mental representation and attentional targeting of salient extrapersonal events. **Philos Trans R Soc Lond B Biol Sci.** 354:1325–1346, 1999.
87. Mesulam MM, Geula C: Nucleus basalis (Ch4) and cortical cholinergic innervation in the human brain: Observations based on the distribution of acetyl-

cholinesterase and choline acetyltransferase. **J Comp Neurol** 275:216–240, 1988.
88. Moniz E: Prefrontal leucotomy in the treatment of mental disorders. **Am J Psychiatry** 93:1379–1385, 1937.
89. Mori S, Crain BJ, Chacko VP, van Zijl PC: Three dimensional tracking of axonal projections in the brain by magnetic resonance imaging. **Ann Neurol** 45:265–269, 1999.
90. Morys J, Narkiewicz O, Wisniewski HM: Neuronal loss in the human claustrum following ulegyria. **Brain Res** 616:176–180, 1993.
91. Moryś J, Słoniewski P, Narkiewicz O: Somatosensory evoked potentials following lesions of the claustrum. **Acta Physiol Pol** 39:475–483, 1988.
92. Narkiewicz O: Connections of the claustrum with the cerebral cortex [in Polish]. **Folia Morphol (Warsz)** 25:555–561, 1966.
93. Narkiewicz O: Degenerations in the claustrum after regional neocortical ablations in the cat. **J Comp Neurol** 123:335–355, 1964.
94. Narkiewicz O: Frontoclaustral interrelations in cats and dogs. **Acta Neurobiol Exp (Wars)** 32:141–150, 1972.
95. Nieuwenhuys R, Voogd J, van Huijzen C: *The Human Central Nervous System*. Berlin, Springler-Verlag, 1988, ed 3.
96. Nimsky C, Ganslandt O, Fahlbusch R: Implementation of fiber tract navigation. **Neurosurgery** 58 [Suppl 2]:ONS292–ONS304, 2006.
97. Nimsky C, Ganslandt O, Hastreiter P, Wang R, Benner T, Sorensen AG, Fahlbusch R: Intraoperative diffusion-tensor MR imaging: Shifting of white matter tracts during neurosurgical procedures—initial experience. **Radiology** 234:218–225, 2005.
98. Nimsky C, Ganslandt O, Hastreiter P, Wang R, Benner T, Sorensen AG, Fahlbusch R: Preoperative and intraoperative diffusion tensor imaging-based fiber tracking in glioma surgery. **Neurosurgery** 56:130–138, 2005.
99. Nishizawa M: Acute encephalopathy after ingestion of "sugihiratake" mushroom [in Japanese]. **Rinsho Shinkeigaku** 45:818–820, 2005.
100. Ono M, Kubik S, Abernathey CD: *Atlas of the Cerebral Sulci*. Stuttgart, Thieme Verlag, 1990, pp 14–16.
101. Papez JW: A proposed mechanism of emotion. **Arch Neurol Psychiatry** 38:725–743, 1937.
102. Pearson RC, Brodal P, Gatter KC, Powell TP: The organization of the connections between the cortex and the claustrum in the monkey. **Brain Res** 234:435–441, 1982.
103. Petrides M, Pandya DN: Association fiber pathways to the frontal cortex from the superior temporal region in the rhesus monkey. **J Comp Neurol** 273:52–66, 1988.
104. Petrides M, Pandya DN: Comparative cytoarchitectonic analysis of the human and the macaque ventrolateral prefrontal cortex and corticocortical connection patterns in the monkey. **Eur J Neurosci** 16:291–310, 2002.
105. Petrides M, Pandya DN: Dorsolateral prefrontal cortex: Comparative cytoarchitectonic analysis in the human and the macaque brain and corticocortical connection patterns. **Eur J Neurosci** 11:1011–1036, 1999.
106. Petrides M, Pandya DN: Projections to the frontal cortex from the posterior parietal region in the rhesus monkey. **J Comp Neurol** 228:105–116, 1984.
107. Peuskens D, van Loon J, Van Calenbergh F, van den Bergh R, Goffin J, Plets C: Anatomy of the anterior temporal lobe and the frontotemporal region demonstrated by fiber dissection. **Neurosurgery** 55:1174–1184, 2004.
108. Poupon C, Clark CA, Frouin V, Régis J, Bloch I, Le Bihan D, Mangin J: Regularization of diffusion-based direction maps for the tracking of brain white matter fascicles. **Neuroimage** 12:184–195, 2000.
109. Rae AS: The connections of the claustrum. **Confin Neurol** 14:211–219, 1954.
110. Rae AS: The form and structure of the human claustrum. **J Comp Neurol** 100:15–39, 1954.
111. Ramón y Cajal S: Neuron theory or reticular theory? Objective evidence of the anatomical unity of nerve cells [in Spanish]. **Archivos Neurobiol** 13:570–646, 1933.
112. Renowden SA, Matkovic Z, Adams CB, Carpenter K, Oxbury S, Molyneux AJ, Anslow P, Oxbury J: Selective amygdalohippocampectomy for hippocampal sclerosis: Postoperative MR appearance. **AJNR Am J Neuroradiol** 16:1855–1861, 1995.
113. Rhoton AL Jr: The cerebrum. **Neurosurgery** 51 [Suppl]:S1–S51, 2002.
114. Ribas GC, Bento RF, Rodrigues AJ Jr: Anaglyphic three-dimensional stereoscopic printing: Revival of an old method for anatomical and surgical teaching and reporting. **J Neurosurg**. 95:1057–1066, 2001.
115. Ribas GC, Yasuda A, Ribas EC, Nishikuni K, Rodrigues AJ Jr: Surgical anatomy of microneurosurgical sulcal key points. **Neurosurgery** 59 [Suppl 2]:ONS177–ONS211, 2006.
116. Rosenfeld JV, Freeman JL, Harvey AS: Operative technique: The anterior transcallosal transseptal interforniceal approach to the third ventricle and resection of hypothalamic hamartomas. **J Clin Neurosci** 11:738–744, 2004.
117. Rubino PA, Rhoton AL Jr, Tong X, Oliveira E: Three-dimensional relationships of the optic radiation. **Neurosurgery** 57:219–227, 2005.
118. Schmahmann JD, Pandya DN: *Fiber Pathways of the Brain*. New York, Oxford University Press, 2006.
119. Shimizu S, Tanaka R, Rhoton AL Jr, Fukushima Y, Osawa S, Kawashima M, Oka H, Fujii K: Anatomic dissection and classic three-dimensional documentation: A unit of education for neurosurgical anatomy revisited. **Neurosurgery** 58:E1000, 2006.
120. Sincoff EH, Tan Y, Abdulrauf SI: White matter fiber dissection of the optic radiations of the temporal lobe and implications for surgical approaches to the temporal horn. **J Neurosurg** 101:739–746, 2004.
121. Spena G, Gatignol P, Capelle L, Duffau H: Superior longitudinal fasciculus subserves vestibular network in humans. **Neuroreport** 17:1403–1406, 2006.
122. Spencer DD, Spencer SS: Surgery for epilepsy. **Neurol Clin** 3:313–330, 1985.
123. Sperner J, Sander B, Lau S, Krude H, Scheffner D: Severe transitory encephalopathy with reversible lesions of the claustrum. **Pediatr Radiol** 26:769–771, 1996.
124. Sperry R: Some effects of disconnecting the cerebral hemispheres. **Science** 217:1223–1226, 1982.
125. Sperry RW: Perception in the absence of the neocortical commissures. **Res Publ Assoc Res Nerv Ment Dis** 48:123–138, 1970.
126. Spiegelmann R, Faibel M, Zohar Y: CT target selection in stereotactic anterior capsulotomy: Anatomical considerations. **Stereotact Funct Neurosurg** 63:160–167, 1994.
127. Standring S, Crossman AR, Turlough FitzGerald MJ, Collins P: Neuroanatomy, in Standring S (ed): *Gray's Anatomy: The Anatomical Basis of Clinical Practice*. New York, Elsevier Churchill Livingstone, 2005, ed 39, pp 227–431.
128. Stevens CF: Consciousness: Crick and the claustrum. **Nature** 435:1040–1041, 2005.
129. Stuss DT, Levine B: Adult clinical neuropsychology: Lessons from studies of the frontal lobes. **Annu Rev Psychol** 53:401–433, 2002.
130. Swanson KR, Bridge C, Murray JD, Alvord EC Jr: Virtual and real brain tumors: Using mathematical modeling to quantify glioma growth and invasion. **J Neurol Sci** 216:1–10, 2003.
131. Szeszko PR, Ardekani BA, Ashtari M, Malhotra AK, Robinson DG, Bilder RM, Lim KO: White matter abnormalities in obsessive-compulsive disorder: A diffusion tensor imaging study. **Arch Gen Psychiatry** 62:782–790, 2005.
132. Talairach J: Limited prefrontal lobotomy performed by electrocoagulation of the thalamo-frontal fibres at their origin from the anterior limb of the internal capsule [in French]. *IV Congres Neurologique International*, Paris, Masson, 1949.
133. Tanriover N, Rhoton AL Jr, Kawashima M, Ulm A, Yasuda A: Microsurgical anatomy of the insula and the sylvian fissure. **J Neurosurg** 100:891–922, 2004.
134. Thiebaut de Schotten M, Urbanski M, Duffau H, Volle E, Lévy R, Dubois B, Bartolomeo P: Direct evidence for a parietal-frontal pathway subserving spatial awareness in humans. **Science** 309:2226–2228, 2005.
135. Tooth JC, Newton MP: Leucotomy in England and Wales 1942–1954. *Reports on Public Health and Medical Subjects*. London, Her Majesty's Stationary Office, no. 104, 1961.
136. Trolard P: Apropos of the claustrum [in French]. **Rev Neurol** 13:1068–1071, 1905.
137. Türe U, Yaşargil DC, Al-Mefty O, Yaşargil MG: Topographic anatomy of the insular region. **J Neurosurg** 90:720–733, 1999.
138. Türe U, Yaşargil MG, Friedman AH, Al-Mefty O: Fiber dissection technique: Lateral aspect of the brain. **Neurosurgery** 47:417–427, 2000.
139. Türe U, Yaşargil MG, Pait TG: Is there a superior occipitofrontal fasciculus? A microsurgical anatomic study. **Neurosurgery** 40:1226–1232, 1997.
140. Van der Werf YD, Scheltens P, Lindeboom J, Witter MP, Uylings HB, Jolles J: Deficits of memory, executive functioning and attention following infarction in the thalamus; a study of 22 cases with localized lesions. **Neuropsychologia** 41:1330–1344, 2003.

141. Villemure JG, Mascott CR: Peri-insular hemispherotomy: Surgical principles and anatomy. **Neurosurgery** 37:975–981, 1995.
142. Wakana S, Jiang H, Nagae-Poetscher LM, van Zijl PC, Mori S: Fiber tract-based atlas of human white matter anatomy. **Radiology** 230:77–87, 2004.
143. Wen HT, Rhoton AL Jr, de Oliveira E: Transchoroidal approach to the third ventricle: An anatomic study of the choroidal fissure and its clinical application. **Neurosurgery** 42:1205–1219, 1998.
144. Wieser HG: Selective amygdalohippocampectomy: Indications, investigative technique and results. **Adv Tech Stand Neurosurg** 13:39–133, 1986.
145. Wieser HG, Yaşargil MG: Selective amygdalohippocampectomy as a surgical treatment of mesiobasal limbic epilepsy. **Surg Neurol** 17:445–457, 1982.
146. Wilson DH, Culver C, Waddington M, Gazzaniga M: Disconnection of the cerebral hemispheres. An alternative to hemispherectomy for the control of intractable seizures. **Neurology** 25:1149–1153, 1975.
147. Witelson SF: Hand and sex differences in the isthmus and genu of the human corpus callosum. A postmortem morphological study. **Brain** 112:799–835, 1989.
148. Yaşargil MG: *Microneurosurgery: CNS Tumors: Surgical Anatomy, Neuropathology, Neuroradiology, Neurophysiology, Clinical Considerations, Operability, Treatment Options*. Stuttgart, Georg Thieme Verlag, 1994, vol 4A.
149. Yaşargil MG, Türe U, Yaşargil DC: Impact of temporal lobe surgery. **J Neurosurg** 101:725–738, 2004.
150. Yen CP, Kung SS, Su YF, Lin WC, Howng SL, Kwan AL: Stereotactic bilateral anterior cingulotomy for intractable pain. **J Clin Neurosci** 12:886–890, 2005.
151. Young P, Young P: *Basic Clinical Neuroanatomy*. Philadelphia, Williams & Wilkins, ed 1, 1997.

Acknowledgments

We thank Robin Barry for assistance in preparation of the figures, Laura Dickinson for helping with the manuscript, and Fernando Carceller, M.D., Carlos Perez, M.D., and Roberto Martinez, M.D., for collaboration with the clinical material. We acknowledge Maria Jose Bolado for constant support to complete this project.

COMMENTS

Fernández-Miranda et al. present a comprehensive overview of the major white matter tracts in the healthy human brain. They applied a standard anatomical fiber dissection technique as well as a straight forward standard visualization of diffusion tensor imaging (DTI)-based fiber tracking.

Reconstruction of major white matter tracts by fiber tracking is becoming more and more important in surgery of lesions located close to these eloquent deep-seated brain structures to prevent postoperative deficits. Integrating fiber tracking in an advanced multimodal neuronavigational setup helps to achieve this goal. Additional application of electrophysiological methods may help by adding further safety and confidence, as well as to confirm the reconstructed fiber bundles in selected cases. Intraoperative events such as brain shift necessitate some kind of intraoperative compensation to allow accurate representation during surgery. This compensation is possible by intraoperative imaging. There are two principal strategies to achieve this: either applying some kind of intraoperative anatomical imaging based on ultrasound, computed tomography, or low-field magnetic resonance imaging that may depict the intraoperative three-dimensional anatomical situation combined with a non-rigid registration of preoperative high-quality fiber tracking data to calculate the actual intraoperative situation of the fiber tracts or the actual measurement of intraoperative DTI data with immediate fiber tracking by the application of intraoperative high-field magnetic resonance imaging.

The increasing application of fiber tracking for neurosurgical use necessitates some kind of standardization of the fiber tracking strategies. The current article provides a good starting point. It is very important to realize that even small differences in the placement of the regions of interest for the tracking algorithm may result in significantly different reconstructed fiber tract bundles. Furthermore, fiber tracking in patients with space-occupying lesions is a much bigger challenge than tracking in the healthy brain. Intracerebral lesions may result in a deviation, interruption, or thinning of an adjacent tract system. Edema and infiltration of major white matter tracts affect the tracking results significantly, so that methods have to be developed in the future to characterize, quantify, and visualize the actual quality of the results of the various tracking algorithms, before these data can be fully trusted in the surgical field.

Christopher Nimsky
Erlangen, Germany

I congratulate Fernández-Miranda et al. on their diligence in producing this important article. Included are 60 excellent three-dimensional images of the brain and the dissected fiber system, as well as 28 excellent colored images of the fiber tracts visualized with DTI technology. Based on this anatomic data, the authors discuss the distinct cognitive centers of the cerebrum and define their interaction by referring to selective research papers of the past century encompassing neuroanatomy, neurophysiology, neurochemistry, neurosurgery, neuroradiology, behavioral neurology, neuropsychology, and psychiatry.

Fernández-Miranda et al. have described a good regime for laboratory training. Young colleagues are strongly advised to assimilate the material on brain anatomy offered here and perform dissections themselves in the laboratory, following these instructions step-by-step. These exercises will form a good foundation in anatomy and will promote the development of a dynamic three-dimensional graphic imagery of the complex white matter of the brain in the mind of the student.

The authors resolved to enter into this delicate field and to complete this article within 3 years, having been introduced to the modern fiber dissection by Professor Türe at annual courses in Braga, Portugal in 2005, 2006, and 2007.

Reviewed historically, we appreciate that philosophers, mathematicians, scientists, and artists have been motivated by the desire to interpret the riddle of the human brain for more than 2500 years. We find notable and realistic concepts, as well as those that are speculative. After a millennium of considerations and opinions that specify mental functions as being located in the ventricles, in the 17th century, attention began to be directed at the gray and white matter with the studies of Willis, Malpighi, Steno, Vieussens, and Riley. Niels Stensen (Steno) designated the white matter as the "nature masterpiece" and demanded, in a famous lecture in Paris, 1665, well programmed research of the brain.

Parallel to the advances in mathematics, basic sciences, and scientific technology in the 19th and 20th centuries, investigations in anatomy and physiology of the primate and human brain progressed in steady, intense, carefully planned research programs. Much attention was paid to the architecture and function of the gray matter, particularly of the neurons, thanks to the technological advances in microscopy, microtome, and chemistry. The study of neuroglia and white matter remained a neglected field to some extent. This was not intentional but was caused by the lack of adequate scientific technology to grasp the specific anatomy and distinctive functions of the brain.

Dr. Josef Klingler at the Anatomy Institute, University of Basel, Switzerland, invented the frozen-technique of formol-fixed cadaver brains, which enabled him to perform meticulous dissections of the connective fibers. He published his unique work together with Professor E. Ludwig in 1956 in a famous atlas.

This pioneering work aroused the interest and curiosity of Professor Türe in Istanbul's Yedi Tepe University Hospital, who became fasci-

nated by fiber dissection and has persisted in perfecting the technique by applying the operating microscope, self-manufactured specific wooden-spatulas, and a low-pressure suction system for accurate handwork since 1990. Professor Türe has spent 17 years studying and documenting the intricacies of the fiber system. He has published essential preliminary articles and has presented his approaches and views in many meetings and courses since 1995. He has distributed his instructional videos to interested colleagues on four continents. With respect to the complex architecture of the white matter, Professor Türe preferred first to study the correlations of his studies with the results of DTI, positron-emission tomography, and functional magnetic resonance imaging before the publication of a monograph together with Professors A. Valavanis and S. Kollias at the University Hospital, Zurich, Switzerland. Professors Valavanis and Kollias have pioneered innovative and essential aspects of tractography of the brain and spinal cord using advanced DTI technology on 3-T magnetic resonance imaging. Their studies were published in *Neuroimaging* in 2003. Their preliminary observations have also been presented at annual meetings and courses. The publication of this monograph will broaden and illuminate our understanding of the unique architecture of the brain white matter and will focus on applying this knowledge to our clinical and surgical practice.

White matter has a seemingly amorphous, homogeneous appearance, but it presents the most ingenious architecture in its anatomical, biophysical, biochemical, and immunological aspects. The known components of white matter are the three-dimensional myriad networks of perfectly organized myelinated and unmyelinated fiber systems, a network of intraparenchymal vascular and cerebrospinal fluid pathways, cellular and fluid components of the endocrine and immune systems, and newly generated glial and neuronal cells migrating between fibers and other pathways. The detailed architecture of the fiber systems remains unknown. Their lamellae are similar to curling leaves stratified in three-dimensional layers, which were described in 1675 to 1679 by Malpighi, who had used a microscope for his studies for the first time.

Fifty years ago, W.J.S. Krieg, an anatomist in Chicago, presented perplexing monographs, which are overwhelming both in their elaborate text and in the inclusion of innovative, artistic three-dimensional diagrams to illustrate the entire connective system of the central nervous system. These illustrations offer a new paradigm reflecting the organization of the connective fibers of the white matter. Dr. Krieg's striking anatomical perspectives should be studied, in particular by neuroradiologists, who are progressively enhancing the visualization of the fiber tract with the aid of diffusion tensor magnetic resonance technology.

The dawn of neurochemical imaging with positron-emission tomography, magnetic resonance spectroscopy, and functional magnetic resonance imaging has the potential to broaden our insights and provide new dimensions to our knowledge.

The dynamic functional anatomy of the human brain merits further study and places emphasis on multidirectional units, which deserve to be expressed in tangible, factual terminology. The three-dimensional, perfectly organized brain parenchyma may appear, in spatial terms, to be a static and unvarying construction. In view of the motion and impulses, however, the constant modulations in multidimensional and multidirectional synaptic activities and interactivities, the biophysical and biochemical transmissions and their instantly changing connections and communication patterns, and the continuous oscillating and merging alliances between compartments of functional units in various topographic areas of the brain are unparalleled characteristics.

Neither the perpetual and generally perfect regulations governing the transmission activities of fiber systems nor the microarchitecture of the fiber systems have been thoroughly investigated. This branch of anatomy awaits further elucidation. Before a comprehensive understanding of human brain function down to the intracellular structures in nanometric dimensions can be gained, the riddle of the fiber system and other components of white matter needs to be resolved.

Impressed by pictograms of fiber tracts obtained using tractography technology with DTI, we are forced to confess that these images have been derived mathematically from prospective illustrations based on currently available anatomical knowledge. Further advances in neuroscience and scientific technology will ultimately decipher the entire parenchymal architecture of the brain and its functional parameters.

Unmistakably, we reap great clinical value from our ongoing research activities and profit from our exchanges with colleagues and our discussion of differing opinions. The coming generation of neuroscientists will be confronted with even more data related to the architecture and function of the normal and diseased central nervous system, which they will need to analyze and coordinate into their own research. In this connection, I recommend paying attention to the excellent monograph of P. Gloor, *The Temporal Lobe and Limbic System,* and another by Per Andersen et al., *The Hippocampus Book.*

I would also like to emphasize the forgotten work of David L. Basset, who pioneered the publication of the first comprehensive stereoscopic atlas of the whole human body in 30 volumes in 1952. He devoted four volumes to the central nervous system, with 28 reels each containing seven instructive stereopictures of the brain and spinal cord, accompanied with excellent drawings and precise texts. These four volumes should be available for young neurosurgeons and neuroradiologists.

Undoubtedly, the article of Fernández-Miranda et al. will greatly enhance and stimulate the critical research activities in this field.

M. Gazi Yaşargil
Little Rock, Arkansas

Nowadays, it is mandatory for neurosurgeons, especially when operating on cerebral low-grade gliomas, to have a great knowledge of the complex architecture of the white matter in order to improve the presurgical strategy, avoid damage of white fibers, and have the opportunity to understand the connections within the brain.

In this study, fiber dissection and DTI techniques are reciprocally enriched in order to better describe the anatomical relationships between white matter tracts. This is an original work, as there are no other articles in which fiber dissection with Kingler's technique, three-dimensional reconstruction of the anatomical images, and DTI-based tractography are compared in order to provide a better understanding of the white matter tracts. Moreover, it is of great interest that DTI-based tractography was validated by comparing their results to fiber dissections rather than classical anatomical descriptions.

This article gives neurosurgeons the opportunity to better understand the complex anatomical relationships between fiber tracts thanks to the great three-dimensional anatomical images provided and to compare the real anatomy of the brain to the findings of DTI-based tractography.

Roberto Delfini
Rome, Italy

In order to fully appreciate the information and visual presentation of this report, the reader will likely have to take it in sections. The article is necessarily long and complete, and the illustrations are remarkable. Our readers should save this issue of the Journal as a reference text, like an anatomy book in their library. I only wish that I had this as a reference when I started to study surgical anatomy.

Joseph M. Piepmeier
New Haven, Connecticut

This is another *tour de force* by Dr. Rhoton and his colleagues, headed up by Dr. Fernández-Miranda, in a study to anatomically depict white matter tracts in relation to DTI. Using formalin-fixed human hemispheres and an elegant fiber dissection technique, they were able to demonstrate the classic white matter fasciculi and their projections, which correspond very nicely to DTI. This is particularly important in light of the fact that we can obtain high resolution DTI of tracts in relationship to intracerebral lesions, which can often be confirmed at the time of surgery to be functional in nature. DTI is extraordinarily complex, especially as various fiber pathways cross each other. New techniques, including 3-T hemispheric array detector for imaging paradigms allow for simultaneous depiction of subcortical tracts in one setting. This is particularly important because most DTI to date has only been able to show one or perhaps two components of a tract at any given time. This is going to provide even greater resolution to the imaging technique which will depict these subcortical tracts prior to surgery. This elegant set of dissections clearly shows the relationship of these anatomical fiber dissection tracts with the DTI that will allow for the practical use for surgical planning. The authors are to be congratulated on a job very well done, and a tedious study that will have great utility for everyday surgery in conjunction with DTI.

Mitchel S. Berger
San Francisco, California

One of the most fascinating developments in 19th-century clinical neuroscience was the teasing out of localized (versus globally distributed) cerebral functionality. This line of investigation was more recently reinvigorated by technological advances in functional imaging such as positron-emission tomography and functional magnetic resonance imaging. Not surprisingly, these studies have oriented most of us towards cortical function; we look for the dime where the light is good. In 1965, Norman Geschwind focused attention on a complementary view of brain function, but also recognized the powerful and critically important role played by connectivity (1, 2). As technological advances increasingly enable visualization of subcortical substructure, it is likely that his contributions will loom even larger.

Fernández-Miranda et al. have once more produced an anatomical *tour de force,* this time integrating findings from an old manual technique with one of the hottest neuroimaging methodologies we have today. This is an enjoyable and rewarding work to read, but more importantly, this work will be a valuable resource to draw upon in the future for everyone trying to understand or work within the brain.

David W. Roberts
Lebanon, New Hampshire

1. Geschwind N: Disconnexion syndromes in animals and man. I. **Brain** 88:237–294, 1965.
2. Geschwind N: Disconnexion syndromes in animals and man. II. **Brain** 88:585–644, 1965.

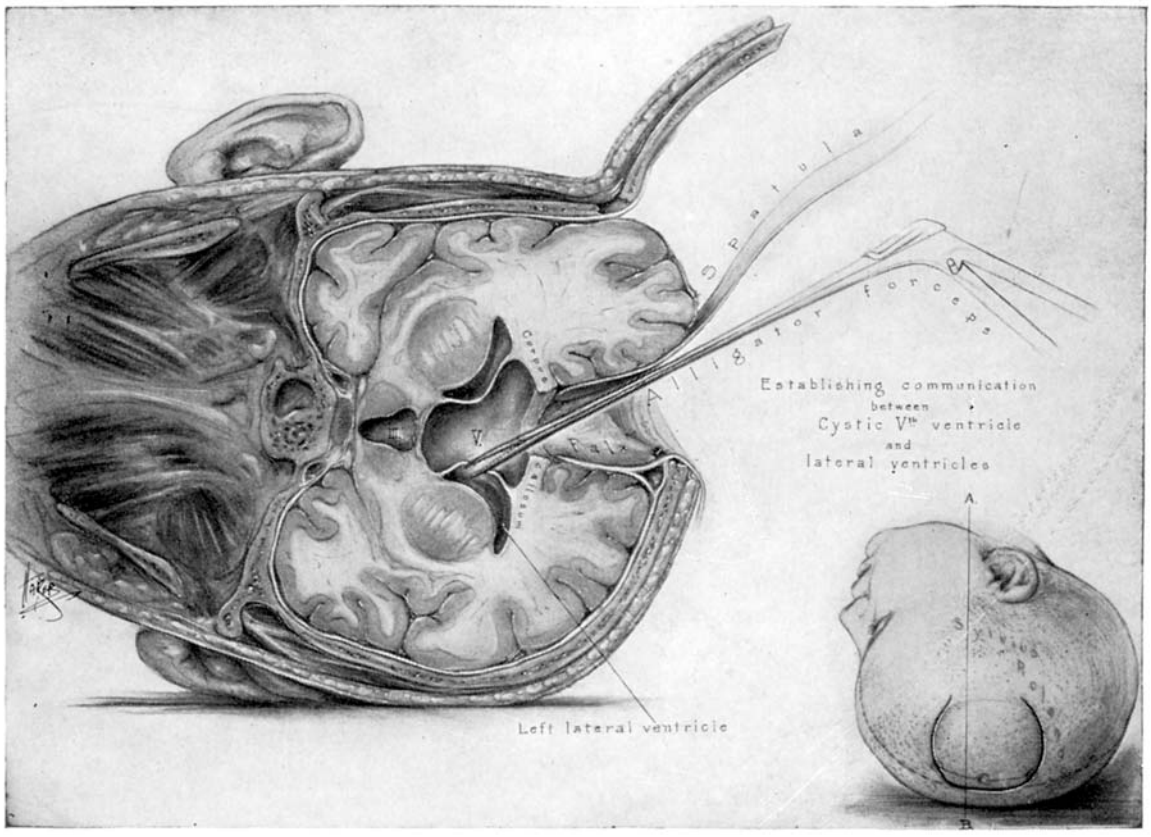

Diagram indicating method of establishing communication between the lateral ventricles and a cyst of the septum pellucidum. (From: Dandy WE: *The Brain.* New York, Harper & Row, Publishers, 1969. Reprinted from *Lewis' Practice of Surgery*, Prior, 1933.)